UNIVERSITY OF VERONA

DEPARTMENT OF

Biotechnology

DOCTORAL PROGRAM IN

Biotechnology

WITH THE FINANCIAL CONTRIBUTION OF

SUS-MIRRI.IT

Cycle / year: 38° / 2022-2023

TITLE OF THE DOCTORAL THESIS

Preservation, Characterization, and Bioremediation Potential of Microbiomes from PFAS-impacted Soil and Sediment

S.S.D. BIO/19

Coordinator: Prof.ssa Flavia Guzzo

Signature _____

Supervisor: Prof.ssa Silvia Lampis

Signature _____

Co-Supervisor: Prof.ssa Nicola Vitulo

Signature _____

Doctoral Student: Dott. Asma Nawaz

Signature _____

The doctoral scholarship was funded by the European Union –NextGenerationEU, National Recovery and Resilience Plan, in the framework of the project “Strengthening the MIRRI Italian Research Infrastructure for Sustainable Bioscience and Bioeconomy”, area ESFRI “Health and Food”, Mission 4 Component 2 Investiment 3.1.

Acknowledgments

I would like to express my sincere gratitude to everyone who, in one way or another, has supported me and contributed to the completion of this work.

First and foremost, I am deeply grateful to my supervisor, Professor Silvia Lampis, for her continuous guidance, encouragement, and unwavering support throughout my Ph.D. journey. Her mentorship has been invaluable to both my academic and personal growth.

I would like to extend my heartfelt thanks to my co-supervisor, Dr. Marco Andreolli, for his constant guidance, invaluable support, and dedication. His assistance in experimental work, data analysis, and overall mentorship has been fundamental to the successful completion of this research. My sincere appreciation also goes to Dr. Davide Righetti for his insightful discussions and support, and to Beatrice Tontini for her assistance and collaboration in the laboratory.

I am especially grateful to my host supervisor, Professor Paula M. L. Castro, for providing me with the opportunity to carry out part of my research at CBQF. I would also like to express my deepest thanks to Dr. Irina S. Moreira for her continuous support, guidance, and hands-on assistance during my experimental work throughout my visit. I would like to acknowledge all the students, fellows, and colleagues who have been part of the laboratory environment, contributing to a collaborative and supportive atmosphere.

My deepest gratitude goes to my parents, Muhammad Nawaz and Rashidan Nawaz, whose unwavering belief in me, endless sacrifices, and constant support have made this journey possible. Coming from a small village to pursuing a Ph.D. in a new country would not have been achievable without their strength, encouragement, and trust. I am forever indebted to them.

I am also sincerely grateful to my siblings—Tehmina Nawaz, Ali Nawaz, and Arman Nawaz—for their unwavering support, love, and encouragement. I would like to extend a special thanks to my partner, Ali Raza, for his understanding, support, and encouragement throughout this journey.

I am grateful to my dear friends for their kindness, and companionship. Last but not least, I would like to acknowledge myself—for my resilience, determination, and inner strength; for continuing to believe in my abilities during the most challenging times; and for having the courage to navigate this journey independently, far from home, while remaining committed to achieving this milestone.

I dedicate this thesis to my parents, whose love, sacrifices, and unwavering support have made everything possible. Without them, this journey would not have been achievable.

Asma Nawaz
21 April 2026

Highlights

- Cryogenic preservation (−80 °C, glycerol) was used to preserve the structural integrity of the PFAS-impacted environmental microbiomes (Soil and Sediment) over a twelve-month storage period.
- Microbial vitality and functional activity were assessed at four time points during preservation: T0 (pre-storage), T1 (3 months), T2 (8 months), and T3 (12 months), showing progressive changes over time
- DNA barcoding analysis revealed that the core community structure remained stable throughout the preservation period in both soil and sediment matrices, with no observable changes related to storage time; however, soil samples displayed higher heterogeneity than sediment samples.
- DNA barcoding analysis revealed that bacterial communities were consistently dominated by *Proteobacteria, Bacteroidota*, and *Actinobacteriota*, while fungal communities were characterized by the high prevalence of *Sordariomycetes*, *Agaricomycetes*, and *Leotiomycetes*.
- New microbiomes were obtained after enrichment cultures from matrices stored at different time points, and the differences among these new microbiomes were more evident in soil than in sediment.
- Microbiomes obtained from enrichment cultures were tested for PFOA and PFHxS degradation, but no significant degradation was observed.
- Isolates from enrichment cultures were identified via partial 16S rRNA and ITS sequencing; despite temporal changes, *Pseudomonas*, *Flavobacterium*, *Microbacterium*, *Brucella*, *Brevundimonas*, and *Rhodanobacter* remained prominent among bacterial genera, while *Galactomyces*, *Trichosporon*, *Candida*, *Geotrichum*, and *Fusarium* dominated fungal communities.
- Only three isolates (*Brevundimonas* sp. 9T2SB, *Sphingobacterium* sp. 5T3SA, and *Candida* sp. 4T2SB) demonstrated co-metabolic defluorination of fluoxetine, indicating potential for transformation of less recalcitrant fluorinated compounds.
- The study highlights the importance of preserving intact microbiomes and the challenges associated with PFAS biodegradation.

Abstract

Poly- and perfluoroalkyl substances (PFASs) are persistent, bio accumulative, and toxic environmental pollutants that adversely affect ecosystems and human health. Traditional physicochemical approaches such as filtration and adsorption (e.g., activated carbon) commonly involve high costs, substantial energy inputs, and secondary environmental pollution, including the release of shorter-chain PFAS. Bioremediation is therefore increasingly explored as a promising and sustainable alternative. Several studies have evidenced that contaminants' transformation may be driven by community-level processes where inter-species interactions play a central role. However, most of the literature is focused on the study of isolated microbial strains on these contaminants and studies focusing on complex environmental microbiomes remain scarce, particularly when considering their functional dynamics. This reinforces the importance of studying natural microbiomes to understand their structural and functional dynamics.

This study aimed to investigate the preservation, propagation, and utilization of environmental PFAS-impacted microbiomes for their potential exploitation in bioremediation protocols. Furthermore, to support this work, methodological standardization was addressed by developing and validating Standard Operating Procedures (SOPs) of sampling and DNA extraction. The interlaboratory validation revealed good reproducibility and consistency of the research units, and no significant differences in the microbial diversity, community structure, and taxonomic composition were found among the samples.

For this study, soil (Soil) and sediment (Sed) matrices were obtained from two sites in the Vicenza Province (Veneto, Italy). These sites have been affected by PFAS contamination resulting from industrial wastewater release. Chemical analysis revealed that sediment was more contaminated (17,700 ng kg^{-1}) than soil (5,370 ng kg^{-1}), with a dominance of PFOS and PFSA in sediment, and PFOA in soil samples. Samples were cryopreserved (with 30% *v/w* glycerol) at -80 °C and preservation impacts were assessed at four time points: T0 (pre storage), T1 (3 months storage), T2 (8 months storage), and T3 (12 months storage). The effect of storage on microbiomes was analyzed through either culture-dependent or -independent methods such as total microbial counts, Biolog EcoPlate analysis, and DNA metabarcoding.

These analyses were performed to study microbial viability, metabolic activity, and community structure shifts at DNA level during preservation. Results showed that bacterial counts were stable up to T2 (8 months) in both matrices followed by a decrease in viable counts at T3 (12 months) particularly in Soil. Fungi showed no change in viability during the preservation process in sediment, but a slight decrease was observed after 12 months in soil. Biolog analysis showed that soil had a higher initial metabolic activity than sediment, and a clear decrease in the number of substrates used mainly from T2 to T3, suggesting the loss of selected metabolic functions. In sediment, there was a gradual decrease in metabolic activities. DNA extraction from the environmental matrixes showed that sediment provided a substantially greater yield of total genomic DNA (15-30 µg g^{-1}) than soil (3-7.5 µg g^{-1}).

Metabarcoding data revealed that sediment and soil-derived microbiomes evidenced with no correlation between microbial communities (both bacteria and fungi) and storage time. Bacterial communities were consistently dominated by *Proteobacteria*, *Bacteroidota*, and *Actinobacteriota*, while fungal communities were characterized by the high prevalence of *Sordariomycetes*, *Agaricomycetes*, and *Leotiomycetes*. Microbial propagation was performed by enrichment cultures adding PFOA (from 300 to 600 mg L^{-1}) as sole source of carbon and energy across the preservation time points (T0, T1, T2 and T3), Genomic DNA was successfully extracted from all enrichment cultures, with higher DNA yields (0.58-1.82 µg ml^{-1}) in sediment than from soil (0.29-0.59 µg ml^{-1}).

The microbial succession after PFOA enrichment revealed distinct banding patterns by DGGE analysis. In sediment, a similarity of about 20% was observed between T0 and T3. In soil, this temporal separation was even greater where similarity dropped to only 5% between T0 and T3. These findings evidenced a change in enriched community structure derived from microbiome stored at different timing, with a more pronounced shift in microbial structure in the soil derived cultures. The new microbiomes obtained from the different enrichment cultures were tested in batch abatement trials using PFOA (25 mg L^{-1}) and PFHxS (10 mg L^{-1}) as the reference

compounds over 87 days. Total count revealed an increased bacterial count in soil and a stable count in sediment during the experiment. On the other hand, no significant abatement of PFAS was observed, suggesting no active biodegradation or transformation of PFAS under these conditions. A total of 158 bacterial (resolved into 103 bacterial operational taxonomic units) and 53 fungal strains were isolated.

Different genera exhibited temporal changes, *Pseudomonas*, *Flavobacterium*, *Microbacterium*, *Brucella*, *Brevundimonas*, and *Rhodanobacter* being prominent bacterial groups. *Galactomyces*, *Trichosporon*, *Candida*, *Geotrichum* and *Fusarium* were prominent fungal groups throughout the different enrichment cultures, suggesting adaptation to stress conditions related to the presence of PFAS. Isolated strains were further characterized. Six isolates showed apparent growth on DM agar plates supplied with 50 mg L^{-1} PFOA: *Brevundimonas* sp. 9T2SB, *Chryseobacterium* sp. 5T2LA, *Sphingobacterium* spp. (9T2LB, 5T3SA), *Geotrichum* sp. 3T2SA, and *Candida* sp. 4T2SB. When these selected isolates were subjected to biotransformation assays of a structurally varied range of PFAS (PFOA, PFOS, 8:2 FTS, GenX, 7:3 FTCA, and NFDHA) revealed no detectable fluoride (F-) release or transformation in both axenic cultures and consortia, indicating high recalcitrance of these compounds.

In contrast, co-metabolic assays demonstrated the transformation of fluoxetine (FLX), with glucose serving as the primary substrate supporting microbial growth and metabolism. Thus, FLX transformation occurred through glucose-supported co-metabolism.

HPLC and ion-selective electrode analysis confirmed substantial FLX removal and steady F^- release, particularly by strains *Brevundimonas* sp. 9T2SB, *Sphingobacterium* sp. 5T3SA, and *Candida* sp. 4T2SB. This suggests that these strains, while lacking inherent pathways to mineralize PFAS, have active co-metabolic defluorination pathways to degrade less complex fluorinated aromatics. In summary, cryogenic preservation showed progressive changes in microbial vitality and functional activity over storage time, whereas core community structure in terms of DNA was maintained. Under PFAS exposure, neither enriched microbiomes nor isolated strains exhibited PFAS biotransformation or defluorination under the tested conditions. However, selected isolates transformed fluoxetine under co-metabolic conditions, with fluoride release, indicating potential for less recalcitrant fluorinated compounds**.**

Overall, these results emphasize both the impact and the importance of preservation of PFAS-associated microbiomes and the inherent challenges of PFAS biodegradation, highlighting the need for further investigation into conditions that support effective transformation.

Keywords

Per- and polyfluoroalkyl substances (PFAS), soil and sediment microbiomes, Cryopreservation, DNA metabarcoding, Community-level physiological profiling (CLPP), Enrichment cultures, Defluorination, Co-metabolism

Highlights (Italian)

- La conservazione criogenica (−80 °C, glicerolo) è stata utilizzata per preservare l'integrità strutturale dei microbiomi ambientali contaminati da PFAS (suolo e sedimento) per un periodo di stoccaggio di dodici mesi.
- La vitalità microbica e l'attività funzionale sono state valutate in quattro punti temporali durante la conservazione: T0 (pre-stoccaggio), T1 (3 mesi), T2 (8 mesi) e T3 (12 mesi), mostrando cambiamenti progressivi nel tempo.
- L'analisi di DNA barcoding ha evidenziato che la struttura della comunità core è rimasta stabile durante l'intero periodo di conservazione in entrambe le matrici, suolo e sedimento, senza variazioni osservabili legate al tempo di stoccaggio; tuttavia, i campioni di suolo hanno mostrato una maggiore eterogeneità rispetto a quelli di sedimento.
- L'analisi di DNA barcoding ha inoltre rivelato che le comunità batteriche erano costantemente dominate da *Proteobacteria*, *Bacteroidota* e *Actinobacteriota*, mentre le comunità fungine erano caratterizzate da un'elevata prevalenza di *Sordariomycetes*, *Agaricomycetes* e *Leotiomycetes*.
- Nuovi microbiomi sono stati ottenuti a seguito di colture di arricchimento a partire da matrici conservate a diversi tempi, e le differenze tra questi microbiomi sono risultate più evidenti nel suolo rispetto al sedimento.
- I microbiomi ottenuti dalle colture di arricchimento sono stati testati per la degradazione di PFOA e PFHxS, ma non è stata osservata alcuna degradazione significativa.
- Gli isolati ottenuti dalle colture di arricchimento sono stati identificati mediante sequenziamento parziale del 16S rRNA e dell'ITS; nonostante le variazioni temporali, *Pseudomonas*, *Flavobacterium*, *Microbacterium*, *Brucella*, *Brevundimonas* e *Rhodanobacter* sono rimasti tra i generi batterici predominanti, mentre *Galactomyces*, *Trichosporon*, *Candida*, *Geotrichum* e *Fusarium* hanno dominato le comunità fungine.
- Solo tre isolati (*Brevundimonas* sp. 9T2SB, *Sphingobacterium* sp. 5T3SA e *Candida* sp. 4T2SB) hanno mostrato defluorinazione co-metabolica della fluoxetina, indicando un potenziale per la trasformazione di composti fluorurati meno recalcitranti.
- Lo studio evidenzia l'importanza della conservazione di microbiomi intatti e le sfide associate alla biodegradazione dei PFAS.

Abstract (Italian)

Le sostanze poli- e perfluoroalchiliche (PFAS) sono inquinanti ambientali persistenti, bioaccumulabili e tossici che compromettono gli ecosistemi e la salute umana. Gli approcci fisico-chimici tradizionali, come la filtrazione e l'adsorbimento (ad esempio mediante carbone attivo), comportano generalmente costi elevati, un significativo consumo energetico e possibili impatti ambientali secondari, inclusa la formazione di PFAS a catena più corta. Pertanto, la bioremediation può essere considerata un'alternativa promettente e sostenibile. Tuttavia, ad oggi, gran parte della letteratura si concentra sullo studio delle capacità di trasformazione di questi composti da parte di singoli ceppi isolati.La trasformazione dei contaminanti può invece essere guidata da processi a livello di comunità microbiche, in cui le interazioni interspecifiche svolgono un ruolo centrale.

Il presente studio ha obiettivo di valutare la conservazione, la propagazione e il loro potenziale utilizzo in protocolli di biorisanamento di microbiomi presenti in matrici ambientali contaminate da PFAS—suolo (Soil) e sedimento (Sed)— A tal fine, campioni di suolo e sedimento sono stati raccolti in due siti nella provincia di Vicenza (Veneto, Italia), contaminati da PFAS a causa di scarichi industriali. Le analisi chimiche hanno evidenziato una maggiore contaminazione nei sedimenti (17.700 ng kg^{-1}) rispetto al suolo (5.370 ng kg^{-1}), con predominanza di PFOS e PFSA nei sedimenti e di PFOA nei campioni di suolo. I campioni sono stati crioconservati (con glicerolo al 30% v/p) a −80 °C e gli effetti della conservazione sono stati valutati a quattro tempi: T0 (prima della conservazione), T1 (3 mesi), T2 (8 mesi) e T3 (12 mesi).

La conservazione dei microbiomi è stata valutata sia con metododiche coltura-dipendenti che indipendenti, tra cui conte microbiologiche totali, analisi Biolog EcoPlate e DNA metabarcoding. I risultati hanno mostrato che le conte batteriche sono rimaste stabili fino a T2 (8 mesi) in entrambe le matrici, seguite da una diminuzione della vitalità a T3 (12 mesi), particolarmente nel suolo. I funghi non hanno mostrato variazioni significative nella vitalità nei sedimenti, mentre nel suolo è stata osservata una lieve riduzione dopo 12 mesi. L'analisi Biolog ha evidenziato una maggiore attività metabolica iniziale nel suolo rispetto al sedimento e una chiara diminuzione del numero di substrati utilizzati, soprattutto tra T2 e T3, suggerendo la perdita di specifiche funzioni metaboliche. Nei sedimenti, invece, si è osservata una diminuzione più graduale dell'attività metabolica.

L'estrazione del DNA ha mostrato rese significativamente più elevate nei sedimenti (15–30 µg g^{-1}) rispetto al suolo (3–7,5 µg g^{-1}). I dati di DNA metabarcoding effettuati sia sulla popolazione batterica che fungina hanno evidenziato che le comunità microbiche presenti nel sedimento e suolo non evidenziavano una significativa correlazione con il tempo di stoccaggio. Le comunità batteriche erano dominate da Proteobacteria, Bacteroidota e Actinobacteriota, mentre quelle fungine erano caratterizzate principalmente da Sordariomycetes, Agaricomycetes e Leotiomycetes.

L propagazione microbica delle matrici conservate è stata condotta tramite colture di arricchimento utilizzando PFOA (ad una concentrazione crescente da 300 a 600 mg L^{-1}) come unica fonte di carbonio ed energia. Lo scopo principale era valutare e confrontare l'arricchimetomicrobico derivante dai campioni durante i diversi tempi di conservazione e per favorire l'isolamento di ceppi tolleranti al PFOA. Il DNA genomico è stato estratto con successo da tutte le colture di arricchimento, con rese più elevate nei sedimenti (0,58–1,82 µg ml^{-1}) rispetto al suolo (0,29–0,59 µg ml^{-1}). L'analisi DGGE ha evidenziato cambiamenti temporali nella struttura delle comunità arricchite, con una similarità del 20% tra T0 e T3 nei sedimenti e solo del 5% nel suolo, indicando una maggiore variazione nelle comunità del suolo.

I microbiomi ottenuti a seguito delle colture di arricchimento (T0 e T3) sono stati testati al fine di valutare la loro capacità di degradazione di composti PFAS. Tuttavia, nei test di abbattimento condotti per 87 giorni con PFOA (25 mg L^{-1}) e PFHxS (10 mg L^{-1}), non è stata osservata alcuna significativa rimozione dei PFAS, indicando l'assenza di biodegradazione o trasformazione attiva nelle condizioni sperimentali adottate.

A seguito delle colture di arricchimento sono stati isolati complessivamente 158 ceppi batterici (103 unità tassonomiche operative) e 53 ceppi fungini. I generi dominanti includevano *Pseudomonas*, *Flavobacterium*, *Microbacterium*, *Brucella*, *Brevundimonas* e *Rhodanobacter* tra i batteri, e *Galactomyces*, *Trichosporon*, *Candida*, *Geotrichum* e *Fusarium* tra i funghi. Sei isolati (*Brevundimonas* sp. 9T2SB, *Chryseobacterium* sp. 5T2LA, *Sphingobacterium* spp. (9T2LB, 5T3SA), *Geotrichum* sp. 3T2SA, and *Candida* sp. 4T2SB) hanno mostrato crescita apparente in presenza di PFOA (50 mg L^{-1}). Tuttavia, i test di biotrasformazione con diversi PFAS non hanno evidenziato rilascio di fluoruro o degradazione. Diversamente, saggi condotti in condizione di co-metabolismo con fluoxetina, è stata osservata una significativa rimozione di fluoruro dal composto fluoxetina, indicando una capacità di defluorinazione di composti fluorurati meno recalcitranti.

In sintesi, la crioconservazione ha determinato cambiamenti progressivi nella vitalità microbica e nell'attività funzionale nel tempo, mentre analisi *colture-dependent* utilizzando come target il DNA non hanno evidenziato variazioni in funzione del tempo di conservazione. Nonostante l'isolamento di numerosi microrganismi a seguito di colture d'arricchimento, non è stata osservata una loro capacità di biotrasformazione dei PFAS. Tuttavia, alcuni isolati hanno mostrato capacità di defluorinazione della fluoxetina in condizioni co-metaboliche. Questi risultati evidenziano sia l'importanza della conservazione dei microbiomi associati ai PFAS sia le difficoltà intrinseche nella loro biodegradazione, sottolineando la necessità di ulteriori studi.

A supporto di questo lavoro, sono state sviluppate e validate procedure operative standard (SOP) per il campionamento e l'estrazione del DNA. La validazione inter-laboratorio ha dimostrato buona riproducibilità e coerenza tra le unità di ricerca, senza differenze significative nella diversità microbica, nella struttura della comunità e nella composizione tassonomica.

Ph.D. Research Aims

This Ph.D. research is conducted within the framework of the SUS-MIRRI.IT project ("Strengthening the MIRRI Italian Research Infrastructure for Sustainable Bioscience and Bioeconomy"), funded under the ESFRI "Health and Food" area by the European Commission through the NextGenerationEU programme (Code N° IR0000005). The SUS-MIRRI.IT initiative aims to strengthen the Italian node of the Microbial Resource Research Infrastructure (MIRRI-IT) by implementing and valorizing microbial resources stored in Italian biobanks, improving their characterization, and optimizing their management through the coordinated involvement of 24 partners. In this context, this Ph.D. project focuses on the investigation, preservation, and characterization of microbiomes associated with PFAS-impacted environmental matrices, with particular emphasis on their long-term stability and functional potential.

The research is also aligned with the activities of the Verona University Culture Collection – Department of Biotechnology (VUCC-DBT), contributing to the development and valorization of microbial resources within this collection. The central research objective of this Ph.D. is to evaluate the impact of preservation on microbiomes originating from PFAS-impacted matrices, while evaluating the impact of PFAS contamination on microbial community structure and functionality. This includes the assessment of microbiomes in terms of (i) preservation, (ii) propagation, and (iii) utilization, with particular attention to microbiome resilience, recovery after long-term storage, and functional stability. The utilization of microbiomes includes the evaluation of both *(i)* new enriched microbiome responses under PFAS exposure and *(ii)* the strain-specific capabilities involved in PFAS biotransformation.

Experimental activities related to microbiome preservation were initiated during the second year of the Ph.D. and continued into the third year. As a supporting methodological component, activities carried out during the first year contributed to the standardization of microbiome analysis workflows through the development and validation of Standard Operating Procedures (SOPs) for sampling and DNA extraction. Although not the primary focus of the thesis, this work provided a robust and reliable framework for subsequent microbiological and molecular analyses. Overall, this Ph.D. provides new insights into the preservation and functional behavior of PFAS-associated microbiomes and highlights their potential as microbial resources for environmental biotechnology applications, while contributing to the broader objectives of the SUS-MIRRI.IT initiative.

Study Design

At the initial stage of the study, standardized operating procedures (SOPs) for water and soil samples were developed and validated to ensure reproducible analysis of environmental microbiomes. These SOPs defined workflows for sample handling, DNA extraction, and downstream metabarcoding analysis. Therefore, the microbiome study was conducted using two PFAS-impaired environmental matrices: Soil and Sediment. To preserve the native microbial communities, samples were aliquoted and amended with sterile glycerol at a final concentration of 30% (*w/v*), homogenized, stored overnight at −4 °C, and subsequently cryopreserved at −80 °C.

The effects of cryopreservation were evaluated using a time-series experimental design, with analyses performed at four defined time points: T0 (pre-storage), T1 (4 months of storage), T2 (9 months of storage), and T3 (12 months of storage). This approach enabled the assessment of long-term impacts of cryopreservation on microbial viability, community structure, and functional potential. Chemical analysis of the samples was performed to determine the concentration of PFAS present in the soil and sediment matrices, providing a baseline for evaluating microbial responses and downstream functional experiments. Culture-dependent analyses were conducted at all time points (T0, T1, T2, and T3) to assess microbial viability and functional diversity during storage.

In parallel, culture-independent analyses based on DNA metabarcoding were performed to investigate changes in microbial community composition over preservation time. In addition to preservation assessment, the stored microbiome was propagated by enrichment cultures to selectively enhance microbial populations with the potential to tolerate and transform PFAS compounds. These enrichment cultures formed the basis for subsequent abatement experiments, as well as for the isolation and identification of microbial strains. Selected isolates were further subjected to biotransformation experiments to evaluate their PFAS transformation potential under controlled laboratory conditions.

This integrated study design allowed the systematic evaluation of microbiome preservation, functional resilience, and PFAS-related microbial activity, providing the conceptual framework for the experimental procedures described in the following Materials and Methodology section.

Contents

List of Figures

List of Tables

Acronyms

Full Name	Acronym
5:3 Fluorotelomer Carboxylic Acid	5:3 FTCA
6:2 Fluorotelomer Acrylate Butyrate	6:2 FTAB
6:2 Fluorotelomer Alcohol	6:2 FTOH
6:2 Fluorotelomer Sulfonate	6:2 FTS
6:2 Fluorotelomer Sulfonic Acid	6:2 FTSA
6:2 Fluorotelomer Unsaturated Carboxylic Acid	6:2 FTUCA
7:3 Fluorotelomer Carboxylic Acid	7:3 FTCA
8:2 Fluorotelomer Alcohol	8:2 FTOH
Amplicon Sequence Variants	ASVs
Aqueous Film-Forming Foams	AFFF
Agency for Toxic Substances and Disease Registry	ATSDR
Boron-Doped Diamond	BDD
Centre for Biotechnology and Fine Chemistry	CBQF
Colony Forming Units	CFU
Drinking Water Directive	DWD
Electrochemical Oxidation	EO
Environmental Protection Agency	EPA
European Environment Agency	EEA
European Food Safety Authority	EFSA
Fluorotelomer Aldehydes	FTAL
Fluorotelomer Alcohols	FTOHs
Fluorotelomer Carboxylic Acids	FTCAs
Fluorotelomer Sulfonic Acids	FTSAs
Fluorotelomer Unsaturated Carboxylic Acids	FTUCA
Fluoxetine	FLX
Granular Activated Carbon	GAC
Hexafluoropropylene Oxide Dimer Acid	GenX
Hydrofluoric Acid	HF
Internal Transcribed Spacer	ITS
International Agency for Research on Cancer	IARC
Interstate Technology and Regulatory Council	ITRC
Ion Exchange	IX
Italian National Agency for New Technologies, Energy and Sustainable Economic Development	ENEA
Malt Yeast Extract	MYE
Microbial Index Quality	MIQ
Minimal Defined Medium	DM
Minimal Medium	MM
N-ethyl Perfluorooctane Sulfonamidoethanol	N-EtFOSE
National Academies of Sciences, Engineering, and Medicine	NASEM

Nanofiltration	NF
Nonafluoro-3,6-dioxaheptanoic Acid	NFDHA
Per- and Polyfluoroalkyl Substances	PFAS
Perfluoroalkyl Acids	PFAA
Perfluoroalkyl Carboxylic Acids	PFCAs
Perfluoroalkyl Phosphonic Acids	PFPA
Perfluoroalkyl Sulfonic Acids	PFSAs
Perfluorobutanoic Acid	PFBA
Perfluorobutane Sulfonic Acid	PFBS
Perfluoroheptanoic Acid	PFHpA
Perfluorohexanoic Acid	PFHxA
Perfluorohexane Sulfonic Acid	PFHxS
Perfluorooctane Sulfonic Acid	PFOS
Perfluorooctanoic Acid	PFOA
Perfluorooctane Sulfonyl Fluoride	POSF
Perfluoropentanoic Acid	PFPeA
Perfluoropolyethers	PFPEs
Polyvinylidene Fluoride	PVDF
Polytetrafluoroethylene	PTFE
Reverse Osmosis	RO
Standard Operating Procedures	SOPs
Tetramethylethylenediamine	TEMED
Total Ionic Strength Adjustment Buffer	TISAB
Tolerable Weekly Intake	TWI
Tris-Acetate-EDTA Buffer	TAE
Tryptic Soy Agar	TSA
Tryptic Soy Broth	TSB
Verona University Culture Collection- Department of Biotechnology	VUCC-DBT
Wastewater Treatment Plants	WWTP
World Health Organization	WHO

Section 1- Standard Operating Procedures (SOPs)

Chapter 1. Overview

Microbiomes are described as characteristic communities of microbial (microbiota) living in a particular environment and interacting in a defined theatre of activity by virtue of specific physicochemical and functional characteristics. Their increasing importance in environmental, agricultural, and biotechnological applications underscores the necessity of consistent and reliable analytical methods (Cocolin et al., 2024). One of the biggest constraints of microbiome studies is that there are no standardized protocols for sampling, DNA isolation, and downstream analysis to limit reproducibility and comparability across studies. This challenge is one of the main goals of the SUS-MIRRI.IT project, the purpose of which is to create and introduce standardized procedures to investigate microbiomes.

In this context, Standard Operating Procedures (SOPs) were formulated on sampling and DNA extracted in various environmental matrices such as soil and water. Subsequently, these SOPs were confirmed by interlaboratory studies to guarantee consistency, accuracy, and reproducibility of microbiome data.

Chapter 2. Materials and Methodology

2.1 Definition of Standard Operating Procedures (SOPs)

The University of Verona was involved in further validation for the sampling and analysis of soil and water samples. It was performed involving different laboratories and operators proceeding with the same sample. Therefore, all laboratories involved are provided with identical soil and water samples from the Leader Unit of the task and perform the analyses according to the previously defined SOPs.

2.2 SOP for Water Sampling

Two different samples were analyzed:

(i) Wastewater was harvest from the Bresso wastewater treatment plant (Milan, Italy), downstream of primary sedimentation, distributed in sterile bottles and sent to the University involved in the analysis using freezer packs. Each unit performed the analysis in triplicate.

(ii) Surface water was harvest from Trasimeno Lake (Umbria, Italy) by immersing a sterile tank in the lake and further transferred into 1 L bottles and shipped with freezer packs. Each unit performed the analysis in triplicate.

Therefore, each Unit stored the samples at room temperature until all laboratories had received them. The filtration of all the samples (0.2 µm filter membranes; 30 mL and 150 mL for wastewater and surface lake water, respectively) was then conducted simultaneously across all the University involved in the analysis.

The commercial DNeasy PowerWater Kit (Qiagen) was used for DNA extraction following the instruction manual. ZymoBIOMICS Microbial Community Standard (Zymo Research, 75 µl) was extracted in triplicate by each unit following the DNeasy PowerWater Kit protocol.

The quality and quantity of DNA were assessed by using both a Qubit 4 Fluorometer (Thermo Fisher Scientific, Waltham, USA), and a NanoDrop™ One/One C UV-Vis spectrophotometer (ThermoScientific, USA).

2.3 SOP for Soil Sampling

Six different units participated in the validation of SOP for soil sampling: University of Verona, Torino, Perugia, Palermo, Milano-Bicocca and the Italian National Agency for New Technologies, Energy and Sustainable Economic Development (ENEA).

The bulk soil microbiota of grapevine was analyzed. Two plants (A and B) of the "Moscato Bianco" cultivar, grafted on "Kober 5BB" rootstocks, were selected from an experimental vineyard located in Grugliasco (Torino, Italy). The soil was harvested, the litter removed and passed through a fine mesh sieve and, thus, homogenized with a sterile spoon. The soil was transferred in 50 ml falcon and sent to each unit at −80 °C in dry ice. Each unit performed the analysis in triplicate.

The commercial DNeasy PowerSoil Pro Kit (Qiagen) was used for DNA extraction from soils. ZymoBIOMICS Microbial Community Standard (Zymo Research, 75 µl) was extracted in triplicate by each unit following the DNeasy PowerWater Kit protocol.

The quality and quantity of DNA were assessed by using both a Qubit 4 Fluorometer (Thermo Fisher Scientific, Waltham, USA), and a NanoDrop™ One/One C UV-Vis spectrophotometer (ThermoScientific, USA).

2.4 Amplicon Sequencing, Bioinformatic and Statistical Analysis

All the further analysis was performed by the University of Torino (Department of Agricultural, Forest and Food Sciences) and detailed described in Ferrocino et al. (2025).

Briefly, the V3-V4 region of the 16S rRNA gene was amplified using the primers 16SF 5'-CCTACGGGNGGCWGCAG-3' and 16SR 5'-GACTACHVGGGTATCTAATCC-3 (Klindworth et al., 2013) for the preparation of Illumina 16S sequencing library. ZymoBIOMICS Microbial Community DNA Standard was used to avoid bias arising from sequencing library. Amplicons were sequenced by Novogene Company. The *fastq* data were analyzed using QIIME2 v. 2022.2.0 (Bolyen et al., 2019).

The taxonomic classification of Amplicon Sequence Variants (ASVs) was performed using the qiime against the reference GreenGenes2 database (version 2024.1). The alpha diversity index was calculated using the *vegan* package of R (Dixon, 2003). Agreement within units, Bland–Altman plots were made for Shannon diversity indices with 95% confidence intervals.

Chapter 3. Results

3.1 Definition of SOP

Standard Operating Procedures (SOPs) are systematic, standardized procedures aimed at providing consistency, repeatability, and quality to scientific processes. SOPs are especially important in microbiome studies, as differences in sampling, storage, and processing may have a considerable impact on the composition of microbial communities and subsequent analyses. According to the SUS-MIRRI.IT infrastructure, SOPs are created so that methodologies can be aligned in laboratories to allow consistent comparison of microbiome data and high-quality preservation of microbial resources.

SOPs are described as step-by-step documented procedures that seek to establish operational consistency, reduce variability, and enhance efficiency. SOPs are used as a basis for quality management, traceability, and reproducibility in both industrial and scientific environments.

In microbiome studies, SOPs typically include:

- Clearly defined objectives and scope
- Standardized sampling procedures
- Tightly regulated storage and transport.
- Step-by-step laboratory workflows
- Metadata collection requirements
- Quality control measures

The SOP document to be employed in the present study can be found here: STANDARD OPERATING PROCEDURES (SOPs) FOR SAMPLING OF MICROBIOME IN DIFFERENT ECOSYSTEMS (Cocolin et al., 2024).

3.2 DNA Extraction

3.2.1 Water Samples

DNA extraction was performed according to Qiagen protocol as described in the SOPs developed within SUS-MIRRI.IT project (Cocolin et al., 2024). Wastewater was collected from the Bresso wastewater treatment plant (located in Milan, Italy), and Sur face water was collected from Trasimeno Lake (Umbria, Italy) (Ferrocino et al., 2025).

DNA quantification showed that there was a variation in the yield among the various water sources. The highest concentration of DNA was found in the samples that were defined as VR-Lago (lake/surface water) (83.5-105.9 ng μL^{-1}). Conversely, VR-Refluo (wastewater/effluent) samples reported moderate DNA yields (37.9-70.9 ng μL^{-1}), with VR-M (Mock) samples having the lowest concentration (22.8-26.2 ng μL^{-1}).

Table 1. DNA concentration and purity assessment of water-derived microbiome samples from different sources.

Source	Sample Name	DNA (ng/µL)	260/280	260/230
VR-Refuo1	VR W R1	46.8	1.93	1.57
VR-Refuo2	VR W R2	37.9	1.91	1.46
VR-Refuo3	VR W R3	62.5	1.93	1.6
VR-Refuo4	VR W R4	61.2	1.89	0.7
VR-Refuo5	VR W R5	44.5	1.94	1.57
VR-Refuo6	VR W R6	70.9	1.89	2.2
VR-Lago1	VR W L1	103.8	1.89	2.09
VR-Lago2	VR W L2	99.4	1.86	1.74
VR-Lago3	VR W L3	105.9	1.86	1.45
VR-Lago4	VR W L4	101.5	1.86	1.18
VR-Lago5	VR W L5	83.5	1.88	1.5
VR-Lago6	VR W L6	92	1.87	2.11
VR-M1	VR W M1	26.2	1.89	0.65
VR-M2	VR W M2	24.1	1.88	1.69
VR-M3	VR W M3	22.8	1.84	0.99

3.2.2 Soil Samples

Soil samples were subjected to DNA extraction following standardized SOP procedures to ensure consistency and reproducibility (Cocolin et al., 2024). Soil samples were collected to investigate the composition of the bulk soil microbiota associated with grapevine (Ferrocino et al., 2025).

DNA extraction from soil samples resulted in low to moderate yields (8.5–32.2 ng μL^{-1}).

Table 2. DNA concentration and purity assessment of bulk soil microbiota associated with grapevine.

Sample Name	DNA (ng/µL)	260/280	260/230
VR A1	15	1.67	0.57
VR A2	8.5	1.65	0.09
VR A3	9.1	1.62	0.07
VR A4	13.4	1.69	0.1
VR A5	15.7	1.66	0.77
VR A6	12.7	1.89	0.09
VR B1	8.9	1.82	0.08
VR B2	15.1	1.86	0.08
VR B3	11.4	1.6	0.14
VR B4	15.7	1.66	0.24
VR B5	14.2	1.63	0.11
VR B6	13.1	1.69	0.09
VR M1	26.5	1.88	0.51
VR M2	30.9	1.86	0.35
VR M3	32.2	1.98	0.13

3.3 Validation of SOP

Following DNA extraction, all samples were transferred to the University of Torino (Department of Agricultural, Forest and Food Sciences), where subsequent analyses were performed as detailed in; STANDARDIZING MICROBIOME RESEARCH: INTERLABORATORY VALIDATION OF SOPS FOR SAMPLE PREPARATION AND DNA EXTRACTION FROM FOOD AND ENVIRONMENTAL ECOSYSTEMS | ENVIRONMENTAL MICROBIOME | SPRINGER NATURE LINK (Ferrocino et al., 2026).

Chapter 4. Discussion and Conclusion

The interlaboratory validation proved that high reproducibility and consistency of microbiome analyses of environmental matrices are guaranteed by the use of standardized SOPs (Cocolin et al., 2024). In both water and soil samples, microbial diversity, community composition, or taxonomic profile did not show a significant difference between research units. The accuracy and reliability of results was also ensured by the high MIQ values (>99%), which showed that there was little deviation in the expected microbial composition. These results indicate that SOP-based workflows can successfully minimize methodological variance and offer a solid structure of similar microbiome investigations in different laboratories (Ferrocino et al., 2025).

Section 2- PFAS-impacted Environmental Microbiomes

Chapter 1. General Introduction

1.1 Background and Context: PFAS Overview

1.1.1 Definition, Chemical Structure, and Classification

PFASs are defined as fluorinated substances that contain at least one fully fluorinated methyl or methylene carbon atom (without any H/Cl/Br/I atom attached to it)*, i.e., with a few noted exceptions, any chemical with at least a perfluorinated methyl group (−CF_3) or a perfluorinated methylene group (−CF_2−) is a PFAS*" (Wang et al., 2021). PFASs are also known as forever chemicals because of the outstanding strength of the carbon-fluorine (C-F) bond that provides high resistance to thermal, chemical, and biological degradation (Evich et al., 2022). Consequently, the compounds are found to be persistent in the environmental systems and have been observed over all levels of the earth with remote areas like the Arctic to high-populated areas.

Structurally, they have a carbon backbone with hydrogen atoms fully (perfluorinated) or partially (polyfluorinated) substituted by fluorine atoms. Substitution results in exceptional physicochemical characteristics, such as high polarity, hydrophobic-lipophobic interaction of the fluorinated chain, and high chemical inertness (Fernandez et al., 2016; Rahman et al., 2014). The simplified form of PFAS structure can be represented as: C_nF_{2n+1}–R, where n is the number of carbon atoms in the fluorinated chain, and R is a functional group that defines the reactivity of the compound and its interactions with the environment (Dias et al., 2024). This general structure is shown in Figure 1.

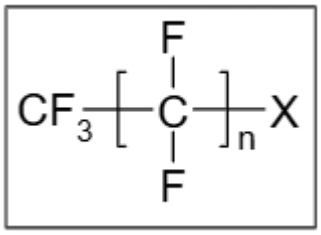

Figure 1. General structure of perfluorinated alkylated substances.

The fluorinated carbon chain is highly stable, and the terminal functional group controls solubility, charge, and the partitioning behavior. This twofold structural character leads to the amphiphilic properties, which allow PFAS to be used as a surface-active agent. These are the properties that make them so extensively used in industry and also make them exhibit convoluted behavior in the environment.

1.1.1.1 Functional Group Diversity

PFAS have a high chemical diversity because their functional head groups may be anionic, cationic, or neutral. Anionic groups are common, e.g. sulfonates ($–SO_3^-$), e.g. perfluorooctane sulfonate (PFOS), and carboxylates ($–COO^-$), e.g. perfluorooctanoic acid (PFOA). The other functional groups are phosphates, sulfonamides, alcohols, and quaternary ammonium moieties. These functional groups significantly affect environmental fate such as solubility, sorption, mobility, and bioavailability which tend to depend on pH (Alexander et al., 2008). As a result, structurally similar PFAS may have significantly different environmental behaviors. Besides terminal functionality, chain length variability and degree of fluorination also add to PFAS diversity.

Long-chain (e.g., PFCAs with $n \geq 7$ and PFSAs with $n \geq 6$) are typically more bio-accumulative and persistent, whereas short-chain analogues (($n \leq 6$) are more mobile but also environmentally stable (Kurwadkar et al., 2022; Yao et al., 2020)

1.1.1.2 Precursors and Transformation Potential

The significant feature of PFAS chemistry is the existence of precursors, especially polyfluoroalkyl substances. These are not entirely fluorinated compounds, which may be abiotically or biotically transformed into more stable perfluoroalkyl acids (PFAAs). An example of this is that fluorotelomer alcohols (FTOHs) can disintegrate to perfluoroalkyl carboxylic acid like PFOA, whereas sulfonamide-based compounds like PFOSA and N-ethyl perfluorooctane sulfonamidoethanol (N-EtFOSE) can be used as precursors of PFOS. Such transformation potential complicates environmental assessment, with precursor compounds potentially being a long-term source of persistent PFAS. In this respect, partially fluorinated telomer-based PFAS are of particular interest.

It is likely that they have a $–CH_2CH_2–$ spacing between the perfluorinated chain and the functional group, and their general formula is $F(CF_2)_n–CH_2CH_2–X$. They are mainly synthesized through telomerization, which leads to even numbered carbon atoms in the linear chains (Alexander et al., 2008).

1.1.1.3 Chemical Classification of PFAS

PFASs are a very diverse group of compounds, and over 4,700 separate substances have been identified, so far (US EPA, 2025). Depending on the structural features, they are broadly categorized into polymeric and non-polymeric PFAS (Harris et al., 2025; Z. Wang et al., 2017).

1. Polymeric PFAS

Polymeric PFAS are compounds of high molecular weight with long carbon backbones, which are fluorinated and include repeating units. These materials usually include over ten carbon atoms and are generally applied in industrial and commercial services that are highly stable and performant. Major categories include:

- **Fluoropolymers**, such as polytetrafluoroethylene (PTFE) and polyvinylidene fluoride (PVDF)
- **Side-chain fluorinated polymers**, including fluorinated polyurethanes
- **Perfluoropolyethers (PFPEs)**, these compounds are typically regarded as less bioavailable because of their high molecular weight but may cause environmental contamination by degradation or processing remnants (Itumoh et al., 2024).

2. Non-Polymeric PFAS

Non-polymeric PFAS are characteristically compounds of lower-molecular-weight and are more environmentally concerned because of their mobility and bioavailability. Both perfluoroalkyl and polyfluoroalkyl substances are found in this group (Williams et al., 2022)

i. Polyfluoroalkyl Substances (Fluorotelomers)

Polyfluoroalkyl compounds are partially fluorinated compounds where not all the hydrogen atoms on the carbon backbone are substituted by fluorine. The importance of these compounds lies in the fact that they may be converted into more recalcitrant perfluoroalkyl compounds.

Key groups include:

- Fluorotelomer alcohols (FTOHs)
- Fluorotelomer carboxylic acids (FTCAs)
- Fluorotelomer sulfonic acids (FTSAs)

ii. Perfluoroalkyl Substances

PFAS subgroups that are the most stable and persistent are perfluoroalkyl compounds that are completely fluorinated along the carbon chain. Among them is the perfluoroalkyl acids (PFAAs). These are acidic compounds that have functional groups bound to a perfluorinated carbon backbone and are commonly found in the environmental matrices (Harris et al., 2025a; Itumoh et al., 2024). Major subclasses include:

- Perfluoroalkyl carboxylic acids (PFCAs) and ether analogues (PFECAs)

- Perfluoroalkyl sulfonic acids (PFSAs)
- Perfluoroalkyl phosphonic acids (PFPAs)
- Perfluoroalkyl phosphinic acids (PFPiAs)

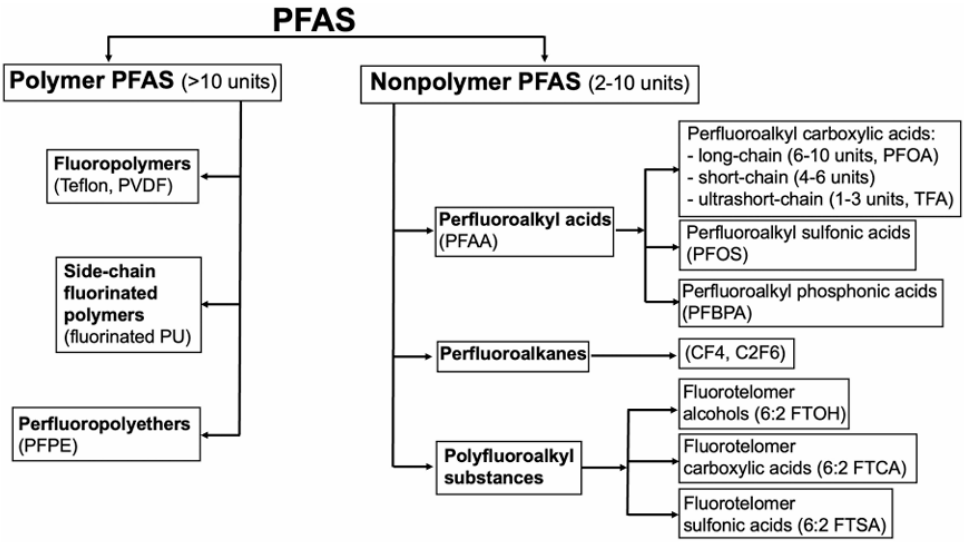

Figure 2. Classification of per- and polyfluoroalkyl substances (PFAS). Adapted from Thakur et al. (2025).

In general, the PFAS are structurally diverse and chemically complex compounds, the abundance of which in the environment is determined largely by the strength of the carbon-fluorine bond. Their transformation potential and their prevalence are the reasons behind this structural diversity which contributes to the increasing concern about their environmental and biological effects.

1.1.2 Physicochemical Properties and Environmental Behavior of PFAS

1.1.2.1 Chemical Structure and Bonding

The nature of the carbon fluorine (C-F) bond in the fluorinated carbon chain controls much of the physicochemical behavior of PFAS. The high electronegativity, high ionization potential, and low polarizability of fluorine are attributed to the difference in the electronic and intermolecular properties of fluorinated chains, compared with their hydrocarbon analogues. Consequently, the C–F bond is one of the strongest organic chemistry bonds, and bond dissociation energies are up to approximately ~531.5 kJ mol^{-1}, which is one of the reasons that makes PFAS exceptionally chemically and thermally stable (Krafft & Riess, 2015; Zhang et al., 2013; Zhou et al., 2013).

The high polarizing influence of fluorine causes C-F bonds to be highly polarized as well as the carbon backbone to be of extremely low polarizability. It does not simply boost the strength of the bonds but also affects intermolecular interactions differently to non-fluorinated compounds. Further replacement of hydrogen by fluorine also changes the electronic environment of the

neighboring functional groups. Specifically, the perfluoroalkyl chain has a strong inductive effect, as it makes the neighboring groups more acidic and the attached organic moieties less basic (Kirsch, 2006; Chambers, 2004).

Collectively, these bonding properties demonstrate the familiar recalcitrance of PFAS, which is largely resistant to hydrolysis, photolysis, oxidation, reduction, and biodegradation in the environment.

1.1.2.2 Surfactant Behavior

PFAS have comparatively high densities, generally between about 1.5 to more than 2.3 g cm^{-3}, depending on the molecular structure, molecular weight, and molecular orientation. Certain short-chain PFAS can be liquids at room temperature, and density variations compared to water can be relevant to subsurface transport, with the heavier liquid layers more likely to move downwards in groundwater systems. Their melting and boiling points are also very diverse and highly dependent on chain length and molecular complexity: short-chain PFAS tend to have lower melting (<0–100 °C) and boiling points (100–150 °C), long-chain and highly fluorinated compounds have very high melting points, even in the 200 °C range, and even higher boiling points, up to or above 300°C. These properties together determine the environmental phase behavior and mobility of PFAS (Naidu et al., 2025).

Substitution of hydrogen by fluorine has a significant effect on the surfactant behavior of these compounds. Perfluorinated surfactants, especially perfluorocarboxylic acid and per fluoroalkane sulfonic acids, are significantly more resistant to heat, chemicals, and acids and bases and are less affective by oxidants and reductants than hydrocarbon analogues, under which conditions conventional surfactants are more readily degraded (Moody & Field, 2000). Fluorine is also a strong electron-withdrawing agent that increases the acid strength of anionic PFAS. The molecules of PFAS are amphiphilic, which means that they are composed of a carbon chain containing fluorine and a polar head group that allows the molecules to be highly active on the surface and accumulate at interfaces including air-water and solid-water interfaces.

They are usually more interfacially active and lower critical micelle concentrations than hydrocarbon surfactants. Chain length has a powerful effect on environmental behavior; the long-chain PFAS have a stronger affinity to solid phase and have a higher bio correlation potential, whereas the short-chain PFAS are more soluble and mobile in water. Such a contrast is one of the reasons that explains the shift toward short-chain alternatives, despite the fact that they remain persistent and have improved mobility in water (Naidu et al., 2025).

1.1.2.3 Environmental Persistence

PFAS are able to survive in the environment due to their persistent nature, which is a direct result of their molecular stability. The carbon chain that is fluorinated is very difficult to chemically and

biologically transform and thus most of the PFAS, especially the perfluoroalkyl acids (PFAAs), tend to persist in the water, soil, sediment, and biota over extended periods. This continuity has significant implications for environmental exposure. PFAS may spread via ground water and surface water after release, and may build up in the environmental matrices, and still be detectable many years after the cessation of emissions. Consequently, the existing contamination patterns tend to be a combination of current input and past releases. The persistence of these compounds is further demonstrated by evidence of long biological half-lives in humans. Some of the PFAAs stay in the body of the human being over a period of years, which is an indication of limited elimination and prolonged exposure (Krafft & Riess, 2015; Z. Wang et al., 2017).

1.1.2.4 Bioaccumulation and Toxicokinetics

PFAS have a bioaccumulation behavior contrary to conventional hydrophobic organic contaminants. In the case of ionic PFAAs, the traditional indicators of octanol-water partition coefficients (KOW) and the standard fish bioconcentration factors fail to correctly describe the accumulation patterns because the compounds are protein-binding compounds, and not lipid-binding compounds. As an example, PFOA is generally relatively lowly bioconcentrated in fish because it is highly eliminated via the gills, which is attributed to its solubility in water. The opposite is true of humans, which eliminates it very slowly and can take several years. This stresses the significance of species-specific toxicokinetics.

This implies that PFAS bioaccumulation evaluation needs to be conducted on a wider level and entails trophic magnification information, field surveys, and chemical-specific toxicokinetic analyses. In this regard, bioaccumulation is not only the main factor of such long-term exposure, but also the persistent of PFAS in the environmental systems (Wang et al., 2017).

1.2 Sources, Uses and Emission Pathways

1.2.1 Primary Manufacturing and Industrial Sources

Mass production of these compounds started in the middle of the 20th century, with 3M and DuPont companies making them in large quantities. In the years 1970-2002, some 96,000 tons of Perfluorooctane sulfonyl fluoride (POSF), a major precursor of PFOS, were manufactured worldwide, of which it is estimated that 450-2,700 tones were discharged into the environment. Likewise, the total production of perfluoro carboxylates (PFCAs) including PFOA and other similar compounds across the globe has been estimated to be 4,400-8000 tones between 1951 to 2004 and the corresponding environmental emissions have been 470-900 tones (Kissa, 2001).

Electrochemical fluorination (ECF) and fluorotelomerization have been the two most common industrial processes used to produce PFAS. ECF forms mixtures of linear and branched isomers and was once used to produce legacy compounds like PFOS, making structurally complex products

that are hard to analyze environmentally and assess fate. Conversely, fluorotelomerization is a method that yields majorly linear PFAS structures, such as fluorotelomer-based products and the products of the reaction (Buck et al., 2011; Q. Wang et al., 2023). As a result of a growing regulatory burden on legacy PFAS, industry has turned to telomer based chemistries, such as their application in aqueous film-forming foams (AFFF). Nevertheless, they are structurally diverse compounds that are difficult to detect and monitor in environmental matrices (ITRC, 2026).

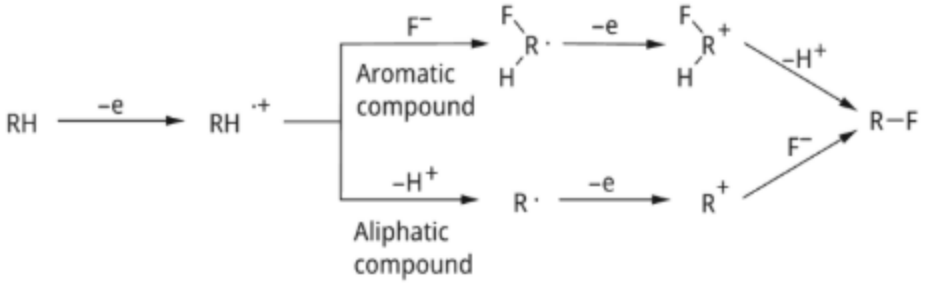

Figure 3. Electrochemical perfluorination: a general reaction mechanism. Adapted from Fuchigami & Inagi (2020).

Manufacturing and processing plants are the key contributors to environmental pollution as they emit PFAS into wastewater, air, solid waste, and accidental spills. Moreover, AFFF discharge in industrial locations and fire-training facilities is one of the major routes of environmental discharge. Released, PFAS may be carried by air and water, resulting in their accumulation in soils and aquatic environments as well as causing both local and regional contamination. Their ubiquitous industrial adoption and numerous emission pathways have led to the widespread and intractable footprint on the environment (Allinson et al., 2019; C. Fang et al., 2017; Gaines, 2023; Itumoh et al., 2024; Thakur et al., 2025; Moody & Field, 2000; Wang et al., 2014)

1.2.2 Consumer Products as Diffuse Sources

PFAS are also actively emitted by consumer products that are considered to be diffuse and continuous sources of contamination. PFAS are added to an extensive selection of materials to make them resistant to water, oil, heat, and stains. These are textiles, upholstery, non-stick cookware, food-contact materials, cosmetics, cleaning agents, and household products (Buck et al., 2011). Ther are emitted at low levels and uniformly over time as consumers use the products, wash them, abrade them, and dispose of them and the resultant products, causing widespread low-level emittance in both indoor and outdoor settings. It is estimated that more than 1,400 PFAS are used across over 200 applications, reflecting the scale and diversity of these diffuse sources.

Deliberately as well as unintentionally introduced PFAS, by-products, play a role in environmental release, making it difficult to determine the source (Curtzwiler et al., 2021; Dewapriya et al., 2023; Glüge et al., 2020). Consumer-produced PFAS can also enter the human environment via a variety

of routes, such as migration of food-contact materials into food, release of textiles during washing, and indoor dust accumulation. Treated fabrics and disposable hygienics are also found to be the possible sources of exposure especially indoors (De Silva et al., 2021; DeLuca et al., 2021; Schellenberger et al., 2022; Yang et al., 2025). Even though the individual contributions can be quite minor, their aggregate impact is a relatively consistent and underestimated source of PFAS contamination.

1.2.3 Waste Management and Secondary Sources

Waste management systems are important in redistribution of PFAS in the environment. PFAS are typically discarded in landfills, wastewater treatment systems, or incinerated; nevertheless, these measures typically do not lead to full degradation. Consequently, they become secondary sources that perpetuate and recycle contamination. PFAS-contaminated leachates produced by landfills may seep into adjacent soils and groundwater. PFAS are not readily removed by wastewater treatment plants (WWTPs), thereby releasing into surface waters where they accumulate in biosolids which are commonly used in fertile soil. However, incineration despite the disposal method could lead to incomplete destruction, and release of fluorinated by-products into air and ash remains (Mishra et al., 2025).

The sources of major waste are landfills, WWTPs, biosolid-amended soils and sites affected by the use of AFFF. These avenues lead to the contamination of PFAS in different compartments of the environment, such as soil, water, and air (Davis et al., 2007; Guelfo et al., 2021; Hunter Anderson et al., 2019; McGuire et al., 2014). The variety of these sources and their overlap complicate the process of identifying the source, especially when history has not been well documented.

1.2.4 Atmospheric Emissions and Long-range Transport

The distribution of PFAS across the globe is significantly influenced by atmospheric dynamics, especially when it comes to volatile/semi-volatile precursor compounds. Emission sources include industrial processes, use of products, disposal of waste, and volatilization of contaminated surfaces. When released, PFAS may be transported to distant locations in the atmosphere and deposited well beyond their sources (Prevedouros et al., 2006; Z. Wang et al., 2014). Direct and indirect pathways contribute to atmospheric inputs. Direct sources entail the emission of terminal PFAS whereas indirect include precursors like fluorotelomer alcohols and sulfonamides which can be oxidized in the atmosphere to produce persistent perfluoroalkyl acids (Ellis et al., 2004; Yarwood et al., 2007).

These processes of transformation successfully produce delayed secondary sources of PFAS in remote settings. PFAS has been found in the precipitation, which demonstrates that wet deposition is one of the main pathways of transferring PFAS between the atmosphere and terrestrial and aquatic systems (Dreyer et al., 2010). In general, the synergistic actions of industrial emissions,

diffuse consumer sources, redistribution through waste, and atmospheric transport cause permanent and extensive PFAS contamination at local and global levels.

1.3 Environmental Distribution of PFAS

1.3.1 Occurrence in Aquatic Systems (Surface Water and Groundwater)

PFAS are extensively found in water bodies, such as rivers, lakes, coastal waters, and groundwater systems. Their presence is an indicator of the constant contributions of point sources, including industrial discharges and wastewater treatment plants (WWTPs), as well as diffuse pathways, such as atmospheric deposition and leaching of contaminated soils and consumer products. Traditional wastewater treatment methods are not usually efficient to eliminate PFAS, and they may be released into water bodies (Rahman et al., 2014). Another characteristic of PFAS in water pollution is the existence of precursors. Fluorotelomer alcohols and sulfonamides are neutral and semi-volatile precursors that can be transformed into persistent perfluoroalkyl acids (PFAAs), so they serve as delayed secondary sources of contamination (Ahrens & Bundschuh, 2014; Ellis et al., 2004).

This contributes to the phenomenon of PFAS in regions without an apparent source of direct emissions. PFAS concentrations in surface water and groundwater are usually in the range of pg L^{-1} to ng L^{-1}, however, much higher concentrations have been detected near industrial facilities and those affected by aqueous film-forming foams (AFFF) (Ahrens et al., 2010; Möller et al., 2010; Rahman et al., 2014; Technology Solutions, 2006). Groundwater contamination is a significant threat to the drinking water supply. Recent surveillance research shows that short-chain homologues and precursor compounds are more mobile and persistent in water systems (Hu et al., 2016).

1.3.2 Distribution in Soils and Sediments

Soils and sediments are significant environmental reservoirs because they have the ability to hold the compounds over a long duration. PFAS sorption is regulated by a mixture of hydrophobic and electrostatic forces between them due to their amphiphilic structure. Organic carbon content exerts a leading role in increasing the retention of PFAS, whereas solution chemistry (pH and ionic strength) also has additional effects on sorption (Higgins & Luthy, 2006). Chain length has a strong influence on partitioning behavior: long-chain PFAS have a higher propensity to be sorbed to soils and sediments and are likely to be found at the surface, whereas short-chain are more mobile and are frequently found at deeper depths (Abou-Khalil et al., 2022; Han et al., 2025; Mussabek et al., 2020; Sharp et al., 2021).

Sediments, in particular, not only serve as sinks but also as secondary sources, and they release PFAS into the surrounding water by the processes of desorption and maintain long-term

contamination (Brusseau et al., 2020; Cao et al., 2019; Pan et al., 2015). PFAS gets into soils through industrial emissions, AFFF application, landfill leachates, and land application of biosolids, whereas the minor contributors are atmospheric deposition and irrigation with contaminated water (Mussabek et al., 2020; Sharp et al., 2021). Other hot spots include firefighting training grounds, where it can be decades, leading to persistent plumes of groundwater and environmental exposure (Guelfo & Higgins, 2013; Ruyle et al., 2023).

1.3.3 Occurrence in Biota

PFAS is commonly found in aquatic and terrestrial organisms, which indicates its persistence and food web transferability. PFAS selectively attach to proteins and phospholipids resulting in deposition in other tissues like blood and liver instead of fat tissue (Kelly et al., 2009). The presence in food-webs has shown that some PFAS, specifically, the PFOS and long-chain perfluoro carboxylic acids, have the ability to bio magnify between trophic levels which is observed in freshwater and marine food webs (Fang et al., 2014; Ren et al., 2022). Recent data indicate that the contamination of aquatic environments can extend into terrestrial food webs through pathways such as via emergent insects (Hedgespeth et al., 2023).

PFAS may also find its way into the soil-plant food chains. Crops absorb it, especially short-chain PFAS, which is of concern to food intake in humans and demonstrates the interdependence of the environmental compartments (Han et al., 2025).

1.3.4 Global Transport and Remote Regions

Remote areas like the arctic and high alpine areas are also a significant receptor area to PFAS since they are highly connected to the lower-latitude source areas. Their pollution is primarily associated with long-range atmospheric and oceanic transportation, as opposed to local sources. Global distillation, cold condensation, repeated cycles of volatilization, and deposition are some of the processes that facilitate the build-up of persistent compounds in cold conditions. PFAS can be long-lived once deposited; the residence time in the Arctic Ocean has been estimated to be 12.5 ± 3.3 years (Macdonald et al., 2000).

Another source of global redistribution is ocean circulation. Basin-scale gradients in perfluoroalkyl acids in open oceans have been observed in surveys of these substances, with the levels of PFOS and PFOA typically being higher in the North Atlantic than in the South Pacific and Indian Oceans, indicating large-scale transport due to ocean circulation. The profiles that are depth-dependent also indicate that PFAS can act as water-mass movement tracers to the thermohaline circulation of the world (Yamashita et al., 2008).

PFAS deposition has also been identified in arctic ice cores as evidence of long-term deposition, which is also linked to atmospheric conversion of volatile precursors, including fluorotelomer alcohols, to short chain perfluoroalkyl acids, and subsequent wet and dry deposition (Hartz et al.,

2023; X. Wang et al., 2019). The same tendencies have been reported in the alpine areas; e.g., the snow cores in the Tibetan Plateau were found to have PFOS and PFOA in concentrations of 61.4–336 pg L^{-1} and 40.8–243 pg L^{-1}, respectively, which point to atmospheric transport as a significant route (Wang et al., 2014).

In addition to such distant environments, United States is another example of the extensive occurrence of PFAS in different environments. The PFAS Project Lab has developed data that has identified over 2,000 contaminated sites in the country including sites related to industry, military bases, airports, and wastewater treatment facilities (PFAS Project Lab, 2024).

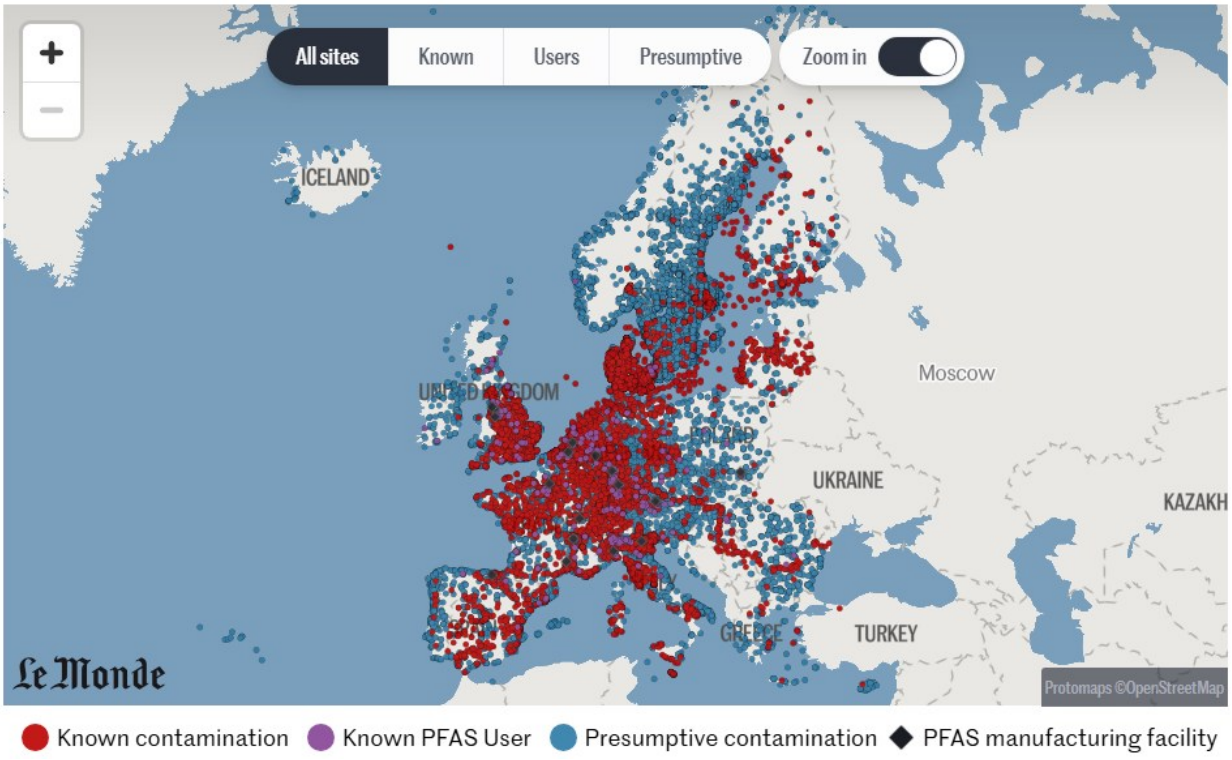

Figure 4. Graphical representation of the global PFASs contamination. In red are reported the known contaminated spots, in purple the known PFASs user, in blue PFASs contaminated spots yet to be confirmed and in black PFAS manufacturing facilities. Adapted from PFAS Data Hub, 2024.

1.3.5 European Distribution Patterns

Monitoring studies in Europe have shown the prevalence of PFAS in marine, freshwater and terrestrial habitats and that the patterns of contamination are closely associated with human activities. It is estimated that there are around 100,000 possible PFAS emission locations in Europe, which reflects the magnitude and intricacy of contamination (EEA, 2019). The presence of spatial gradients has been found in large-scale studies in European seas, such as the North Sea, Baltic Sea, and Norwegian Sea, with increased concentrations in coastal waters,

and decreased concentrations in remote waters. The patterns are a product of the combined effect of riverine contributions, oceanic transport, and closeness to sources of emissions (Ahrens, Gerwinski, et al., 2010).

The scope of contamination, including tens of thousands of contaminated or potentially contaminated locations in Europe, has been further highlighted in recent projects like the Forever Pollution Project and the PFAS Data Hub, indicating that the issue is probably underreported (Cordner et al., 2024; PFAS Data Hub, 2024). Localized case studies also indicate the intensity of contamination. As a case in point, in the 3M plant in Zwijndrecht (Belgium), long-term industrial activity led to the very high levels of PFOS in soils and groundwater, necessitating massive cleaning work.

1.3.6 PFAS Contamination in Italy

In the European context, Italy is one of the most widely documented cases of PFAS contamination. The existence of PFOS, PFOA, PFHxS, and PFBS has been reported in the monitoring studies in different water bodies. It is worth noting that the PFBS concentrations in the Po River delta were 16-21 times more than the PFOS, and the trend shifted towards the use of the short-chain PFAS substitutes (Aminot et al., 2019). PFAS contamination has been also seen in agricultural systems, where biosolids, a byproduct of wastewater treatment, have been found to contribute to soil contamination with a range of 28 to 637 ng g^{-1} (Higgins & Luthy, 2006; Lindstrom et al., 2011; Sun et al., 2011). Decades of fluorochemical manufacture (at a chemical plant in Trissino) in the Veneto region of northern Italy resulted in widespread PFAS pollution found in 2013 affecting an estimated 3,000–3,600 km² area (Giglioli et al., 2023).

Along with the contamination of groundwater, industrial discharges have also affected soils and sediments of the Bacchiglione / Agno River systems. Groundwater flow and basin-level transport processes have a significant impact on the distribution of PFAS in this area and lead to contamination over long distances relative to the location of the initial source of emissions (Schiavo et al., 2025). The fact that PFAS can be transferred to biological systems further underscores their relevance in the environment. It has been reported in freshwater organisms, such as fish in Alpine and subalpine lakes, and the accumulation varies according to anthropogenic contributions, as well as environmental influences (Valsecchi et al., 2021). Likewise, selective bioaccumulation of PFOS has been found in organisms like mussels in European coastal settings, despite other PFAS prevailing in adjacent waters (e.g., PFBS) (Aminot et al., 2019).

In general, the European evidence, along with the case study of Italy and the Trissino hotspot of contamination, reveals that the distribution of PFAS is extremely heterogeneous.

1.3.7 Regulatory Monitoring Data

PFAS persistence and health hazards have escalated regulatory surveillance of PFAS at the European and international levels. In the European Union, the recast Drinking Water Directive (DWD; Directive (EU) 2020/2184) sets the harmonized drinking water PFAS standards. The directive has two parameters: the Sum of PFAS (20 chosen compounds) and the Total PFAS with parametric values of 0.10 µg L^{-1} and 0.50 µg L^{-1} respectively. These limits will be compulsory by January 2026 in Member States (European Commission, 2026).

The European Food Safety Authority (EFSA) has taken a cumulative exposure approach and has set a tolerable weekly intake (TWI) of four major PFAS (PFOA, PFOS, PFNA and PFHxS) at 4.4 ng kg^{-1} of body weight. This is an indication of concern about combined exposure, especially among the vulnerable population like children. The World Health Organization (WHO) advocates precautionary management by the "As Low As Reasonably Achievable" (ALARA) principle at the international level. Nevertheless, these initiatives have not yet resulted in the desired outcomes, as the data provided by the European Environment Agency (EEA) show that the levels of PFOS and PFOA are often above the ecological quality thresholds in surface waters (EEA, 2024).

The case of Italy can illustrate the current regulatory issues. After the introduction of the DWD into law (Legislative Decree 18/2023), tracking programmes have revealed the contamination outside of the industrial regions that were previously identified. PFAS groundwater concentrations in the Veneto region are still high above the regulatory levels despite efforts to manage the situation using granular activated carbon (GAC) filtration. Moreover, surveillance in the Piedmont area, especially around the Spinetta Marengo industrial facility, has shown that there are new compounds emerging including C_6O_4. Recent biomonitoring results also highlight persistent exposure, and about 9 % of the local population has serum PFAS concentrations exceeding health-based reference values (Randazzo et al., 2025; Regione Piemonte, 2025).

1.4 Toxicity of PFAS

1.4.1 Environmental (Ecotoxicological) Effects

Exposure to PFAS has been associated with decreased survival, slowed growth and development, oxidative stress, neurotoxicity, and reproductive dysfunction, especially in invertebrates, plankton, and microorganisms (Ma et al., 2022; Nayak et al., 2023). Primary producers are particularly vulnerable. Phytoplankton species, including *Daphnia magna,* have been extensively used to determine PFAS toxicity. They experience reduced reproduction, growth, and photosynthetic activity, which could disrupt primary production and energy flow within aquatic ecosystems. On the microbial level, exposure to PFAS has been linked to oxidative stress, membrane damage, and metabolic changes, indicating effects on the ecosystem functioning (Ma et al., 2022).

They may also change the soil microbial communities, including abundance, diversity, and metabolic activity, with many more tolerant taxa, such as Proteobacteria, increasing, and overall

microbial activity decreases (Senevirathna et al., 2022a; Wu et al., 2023; Xu et al., 2022). These changes can potentially affect the nutrient circulation and organic matter decomposition. PFAS exposure in terrestrial systems has caused negative impacts on the soil invertebrates, including reduced survival, growth, and reproduction (Houde et al., 2011a; Zhang et al., 2025).

1.4.2 Bioaccumulation and Trophic Transfer

A defining characteristic of PFAS is their ability to bioaccumulate and transfer across food webs. Unlike traditional hydrophobic contaminants, PFAS are selective to bind proteins and phospholipids but not lipids, thus accumulating mainly in tissues that are rich in proteins like liver and blood (Kelly et al., 2009). Some PFAS, especially PFOS and long-chain perfluoro carboxylic acids have been found to bio magnify throughout trophic levels in freshwater and marine systems. Dietary exposure and low elimination rates contribute greatly to accumulation, particularly in long-lived organisms like marine mammals (S. Fang et al., 2014; Kelly et al., 2009; Ren et al., 2022).

The PFAS transfer is also across the ecosystem boundaries. Aquatic insects may serve as vectors, moving PFAS between aquatic and terrestrial food webs and exposing terrestrial predators (Hedgespeth et al., 2023; Kotalik et al., 2025). Soil-plant pathways also play a role in terrestrial systems in terms of trophic transfer, especially those of short-chain PFAS, which are more mobile and easily absorbed by plants (Han et al., 2025). All these interrelated pathways raise the likelihood of ecological and human exposure.

1.4.3 Human Health Effects

Humans are exposed to PFAS via a variety of routes, such as contaminated drinking water, food, inhalation of indoor dust, and contact with consumer products. Among them, the primary exposure pathways of the general population include drinking water and consuming food, especially fish and animal products (Domingo & Nadal, 2017; Houde et al., 2011b). Their high affinity to proteins and metabolic resistance results in long biological half-lives of many PFAS, which means that some are accumulated internally over time (EFSA, 2020; ATSDR, 2021).

One of the most reproducible effects is immunotoxicity and studies have associated PFAS exposure, particularly PFOA and PFOS, with decreased vaccine response and increased susceptibility to infections, especially in children. These results are the basis of the modern methods of risk assessment, such as the introduction of a group of Tolerable Weekly Intake (TWI) of the group once a week by EFSA, regarding immune-related endpoints (EFSA, 2020).

PFAS are also considered endocrine-disrupting chemicals, with reported associations to altered thyroid hormone levels, disrupted lipid metabolism, and effects on reproductive hormones, which are probably mediated by interactions with nuclear receptors and hormone transport systems (ATSDR, 2021; EFSA, 2020; Sunderland et al., 2019).

Carcinogenicity of some of the PFAS has also been assessed. PFOA is categorized as carcinogenic to humans and PFOS is possibly carcinogenic with experimental and mechanistic evidence (IARC, 2023; NASEM, 2024). It has been reported to be associated with liver and breast cancer although there are uncertainties (ATSDR, 2021). Moreover, there is concern about the developmental and reproductive effects, where maternal exposure is associated with less fetal growth, low birth weight, and poor pregnancy outcomes. Exposure during the early life could be due to placental transfer and breastfeeding (Gao et al., 2019; Manzano-Salgado et al., 2015; Zheng et al., 2021).

In general, the effects of PFAS exposure on health have a wide spectrum of negative outcomes related to various physiological systems. Their perseverance and prevalence support their significance to be a global health concern.

1.5 PFAS Remediation Approaches: Current State of Knowledge

PFAS pose a significant dilemma in remediation because of their extreme persistence, water mobility, and their ability to resist natural attenuation. The potency of the carbon fluorine (C–F) bond restricts the efficiency of conventional treatment techniques normally applied to the removal of organic contaminants. Consequently, the majority of the existing methods are based on either physical separation or energy-demanding destructive reactions, both of which are highly constrained both technically and practically (Renella et al., 2025; Tshangana et al., 2025).

1.5.1 Conventional Remediation Technologies

1.5.1.1 Adsorption and Ion Exchange

PFAS removal in contaminated water is commonly achieved with adsorption-based technologies, specifically with granular activated carbon (GAC), it works depending on hydrophobic interactions and van der Waals forces to a great extent, which prefer retention of PFAS in the porous carbon matrix. GAC tends to be more efficient with long-chain PFAS than short-chain counterparts (Tshangana et al., 2025).

Ion exchange (IX) resins have been developed to enhance removal efficiency, especially of anionic PFAS. These materials usually include quaternary ammonium functional groups which facilitate electrostatic attraction as well as hydrophobic partitioning. IX resins in most instances have a greater sorption capacity compared to GAC, particularly when it comes to sulfonated PFAS like PFOS and PFHxS (Milinovic et al., 2015; Nkin, 2025).

1.5.1.2 Membrane Based Separation

Nanofiltration (NF) and reverse osmosis (RO) are considered to be among the best membrane technologies as physical barriers. Their separation principle is founded on both the size exclusion and electrostatic repulsion, which can frequently result in rejection rates of more than 99% of both legacy and emerging PFAS, as well as short-chain (Tshangana et al., 2025).

1.5.1.3 Thermal and Destructive Approaches

In contaminated solids, PFAS can be volatilized by thermal desorption, usually in the range of 350 to 550°C, then the volatilized compounds should be collected and treated. Total destruction is usually achieved by high-temperature above 1,100 °C in order to be effective in breaking the C-F bond (Aggelopoulos, 2026; Renella et al., 2025).

1.5.2 Limitations of Conventional Remediation Approaches

Although these technologies have become very common, traditional remediation technologies have a number of serious limitations.

To begin with, most methods are non-destructive and are phase-transfer processes and produce secondary waste streams such as spent sorbents or concentrated brines, which also need to be treated with further energy-intensive incineration (Renella et al., 2025; Tshangana et al., 2025).

Second, short-chain PFAS and precursor compounds are less easily handled by these technologies and are more mobile than other pollutants, further developing into persistent end-products in the environment (Nkin, 2025; Renella et al., 2025)

Third, the operation of advanced destructive technologies is still economically and energetically intensive, which restricts the applicability to a large scale, especially to dilute environmental matrices such as groundwater and sediments (Aggelopoulos, 2026; Olawade et al., 2025).

1.5.3 Toward Biological Alternatives

The shortcomings of traditional remediation have generated the interest of biological methods as supplementary measures to deal with PFAS. Biological systems can be used under relatively mild conditions unlike physical or thermal treatments and can provide lower-energy, more sustainable long-term treatment. At present, however, PFAS bioremediation remains an emerging field rather than an established solution. The primary focus of bioremediation is not the demonstration of the large-scale destruction of all PFAS as the complete mineralization of heavily fluorinated substances is exceptionally challenging. Instead, it has a potential in the transformation of the chosen PFAS precursors, alteration of PFAS speciation, and the potential of decreasing the mobility of contaminants or long-term risk at environmentally relevant conditions (Olawade et al., 2025).

This has shifted focus to microbial processes which could lead to PFAS transformation, especially in polluted soils, sediments, and wastewater related systems. Accordingly, recent research has increasingly focused on the role of microorganisms not only as passive recipients of contamination but also as potential contributors to PFAS transformation and environmental response. This perspective provides the basis for examining PFAS–microbe interactions in greater detail.

1.6 PFAS and Microbes

1.6.1 Microbial Responses to PFAS Contamination

PFAS when exposed to the environment has the potential to cause selective pressure on microbial communities, which results in structural and functional shifts. A number of studies have reported changes in microbial communities in polluted soils, sediments, and wastewater systems, which are usually marked by the increase in taxa that are more resistant to chemical stress. *Proteobacteria* and other group members have often been found to rise in relative abundance during PFAS exposure, which is associated with adaptive responses related to membrane reorganization, efflux systems, or stress signaling (Senevirathna et al., 2022a; E. Wu et al., 2023; Xu et al., 2022).

Microbial activity may also be affected with PFAS exposure. There are experimental studies that have revealed a decrease in microbial biomass, change in the activity of enzymes, and interference with the metabolic processes especially at the higher contaminant concentration. These impacts are different and depend on the type of PFAS, level, duration of exposure, and environmental factors. Some microbial communities seem to be suppressed, but others survive or even grow, which suggests that the PFAS contamination does not suppress microbial communities, but it alters them (Senevirathna et al., 2022a; J. Zhang et al., 2025).

These findings suggest that PFAS contaminated environments are still biologically active environments where microbial communities persist in operating under chemically altered conditions.

1.6.2 Microbial Transformation of PFAS

Direct microbial degradation of PFAS has little evidence and is mostly restricted to specific compounds and in controlled experimental conditions. The majority of reported interactions between microbes are during co-metabolic interactions, where transformation happens when microbes grow on other substrates and not through direct exploitation of PFAS as a carbohydrate or energy source (Liu & Mejia Avendaño, 2013; Shahsavari et al., 2021).

Polyfluorinated precursor compounds are generally more susceptible to microbial transformation than fully fluorinated perfluoroalkyl acids. In contrast, terminal PFAS such as PFOA and PFOS show strong resistance to biological breakdown under environmentally relevant conditions. Although both aerobic and anaerobic systems have been shown to support transformation processes, these interactions typically involve partial modification rather than complete

degradation. Reports of microbial defluorination remain limited and are associated with specific compounds and controlled conditions, indicating that cleavage of the carbon–fluorine bond is not a widespread microbial capability (Che et al., 2021; Yu et al., 2022).

Overall, microbial processes tend to result in transformation or redistribution of PFAS rather than mineralization, often leading to the persistence of stable end-products.

1.6.3 Key Microbial Taxa in PFAS-Impacted Environments

Most reported microbial responses involve physiological adaptation and interaction with PFAS precursors rather than complete degradation, and current evidence is largely correlative. The microbial genera summarized below represents taxa most frequently reported in PFAS-contaminated environments, along with their proposed adaptive or functional traits.

Table 3. This table summarizes representative microorganisms, plants, and algae for which experimental evidence of PFAS interaction has been reported, including uptake, tolerance, or transformation of PFAS or PFAS precursors under laboratory conditions. The listed examples are not exhaustive and are intended to highlight well-documented cases discussed in the primary literature. More comprehensive and extended compilations of PFAS-associated biological systems, including emerging and indirect evidence, are available in recent critical reviews of PFAS bioremediation strategies (Bhattacharya et al., 2025; Shahid & Shafi, 2026).

Biological system	Representative organism(s)	PFAS / precursor studied	Reported outcome	Key reference(s)
Bacteria (iron-reducing / anaerobic)	*Acidimicrobium* sp. A6	PFOA, PFOS	Reported transformation and fluoride release under Feammox conditions (contested)	(S. Huang et al., 2024; S. Huang & Jaffe, 2019; Ruiz-Urigüen et al., 2022)
	Dehalococcoides spp.	PFMeUPA, 6:2 FTUCA	Reductive transformation of unsaturated PFAS under anaerobic conditions	(Yu et al., 2020, 2022)
Bacteria (aerobic heterotrophs)	*Labrys portucalensis* F11	PFOS, 6:2 FTS, 5:3 FTCA	Co-metabolic transformation under aerobic conditions	(Wijayahena et al., 2025)
	Pseudomonas spp. (*oleovorans*, *butanovora*, *fluorescens* DSM 8341)	6:2–8:2 FTOH	Aerobic oxidation of fluorotelomer alcohols	(M. H. Kim et al., 2012, 2014)
	Dietzia aurantiaca J3	6:2 FTSA	Transformation of PFAS precursor	(Méndez et al., 2022)
	Gordonia sp. NB4-1Y	6:2 FTAB, 6:2 FTSA	Aerobic transformation of PFAS precursors	(Shaw et al., 2019)
Bacteria (tolerance / interaction studies)	*Pseudomonas parafulva* YAB1	PFOA	Uptake and partial removal under laboratory conditions	(Mudumbi et al., 2014)
	Pseudomonas aeruginosa HJ4	PFOS	Reduction in aqueous PFOS concentration; no confirmed defluorination	(Kwon et al., 2014)
	Pseudomonas plecoglossicida 2.4-D	PFOS	Physiological response and stress tolerance; no mineralization	(Chetverikov et al., 2017)

Fungi (white-rot / ligninolytic)	*Pleurotus ostreatus*	PFOA	Uptake and partial transformation	(Luo et al., 2015)
	Phanerochaete chrysosporium	8:2 FTOH	Transformation of fluorotelomer alcohol	(Tseng et al., 2014)
	Gloeophyllum trabeum, *Trametes versicolor*	6:2 FTOH	Fungal-mediated precursor transformation	(Merino et al., 2018)
Plants (phytoremediation)	*Eichhornia crassipes*, *Xanthium strumarium*, *Polygonum salicifolium*	PFOA	Uptake and accumulation in plant tissues	(Mudumbi et al., 2014)
Algae	*Chlorella sorokiniana*	PFOA	Uptake and physiological stress response	(Bah Abbas, 2022)
	Chlorella vulgaris, *Scenedesmus obliquus*	PFOA, PFOS	Bioaccumulation and tolerance	(Mojiri et al., 2023)

1.6.4 Mechanisms Involved in PFAS Transformation

The transformation mechanisms that regulate the interaction between microorganisms and PFAS are based on molecular structure, environmental conditions, and metabolic context. Most of the reported processes do not entirely mineralize but transform partially, typically mediated by co-metabolic processes. Below, these mechanisms are described regarding dominating reaction pathways and related enzymatic activities.

1.6.4.1 Aerobic Oxidation of Fluorotelomer Alcohols (FTOHs)

PFAS-related compounds that have been the most frequently reported to be transformed by microbes under aerobic conditions include fluorotelomer alcohols (FTOHs). The oxidation of non-fluorinated alcohol moiety is usually the initial step in transformation, which is usually linked to oxygenase activity.

The result of this process is the formation of sequentially fluorotelomer aldehydes (FTAL), fluorotelomer carboxylic acids (FTCA), and fluorotelomer unsaturated carboxylic acids (FTUCA). These intermediates can take various pathways of transformation, leading to the x:3 acids and in certain systems, to terminal perfluoroalkyl carboxylates (PFCAs). These are mostly co-metabolic pathways that do not directly utilize PFAS as growth substrates (Kim et al., 2012).

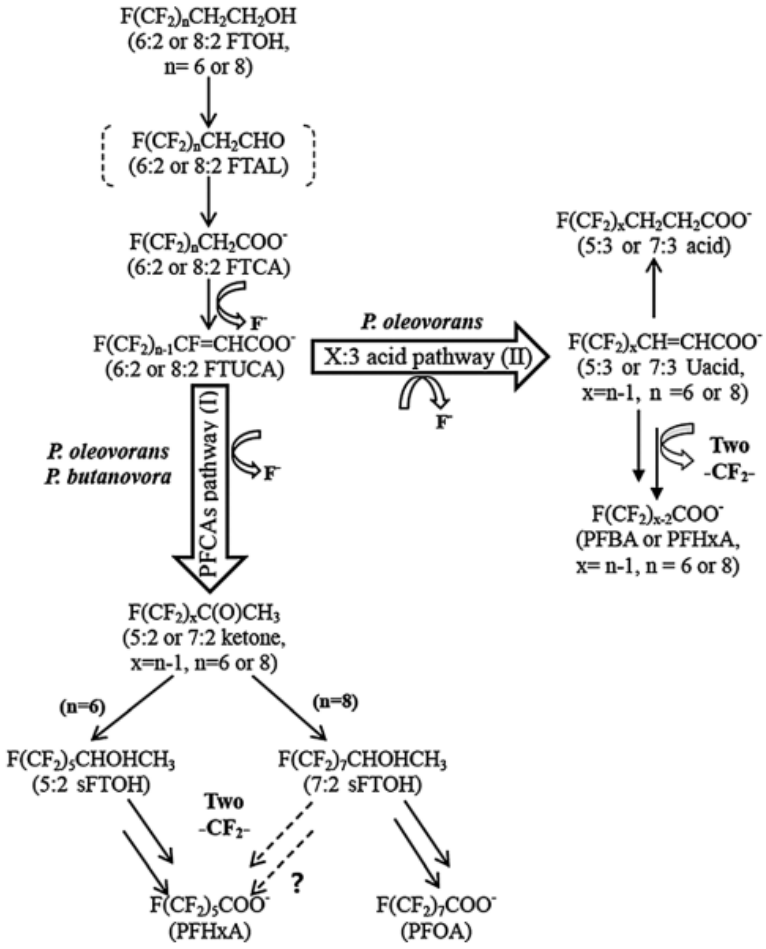

Figure 5. Proposed aerobic biotransformation pathways of 6:2 and 8:2 fluorotelomer alcohols (FTOHs) by Pseudomonas oleovorans and Pseudomonas butanovora. The schematic illustrates two co-metabolic transformation routes. Pathway I predominantly result in the formation of terminal perfluoroalkyl carboxylic acids (PFCAs), whereas Pathway II leads primarily to x:3 acids (5:3 or 7:3 acids) with minor production of shorter-chain PFCAs. P. oleovorans were observed to utilize both pathways, while P. butanovora predominantly followed Pathway I. Adapted from Kim et al. (2012).

1.6.4.2 Anaerobic Biotransformation of Fluorotelomer Compounds

In anaerobic conditions, the transformation of PFAS is typically less extensive and follows the route of altering the non-fluorinated part of the molecule. Methanogenic sludge systems have demonstrated that intermediates including FTAL, FTCA, and FTUCA can be converted to FTOHs, with x:3 acids generally depicting the most prevalent transformation products. Compared to aerobic systems, terminal PFCAs are typically insignificant, and minimal to no fluoride emission is noted. These results point to the fact that anaerobic transformation is more associated with functional group modification than breakage of carbon–fluorine bonds (Zhang et al. 2013).

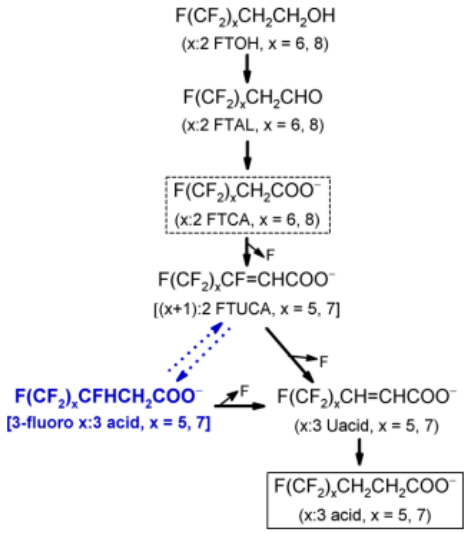

Figure 6. Anaerobic biotransformation pathways of 6:2 and 8:2 fluorotelomer alcohols (FTOHs) in digester sludge under methanogenic conditions. Polyfluorinated acids are shown in deprotonated form, consistent with the slightly alkaline conditions of anaerobic digesters. Dashed boxes indicate major intermediate products, while solid boxes represent the dominant stable transformation of products. Adapted from Zhang et al., (2013).

1.6.4.3 Reductive Defluorination of Unsaturated PFAS

Direct cleavage of the carbon–fluorine bond has been reported only in limited cases and is largely restricted to specific unsaturated PFAS compounds. In these systems, the presence of carbon–carbon double bonds appear to increase susceptibility to microbial attack.

Experimental studies using anaerobic enrichment cultures have demonstrated that certain compounds can undergo reductive defluorination, resulting in fluoride release and the formation of partially defluorinated intermediates. These reactions are typically selective and structure-dependent and have not been demonstrated for fully fluorinated compounds such as PFOA or PFOS (Yu et al., 2022).

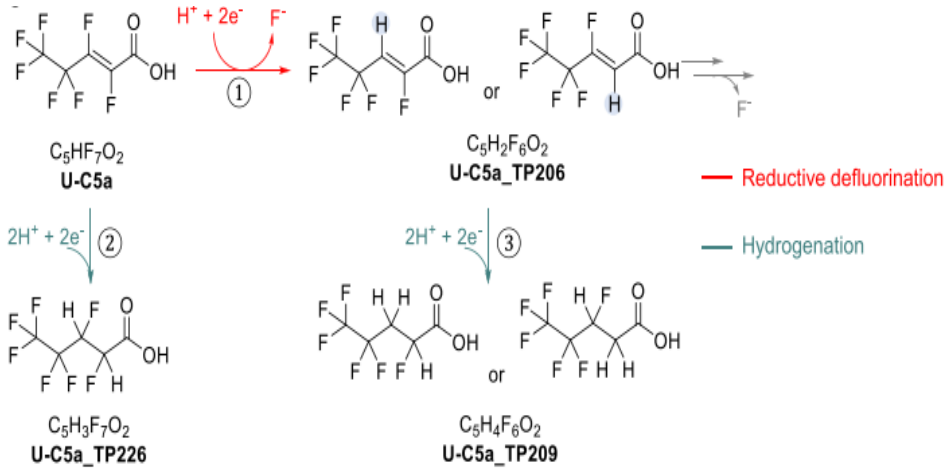

Figure 7. Proposed anaerobic biotransformation pathways of U-C5a. The scheme illustrates sequential reductive reactions leading to the transformation of U-C5a through a combination of reductive defluorination and hydrogenation steps under anaerobic conditions. Red arrows indicate reductive defluorination reactions associated with fluoride release. Adapted from Yu et al. (2022).

1.6.4.4 Enzymatic Involvement in PFAS Transformation

Although several transformation pathways have been described, the enzymatic basis of PFAS transformation remains only partially understood. Most reported processes are associated with non-specific enzymes involved in xenobiotic metabolism rather than dedicated PFAS-degrading systems.

Fluoroacetate dehalogenases: Fluoroacetate dehalogenases are among the few enzymes capable of cleaving carbon–fluorine bonds, but their activity is largely restricted to short-chain substrates and decreases with increasing fluorination (Berhanu et al., 2023; Wackett, 2022).

Oxygenases and co-metabolic oxidation: Oxygenases, particularly monooxygenases, play a central role in the aerobic transformation of PFAS precursors by initiating oxidation of non-fluorinated functional groups (Kim et al., 2012, 2014; Liu & Mejia Avendaño, 2013).

Extracellular oxidative enzymes: Fungal enzymes such as laccases and peroxidases have been investigated for their potential to induce partial PFAS transformation through oxidative mechanisms, although their effectiveness remains variable (Colosi et al., 2009; Cranwill, 2022; Luo et al., 2015).

Feammox-associated processes: Feammox-related processes, linking ammonium oxidation to Fe(III) reduction under anoxic and mildly acidic conditions, have been proposed as a potential framework for PFAS defluorination in *Acidimicrobium* sp. A6. While fluoride release and shorter-chain PFAS products have been observed in Feammox-enriched systems, the enzymatic basis of

these reactions remains unresolved, and the relative contributions of biological and abiotic mechanisms continue to be investigated (S. Huang & Jaffe, 2019; Jaffé et al., 2024).

Comprehensively, existing evidence suggests that microbial relationships with PFAS are predominantly restrained to partial transformation mechanisms, frequently including precursor molecules and co-metabolic routes, as opposed to full mineralization. Although strain-level systems have given significant information about these mechanisms, they are oversimplified systems that do not represent the complexity of the environment. In the natural environments, microorganisms operate in interdependent communities, with metabolic processes spread across a variety of taxa. This underscores the need to think of microbiomes as systems when analyzing PFAS behavior in the environment.

1.7 Microbiomes as Functional Systems in PFAS-Impacted Environments

The microorganisms in the natural environment rarely act as single organisms; instead, they occur as structured and interacting communities within certain physicochemical conditions. In this broader sense, the microbiome encompasses not only the microorganisms themselves but also their collective genetic potential (Berg et al., 2020; Marchesi & Ravel, 2015). The definition is especially applicable to environmental systems, where interactions between multiple taxa give rise to microbial processes.

In contaminated environments, community composition, metabolic diversity, and interspecies relations collectively affect the fate of contaminants. Although strain-based studies have been useful in determining particular transformation pathways or tolerance characteristics, they only provide a small percentage of the biological heterogeneity evident in soils, sediments, and other environmental matrices. A community level framework is needed to better understand the way microbial systems react to PFAS contamination and the distribution of functional roles among taxa (Berg et al., 2020; Shahsavari et al., 2021).

1.7.1 From Single Organisms to Community-Level Processes

Microbial interactions with PFAS have been extensively studied in pure cultures or enriched isolates. Controlled studies on tolerance, uptake, and limited transformation processes are useful. Nevertheless, they are not indicative of the ecological structure of natural communities in which functions are shared among multiple organisms and that emerge as a result of metabolic cooperation, competition, and succession. It is a fact that strain-level measurements are not sufficient to predict how behaviors will be in the context of complex microbial systems (Marchesi & Ravel, 2015; Shahsavari et al., 2021). Conversely, intact microbiomes are complementary distributed processes that lie in the functional capability of taxa. One group can bring about transformation of precursor compounds; others can process intermediates or control environmental

factors such as redox state. This type of interdependence between the metabolisms is especially applicable to PFAS because the interactions are generally slow, co-metabolic, and highly reliant on the environmental context (Liu & Mejia Avendaño, 2013; Shahsavari et al., 2021).

The implication of methodological aspects is significant. Disruption during sampling, storing, or subculturing can not only change composition but functional capacity when the functional traits are community distributed. Intact microbiomes preservation is not only concerned with preserving biomass, but also with preserving ecological interactions and emergent functions that can be lost by change of community structure (Prakash et al., 2020). Collectively, these points favor a transition between reductionist methods to a community-level perspective. Microbiomes in PFAS-affected environments have to be regarded as dynamic systems whose structure and functional integrity should be at the core of the understanding of contaminant response and evaluation of the long-term preservation impact (Berg et al., 2020; Shahsavari et al., 2021).

1.7.2 Microbiome Adaptation under PFAS Exposure

The long-term exposure to per- and polyfluoroalkyl substances (PFAS) can become a selective pressure on the microbiomes present in the environment, resulting in an alteration of the composition and functional capacity. PFAS frequently lead to reorganization of the community, but instead of complete inhibition, sensitive taxa are more frequently killed off and stress-tolerant populations enriched. This has been seen in soils, sediments, and wastewater systems, where taxa including *Proteobacteria* and *Actinobacteria* are usually enriched. The patterns are adaptive, such as a change in membranes, efflux activity, and systems of general stress responses that aid survival in chemical stress (Senevirathna et al., 2022b; Xu et al., 2022).

Microbiome functioning is also affected by exposure to PFAS. Research indicates biomass decreases, alterations in the enzyme activity, and carbon and nutrient cycle disruptions especially in high concentrations (Ye et al., 2022; Zhang et al., 2013). Nevertheless, microbial activity is neither entirely inhibited but is reallocated to taxa meaning that PFAS-contaminated environments remain biologically active at changed conditions. These reactions are a response to ecological adaptation and not the appearance of specific PFAS-degrading organisms. These adaptations are also influenced by environmental context.

The heterogeneity and differences in properties of organic matter content, redox conditions and heterogeneity affect the degree of community restructuring with the more stable systems being more conserved structurally and the environments with heterogeneity being more divergent. In general, PFAS pollution triggers the adaptation of the microbiome mainly by restructuring the communities and the functional changes within the environmental limitations (Liu & Mejia Avendaño, 2013; Shahsavari et al., 2021).

1.7.3 Functional Potential of Microbiomes in PFAS Transformation

Microbiomes have a functional role in the PFAS-impacted environment that is largely linked to restricted structure-specific transformation processes instead of full degradation. The existing evidence suggests that microbial communities respond to polyfluorinated precursors much easier than to completely fluorinated perfluoroalkyl acids, which can be explained by the ease of access to non-fluorinated functional groups by microbial metabolism (Butt et al., 2014; Liu & Mejia Avendaño, 2013). Such transformations are commonly co-metabolic in microbiomes, as they happen as a by-product of the metabolism of other substrates. General organic matter turnover enzymes might trigger the conversion of precursor compounds into intermediate products and, in most instances, terminal perfluoroalkyl acids which remain in the environment (Harding-Marjanovic et al., 2015; Shahsavari et al., 2021).

Consequently, microbial activity is likely to change PFAS composition, but not fluorine. Besides direct transformation, microbiomes may also affect the behavior of PFAS indirectly by altering the environmental conditions. The redox status and organic matter composition are some of the factors controlled by microbial processes and influence the sorption and mobility of PFAS in soils and sediments (M. A. Nguyen et al., 2017). Nevertheless, despite these interactions, most PFAS, especially long-chain compounds, including PFOA and PFOS, have not been shown to undergo any consistent defluorination or mineralization. Altogether, microbiomes contribute to the determination of the fate of PFAS not by direct degradation but instead via co-metabolic transformation of precursors and environmentally mediated mechanisms.

1.7.4 Relevance for Environmental Biotechnology and Remediation

Although these interactions of microbiomes with PFAS are also limited, they have significant impact on environmental biotechnology. Instead of facilitating total degradation, microbial systems play a major role in transforming and changing the behavior of PFAS precursors and modifying them under environmental conditions. This implies that microbiomes can be regarded as part of an integrated remediation, in which the biological processes will be used as supplements to the physical and chemical ones. In this regard, it is crucial to comprehend the stability, functional capacity, and reproducibility of microbiomes, especially in applications where there is a need for a consistent performance of microbiomes in environmental conditions over time.

1.8 Preservation of Intact Environmental Microbiomes

Maintaining the microbiomes of the environment in a manner that does not alter their original composition, and functionality is also a major challenge. Isolation of microbial communities out of the environmental matrix is typically done in two major ways, or preservation of the intact sample containing the microbial communities. The latter method preserves the physical structure and chemical gradients of the matrix, which may affect community stability in the course of

storage. The preservation of intact samples is not however simple. Managing and storage may cause disruptions which change the community structure and recovery. On the contrary, isolation-based methods make the system easy but might not capture the original environmental conditions. Although it is relevant, the long-term maintenance of intact environmental microbiomes is under-studied, especially when it comes to stability and functional recovery after storage (Prakash et al., 2020).

1.8.1 Fundamental Challenges in Microbiome Preservation

Preservation of environmental microbiota is more complicated than preservation of pure cultures: they exist in organized communities instead of being individual organisms. Maintaining a microbiome thus involves not just maintaining a taxonomic composition but also the conditions that enable the activity of it (Berg et al., 2020; Marchesi & Ravel, 2015). The main issue is that even when the composition of a community may seem to be stable, any disruption during sampling or storage may result in functional loss. This is of especially high concern to environmental microbiomes, where uncultivable organisms constitute a proportion of the total population and cannot be regained after being lost. Moreover, DNA-based measurements can be inaccurate in terms of preservation success, since the stability of nucleic acids does not always indicate the viability and activity of microbes (Prakash et al., 2020; Vartoukian et al., 2010)

Microbial populations are also very delicate to external disturbances. Changes in temperature, oxygen or storage environments may selectively advantage select taxa leading to changes in community structure and functionality. In general, preservation of microbiomes is still a difficult task as it is hard to preserve the community structure and functioning across time (Lauber et al., 2010).

1.8.2 Effects of Sampling and Storage on Microbiome Structure and Function

Microbiome structure and function can be affected by sampling and storage greatly. The microbial community will start to react as soon as it is sampled, and the time between the collection and preservation can produce changes in the composition, which usually benefit fast-growing or stress-tolerant microorganisms. The changes may modify the initial ecological profile of the sample, in particular, when the conditions are poorly controlled (Lauber et al., 2010; Rubin et al., 2013)

Storage conditions, particularly temperature, are also important in identifying microbiome stability. Ambient or refrigerated storage is linked to the further microbial activity and restructuring of the community, and freezing lessens but does not remove selective forces. Subsequently, relative abundance shifts can be experienced, and vulnerable populations would be lost even at frozen temperatures. Besides compositional effects, storage may have an effect on microbiome functioning. After storage, decreases in metabolic activity, enzyme activity, and substrate use have been described, which means that even taxonomically stable functional potential may be lost (Prakash et al., 2013, 2020).

In general, sampling and storage both cause biases, which may affect the integrity of microbiomes, which underscores the need to use standardized handling and preservation techniques in environmental research.

1.8.3 Limitations of Current Microbiome Preservation Strategies

The majority of microbiological preservation methods are optimized to handle pure cultures and do not entirely apply to microbiomes of complex environments. Freezing and cryopreservation at −20 °C or −80 °C are common methods to reduce microbial activity and conserve nucleic acids but will lead to cellular damage because of ice crystal formation and osmotic stress, resulting in different taxa surviving better than others and causing a change in community composition (Kerckhof et al., 2014; Prakash et al., 2013).

Cryoprotectants like glycerol are also usually added to minimize the effects of freezing by stabilizing cell membranes. Although they enhance survival, the extent of their effectiveness in different microorganisms is different, and disparities in physiological tolerance may still lead to biases in community structure (Kerckhof et al., 2014). Storage at 4 °C, common in handling the samples, can only be used for short term storage as it permits further microbial activity and alteration of composition. In this case, stress-resistant or fast-growing organisms can be preponderant and change the initial microbiome profile (Lauber et al., 2010).

Notably, success in preservation is commonly determined by the viability of DNA and not functional recovery. Even though the taxonomic profiles can seem to be stable following storage, microbial viability and activity declines are often observed, and modern methods are not sufficient to preserve the microbiome performance over time (Prakash et al., 2020). In conclusion, the current measures offer partial preservation and might not sufficiently preserve the integrity of environmental microbiomes in long-term storage.

1.8.4 Structural–Functional Limitations and Study Gaps

The most important limitation of the microbiome preservation literature is the lack of connection between structural stability and functional integrity, especially when storing the microbiome over time. The majority of studies are based on DNA-based analyses, which characterize the composition of a community, but are not indicative of microbial viability and activity. Consequently, microbiomes can be taxonomically stable with a low culturability, lower enzymatic activity, and substrate use (Kerckhof et al., 2014; Prakash et al., 2020).

This is due to the fact that even when cells are damaged or inactive, nucleic acids may still be left there and, as a result, the success of preservation is overestimated. Moreover, there is scanty current literature on the long-term conservation of intact environmental microbiomes. Available literature is mostly concerned with short-term storage or simplified mechanisms, whereas the more complicated matrices, including soils and sediments, are underrepresented. Moreover, structural,

and functional recovery are rarely measured concurrently, such that the outcomes of preservation cannot be understood in the long term (Prakash et al., 2013, 2020).

The long-term storage may also lead to cumulative stress, selective survivance of resistant taxa and breakdown of community interactions, leading to disillusionment of the initial microbiome. These changes cannot be adequately reflected in compositional analyses but can have a notable impact on functional performance. Altogether, the absence of unified, longitudinal analyses of structure and functionality is a significant gap in the research concerning the preservation of microbiomes.

1.8.5 Relevance to the Present Study

Considering these constraints, systematic assessment of microbiome preservation under environmental conditions of interest is required. It is especially relevant to contaminant affected systems, in which repeated sampling is frequently limited. To fill this gap, this study considers the long-term preservation of soil/sediment microbiomes. It determines structural stability and functional recovery, such as microbial viability, community composition, and response to enrichment conditions through the combination of culture-dependent and culture-independent methods. The purpose of this approach is to find out whether preserved microbiomes can be considered useful and reproducible tools to study microbial processes in contaminated environments.

Chapter 2. Materials and Methods

2.1 Sample Description and Storage Conditions

Two PFAS-impacted matrices were collected, a soil and a sediment sample from contaminated sites in the Veneto region (Italy). The sites are in areas subject to historical PFAS contamination and were selected to provide different environmental matrices with different physio-chemical properties.

2.1.1 Sampling Sites

- **Soil sample (Soil; Lonigo, VI)**
  - Location: Lonigo, Vicenza Province, Veneto region, Italy
  - Geographic coordinates: 45.37996°N, 11.37743°E
  - Environmental matrix: Agricultural Soil
  - Sampling was planned in collaboration with, and site access was granted by, the Municipality of Lonigo and "Mamme no PFAS"
- **Sediment sample (Sed; Trissino, VI)**
  - Location: Trissino, Vicenza Province, Veneto region, Italy
  - Geographic coordinates: 45.549694°N, 11.386583°E
  - Environmental matrix: Sediment
  - Sampling was planned in collaboration with, and site access was granted by,the Municipality of Lonigo and "Mamme no PFAS"

2.1.2 Determination of Moisture Content

Three subsamples (approximately 10g each) of soil and sediment were weighed to determine the initial mass and then dried in an oven at 60°C for 72 hours until constant weight was reached. The dry weight was determined, and moisture content was calculated on the weight lost after drying. The moisture content of the sediment sample (55.3 ± 0.4%) was much higher than that of the soil sample (27.3 ± 1.6%), which is likely due to the inherent differences in the composition and water holding capacity of the two matrices.

Table 4. Moisture content of soil and sediment samples.

#	Samples	Replicates	Initial Weight	Final Weight*	Humidity (%)
1.	Soil (Lonigo)	A	10.00	7.33	27.3 ± 1.6
		B	10.06	7.44	
		C	10.06	7.13	
2.	Sediment	A	10.13	4.57	55.3 ± 0.4
		B	9.94	4.42	

	(Trissino)	C	10.07	4.48	

2.1.3 PFAS Concentrations in Soil and Sediment

The concentrations of selected per- and polyfluoroalkyl substances (PFAS) measured in the soil and sediment samples were previously analyzed through liquid chromatography-mass spectrometry (LC-MS) and reported in Table 5. The sediment sample showed a markedly higher total PFAS burden (17,700 ng/kg) compared to the soil sample (5,370 ng/kg). In sediment, PFOS and PFSA were the dominant compounds, whereas PFOA represented the most abundant PFAS detected in the soil matrix.

Table 5. PFAS concentrations in soil and sediment samples (ng/kg).

	Soil	**Sed**
	ng/Kg	ng/Kg
PFBA	1 400	2 340
PFPeA	800	<50
PFHxA	420	<50
PFHpA	120	<50
PFOA	3 000	3 100
PFBS	100	<50
PFHxS	<50	<50
PFOS	370	9 330
PFSA	<50	2 880
Total	**5 370**	**17 700**

2.1.4 Sample Preparation and Preservation Scheme

Environmental samples were subdivided into aliquots according to the analytical workflow and time-point design (T0–T3). All aliquots were prepared in sterile falcon tubes and preserved for downstream analyses, including microbiological, molecular, and chemical investigations.

Table 6. Sample allocation and storage scheme for downstream analysis.

Analysis	**T0**	**T1**	**T2**	**T3**	**Spare**	**Total Falcons**
Total Count	16g	16g	16g	16g	3 Spare	7
DNA Extraction	5g	5g	5g	5g	3 Spare	7
Enrichment Culture	16g	16g	16g	16g	3 Spare	7
Biolog	16g	16g	16g	16g	3 Spare	7
						28

Each soil or sediment aliquot was weighed according to the quantities reported above prior to preservation. For each environmental matrix, two independent biological replicates were processed throughout the study (Soil A and Soil B; Sed A and Sed B).

2.1.5 Cryopreservation Procedure

Sterile glycerol was used as a cryoprotectant at a final concentration of 28.25% (w/v). After glycerol addition, each Falcon tube was vortexed for 2 minutes to ensure homogeneous mixing. Samples were then stored at −4°C overnight to allow gradual equilibration, followed by long-term preservation at −80°C until further analyses.

2.1.6 PFASs Used in this Study

Two per- and polyfluoroalkyl substances (PFASs) were selected for use in the experimental assays, including tridecafluorohexane-1-sulfonic acid (PFHxS) and perfluorooctanoic acid (PFOA). Both compounds were obtained from Sigma-Aldrich with a stated purity of ≥97%. For stock preparation, each PFAS was dissolved in dimethyl sulfoxide (DMSO; Sigma-Aldrich, USA) to obtain concentrated stock solutions at 200,000 mg L^{-1}. Stock solutions were sterilized by filtration through 0.22 µm polyvinylidene fluoride (PVDF) membrane filters (StarLab, Germany). The sterile PFAS stocks were subsequently diluted with the appropriate medium to achieve the desired working concentrations for the different experimental setups.

A range of additional PFASs was used in defluorination experiments at Center for Biotechnology and Fine Chemistry (CBQF), including fluoxetine, 8:2 fluorotelomer sulfonic acid (8:2 FTS), perfluorooctane sulfonate (PFOS), GenX (HFPO dimer acid), 3-perfluoroheptyl propanoic acid (7:3 FTCA), and nonafluoro-3,6-dioxaheptanoic acid (NFDHA).

2.1.7 Culture Media

The culture growth media, buffers, and solutions used throughout this study, along with their compositions and concentrations, are summarized in Table 7.

Table 7. Culture growth media, buffers, and solutions used in this study, including composition and concentrations.

Medium / Solution	Components	Concentration
Tryptic Soy Broth (TSB)	Tryptic soy broth	30 g L^{-1}
Malt Yeast Extract (MYE)	Malt extract broth	20 g L^{-1}
	Yeast extract	5 g L^{-1}
	Rifampicin	10 mg L^{-1}
Vitamin Solution (1000×)	Biotin	2 mg L^{-1}
	Folic acid	2 mg L^{-1}
	Riboflavin	5 mg L^{-1}
	Pyridoxine hydrochloride	5 mg L^{-1}

	Thiamine hydrochloride	5 mg L^{-1}
	Cyanocobalamin	10 mg L^{-1}
	Nicotinic acid	0.1 mg L^{-1}
	p-Aminobenzoic acid	5 mg L^{-1}
	Calcium pantothenate	5 mg L^{-1}
	Lipoic acid	5 mg L^{-1}
Wolfe Mineral Solution (100×)	Nitrilotriacetic acid	1.6 g L^{-1}
	$MgSO_4 \cdot H_2O$	3.5 g L^{-1}
	$MnSO_4 \cdot H_2O$	0.56 g L^{-1}
	NaCl	1.0 g L^{-1}
	$Fe_2(SO_4)_3$	0.076 g L^{-1}
	$CoSO_4 \cdot 7H_2O$	0.18 g L^{-1}
	$CaCl_2 \cdot 2H_2O$	0.13 g L^{-1}
	$ZnSO_4 \cdot H_2O$	0.11 g L^{-1}
	$CuSO_4 \cdot 5H_2O$	0.01 g L^{-1}
	$AlK(SO_4)_2 \cdot 12H_2O$	0.018 g L^{-1}
	H_3BO_3	0.01 g L^{-1}
	$Na_2MoO_4 \cdot 2H_2O$	0.04 g L^{-1}
Minimal Defined Medium (DM)	Na_2HPO_4	2.2 g L^{-1}
	KH_2PO_4	0.8 g L^{-1}
	NH_4NO_3	3.0 g L^{-1}
	Vitamin solution (1000×)	1 mL L^{-1}
	Wolfe mineral solution (100×)	10 mL L^{-1}
	Carbon source	As required
Oligoelement Solution	NaOH	2 g L^{-1}
	$EDTA \cdot 2H_2O$	12 g L^{-1}
	$FeSO_4 \cdot 7H_2O$	2 g L^{-1}
	$CaCl_2$	1 g L^{-1}
	Na_2SO_4	10 g L^{-1}
	$ZnSO_4 \cdot 7H_2O$	0.40 g L^{-1}
	$MnSO_4 \cdot 4H_2O$	0.40 g L^{-1}
	$CuSO_4 \cdot 5H_2O$	0.10 g L^{-1}
	$Na_2MoO_4 \cdot 2H_2O$	0.10 g L^{-1}
	H_2SO_4 (conc)	0.50 mL L^{-1}
Minimal Medium (MM)	$Na_2HPO_4.2H_2O$	2.67 g L^{-1}
	KH_2PO_4	1.40 g L^{-1}
	$MgSO_4.7H_2O$	0.20 g L^{-1}
	$(NH_4)_2SO_4$	0.50 g L^{-1}
	Oligoelements Solution	10 mL $^{-1}$
TAE buffer (50×)	Tris base	242 g L^{-1}
	Acetic acid (glacial)	57.1 mL L^{-1}
	EDTA (disodium salt)	100 mL L^{-1}
Total Ionic Strength	NaCl	58.44 g L^{-1}

Adjustment Buffer (TISAB)	$NaCH_3COO$	61.52 g L^{-1}
	$Na_3C_6H_5O_7.2H_2O$	0.59 g L^{-1}
	CH_3COOH	14.24 mL L^{-1}
Physiological solution	NaCl	9 g L^{-1} (0.9%)

All chemicals and culture media components were obtained from Sigma-Aldrich, USA, unless otherwise indicated. Microbiological Agar (Sigma-Aldrich, USA) was supplied (15 g L^{-1}) to TSB, MYE, and DM to solidify the culture media. The above media, TAE buffer, and physiological solutions were sterilized by autoclaving at 121 °C for 15 min under overpressure conditions. On the other hand, Vitamin and Wolfe solutions were sterilized by filtration through 0.22 µm polyvinylidene fluoride (PVDF) membrane filters (StarLab, Germany).

2.2 Culture-Dependent Analysis

2.2.1 Total Count Protocol

Total microbial counts were determined for soil and sediment samples at four experimental time points (T0, T1, T2, and T3). From each sample (SoilA, SoilB, SedA and SedB) 3.5g of soil was collected, diluted 1:10 with sterile physiological solution (0.9 % *w/v* NaCl) and stirred for 1h to promote detachment of microbial cells from the solid matrix. Following homogenization, serial dilutions were prepared using the physiological solution.

For microbial enumeration, dilution ranges of 10^{-3} to 10^{-5} were plated for bacteria and 10^{-1} to 10^{-3} for fungi. The bacterial count was conducted in Tryptic Soy Agar (TSA) and the fungal count on the Malt-Yeast Extract (MYE) agar. The experiment was conducted with two biological replicates (A and B) of each matrix, and three technical replicates per sample. The plates were incubated at 27 °C for 5 days, and CFUs were counted.

2.2.2 Biolog EcoPlate™ Analysis

The analysis was performed at each time points (T0, T1, T2, and T3). A 2g sample of soil or sediment was suspended in 18 mL of sterile physiological solution (0.9% w/v NaCl) in sterile glass vials (1:10 dilution). The samples were then shaken on a horizontal shaker at 150 rpm for 30 minutes to allow microbial detachment. Subsequently, 12 mL of the homogenized suspension were transferred into sterile 15 mL screw-cap centrifuge tubes and centrifuged at 800 × g for 2 minutes to remove coarse particles. From the resulting supernatant, 2 mL were collected and further diluted 1:10 by adding 18 mL of sterile physiological solution in sterile 50 mL Falcon tubes.

A volume of 120 µL of the final dilution was inoculated into each well of the Biolog EcoPlates™. The plates were incubated at 27 °C in the dark under shaking conditions (110 rpm) for five days. The plates were read after 48 hours at both 700 nm and 590 nm by using BioTek Synergy Neo2 Hybrid Multimode Reade (Agilent; Santa Clara, US). Multivariate statistical analyses, including

cluster analysis based on the UPGMA algorithm, were performed using PAST software (version 4.03). The analysis was performed in duplicate.

2.3 Culture-Independent Analyses (DNA Metabarcoding)

2.3.1 DNA Extraction from Environmental Samples

At T0, T1, T2, and T3 DNA was extracted in duplicate from each sample (SoilA, SoilB, SedA, and SedB) using the DNeasy PowerSoil Pro Kit® (Qiagen, Hilden, Germany), following the manufacturer's instructions. DNA was eluted in 75 µL of Buffer C6.DNA concentration was initially estimated by measuring absorbance at 260 nm, and purity was assessed using the A260/A280 and A260/A230 ratios with a NanoDrop™ One/One C UV–Vis spectrophotometer (Thermo Fisher Scientific, USA). In parallel, DNA concentration was also quantified using a Qubit™ 4 Fluorometer (Invitrogen, USA).

2.3.2 Metagenomic Analysis

The hypervariable V5–V6 region of the 16S rRNA gene and the internal transcribed spacer (ITS) region were selected as targets for bacterial and fungal community profiling, respectively. PCR amplification was performed in-house, and subsequent sequencing was carried out by the University of Milano-Bicocca, which provided the resulting sequence of files for analysis. The further amplicon sequencing and bioinformatic processing were performed as described in (Gandolfi et al., 2024).

2.3.2.1 Protocol for Sample Preparation for Illumina 16S Bacterial Sequencing (MiSeq 2×300)

The 16S rRNA gene fragment selected for amplification includes the hypervariable regions V5 and V6 and is flanked by the primers 783F and 1027R. The primers were tagged with a barcode so that several amplicons from different samples could be combined in a single sequencing library. In particular, three different barcodes were chosen for the forward primer, and one barcode for the reverse primer, resulting in nine different combinations.

Primers

The primers used in this study were as follows:

ill4_1B_783F	TCGTCGGCAGCGTCAGATGTGTATAAGAGACAGAGCAGCCAGGATTAGATACCC
ill4_3B_783F	TCGTCGGCAGCGTCAGATGTGTATAAGAGACAGAGAGAGCAGGATTAGATACCC
ill4_4B_783F	TCGTCGGCAGCGTCAGATGTGTATAAGAGACAGAGATGCCAGGATTAGATACCC
ill4_10B_1027R	GTCTCGTGGGCTCGGAGATGTGTATAAGAGACAGATGCAGCGACRRCCATGCANCACCT

The part marked in black is the gene-specific primer sequence; the part marked in red is the barcode, which is primer-specific, and the part marked in blue is the Illumina adapter sequence, as

supplied by the sequencing company. The expected size of the fragment including barcodes and adapters is 361 bp.

PCR Program

PCR amplification was performed using the following thermal cycling conditions for bacterial 16S rRNA gene amplification:

- Initial denaturation at 94 °C for 4 minutes
- 27 cycles of:
  - Denaturation at 94 °C for 50 seconds
  - Annealing at 50 °C for 30 seconds
  - Extension at 72 °C for 30 seconds
- Final extension at 72 °C for 5 minutes
- Hold at 10 °C

2.3.2.2 Protocol for Sample Preparation for Illumina ITS Sequencing (MiSeq 2×300)

The region targeted for amplification is the ITS region. Primers were barcoded, enabling the pooling of several amplicons (corresponding to different samples) in a single sequencing library. Three barcodes were chosen for the forward primer, and three for the reverse primer, leading to nine combinations.

Primers

ill4_1B_ITS1F	TCGTCGGCAGCGTCAGATGTGTATAAGAGACAGAGCAGCCTTGGTCATTTAGAGGAAGTAA
ill4_3B_ITS1F	TCGTCGGCAGCGTCAGATGTGTATAAGAGACAGAGAGAGCTTGGTCATTTAGAGGAAGTAA
ill4_4B_ITS1F	TCGTCGGCAGCGTCAGATGTGTATAAGAGACAGAGATGCCTTGGTCATTTAGAGGAAGTAA
ill4_13B_ITS2R	GTCTCGTGGGCTCGGAGATGTGTATAAGAGACAGCAGATGGCTGCGTTCTTCATCGATGC

The black region of the primer corresponds to the specific primer for the gene, the red region corresponds to the barcode (specific to each primer) and the blue region corresponds to the Illumina adapter sequence (as provided by the sequencing company). The amplified fragment, including the barcodes and adapters, is expected to be 383 bp long.

PCR Program

PCR amplification for fungal ITS regions was performed using the following thermal cycling conditions:

- Initial denaturation at 94 °C for 5 minutes
- 30 cycles of:
  - Denaturation at 94 °C for 40 seconds
  - Annealing at 50 °C for 30 seconds

    - Extension at 72 °C for 1 minute
- Final extension at 72 °C for 5 minutes
- Hold at 10 °C

PCR Reaction

For each sample (both in case of ITS and 16S sequencing), two PCR reactions of 50 µL each were prepared. Each PCR reaction mixture consisted of the following components:

- GoTaq® Reaction Buffer 1× (stock 5×, Promega): 10 µL
- Forward primer, 10 µM (final concentration 1 µM): 5 µL
- Reverse primer, 10 µM (final concentration 1 µM): 5 µL
- dNTPs (0.4 mM; stock 10 mM, Promega): 2 µL
- Taq DNA Polymerase (5U/ µL): 0.2 µL
- Template DNA: 2 µL
- Nuclease-free water: 25.8 µL

At the end of the amplification, two PCR reactions corresponding to the same sample were pooled. The amplified products were then separated by electrophoresis on a 1–1.5% agarose gel, excised, and purified using the Wizard SV Gel and PCR Clean-Up System (Promega), with a final elution volume of 50 µL of water. DNA concentration in the eluate was quantified using a Qubit fluorometer with the dsDNA Broad Range reagent, measuring 2 µL per sample. For sequencing, a minimum DNA concentration of 2 ng/µL per sample was required

2.3.3 Biodiversity Indexes and Multivariate Analysis

Alpha diversity reflects both the richness and evenness of microbial communities, whereas beta diversity provides information on compositional dissimilarities and temporal or spatial shifts in community structure. Alpha diversity was assessed using the Shannon diversity index (H′), calculated with PAST software (version 4.03).

Furthermore, cluster analysis was conducted using the Unweighted Pair Group Method with Arithmetic Mean (UPGMA) algorithm, with the Bray-Curtis method and 1000 bootstraps. This analysis was used to cluster samples based on overall community similarity and to assess sample relationships with respect to time and matrix type. The use of alpha diversity indices and beta diversity analyses together allowed a holistic assessment of community diversity, structure, and temporal dynamics.

2.4 Enrichment Cultures

At each time point (T0, T1, T2, and T3), enrichment cultures were performed on microbiome associated with each sample (SedA, SedB, SoilA, and SoilB) using PFOA as the sole carbon and energy source. The enrichment procedure was performed in technical duplicate for each sample. Briefly, 5 g of soil or sediment was incubated in 45 mL of DM minimal medium (Frassinetti et al.,

1998) supplemented with 300 mg L^{-1} PFOA and incubated for 7 days at 27 °C under shaking conditions (200 rpm).

Following this initial enrichment phase, a 1:10 refreshment was carried out by transferring 5 mL of the enrichment culture into 45 mL of fresh DM minimal medium supplemented with 600 mg L^{-1} PFOA, resulting in a final volume of 50 mL per flask. This refreshed enrichment was incubated for an additional 7 days at 27 °C under shaking conditions (200 rpm). At the end of the incubation, the enrichment cultures containing new microbiomes were subdivided for downstream analysis as follows:

- **New Microbiome preservation:**

To preserve the enriched microbiomes, an aliquot of 15 mL of enrichment culture was transferred into a 50 mL Falcon tube and mixed with 5 mL of glycerol (30%, v/v) followed by storage at –80 °C.

- **Total microbial count and isolation:**

An aliquot of 1 mL of enrichment culture was collected at the end of enrichment culture in a 2 mL Eppendorf tube for total microbial enumeration, followed by microbial isolation.

- **DNA extraction:**

A 29 mL aliquot of enrichment culture was transferred to a 50 mL Falcon tube; 10 mL was immediately subjected to DNA extraction, and the remaining pellet was preserved at –80 °C for future analysis.

2.5 PCR-DGGE Analysis

At each time point (T0–T3), DNA was extracted in duplicate from enrichment cultures using the DNeasy® PowerWater® Pro Kit (Qiagen, Hilden, Germany), following the manufacturer's instructions. DNA concentration and purity were assessed using a NanoDrop™ One/One^{c} UV–Vis spectrophotometer (Thermo Scientific, USA) by measuring absorbance at 260 nm and evaluating the A260/A280 and A260/A230 ratios.

To assess community composition at different time points during the enrichment procedure, the V3 region of the 16S rRNA gene was amplified for Denaturing Gradient Gel Electrophoresis (DGGE) analysis. The amplification of the V3 hypervariable region of the 16S rRNA gene, the DGGE electrophoresis, and further statistical analysis were performed as described in (Andreolli et al., 2021).

PCR Reaction (V3 Amplification)

PCR reactions were performed in a final volume of 25 µL per replicate, with three technical replicates pooled to obtain a total volume of 75 µL for each sample. A negative control, containing all reaction components except template DNA, was included in each PCR run.

Each PCR reaction mixture consisted of the following components:

- DNA (20–50 ng): 1 µL
- GoTaq® Reaction Buffer 1× (stock 5×, Promega): 5 µL
- Primer P1-GC (Muyzer et al., 1993), 0.4 mM; stock 10 mM): 1 µL
- Primer P2 (Muyzer et al., 1993), 0.4 mM; stock 10 mM): 1 µL
- dNTPs (0.4 mM; stock 10 mM, Promega): 1 µL
- $MgCl_2$ (1.5 mM; stock 25 mM): 1.5 µL
- Taq DNA polymerase (1 U; stock 5 U μL^{-1}, Promega): 0.2 µL
- Sterile distilled water: 14.3 µL

PCR Program

- 94 °C for 5 min
- 30 cycles:
    - Denaturation: 94°C, 1 min
    - Annealing: 55°C, 1 min
    - Extension: 72°C, 40 sec
- Final extension: 72°C, 5 min

Amplicons were verified on a 2% agarose gel, using 100 bp ladder.

DGGE Conditions

DGGE was performed using an 8% (w/v) polyacrylamide gel containing a 30–60% linear denaturing gradient of formamide and urea (100% denaturant defined as 7 M urea and 40% (v/v) formamide). Electrophoresis was carried out using a Bio-Rad DCode™ DGGE system with 1× TAE buffer as the running buffer. The electrophoretic run consisted of an initial equilibration step at 60 °C for 10 min at 100 mV, followed by separation at 50 mV for 16 h under constant temperature conditions.

Reagents and Concentrations used for DGGE Gel Preparation

Gels were degassed for 2 h prior to polymerization. Polymerization was initiated by the addition of TEMED (Sigma Aldrich, 55 µL) and APS (0.1 g/mL; 88 µL). For DGGE analysis, 75 µL of PCR product (about 2000 ng) per sample was loaded.

Table 8. Reagents and concentrations used for DGGE gel preparation.

Reagent	30% Denaturant Solution	60% Denaturant Solution
Acrylamide	3.6 mL	3.6 mL
50× TAE buffer	360 µL	360 µL
Formamide (40%)	2.16 g	4.32 g
Urea (7 M)	2.27 g	4.54 g

Deionized water	Up to 18 mL	Up to 18 mL

Image Acquisition and Data Analysis

Following electrophoresis, DGGE gels were stained for 30 min in 1× TAE buffer supplemented with 12.5 µL DNA ClearSight™ dye (BIOATLAS). Gel images were acquired using a FireReader Max imaging system (UVITEC). Digital images were imported into UVISoft UVIBandMap software (UVISoft UVIBandMap) for band pattern analysis. Lanes and corresponding band positions were manually identified. The presence/absence of bands was used to determine the similarity of samples, which are represented by building a dendrogram using the unweighted pair group method with arithmetic mean (UPGMA).

2.6 Total Microbial Count from Enrichment Cultures

Total microbial enumeration of enrichment cultures (T0, T1, T2, and T3) for all samples (Soil A, Soil B, Sed A, and Sed B). Each biological replicate was further analyzed in duplicate (technical replicates). Colony-forming units (CFUs) were determined following serial dilution and plating as described in Section 2.2.1.

2.6.1 Isolation and Identification of Microbial Strains

Microbial isolation was performed by direct isolation procedure following the same method as described in Section 2.6. Plates were incubated at 27 °C for 5 days. After incubation, well-isolated and morphologically distinct colonies were selected and transferred onto fresh media. Selected colonies were sub-cultured through three consecutive transfers on the corresponding media to obtain pure cultures.

2.6.1.1 DNA Extraction from Bacterial Liquid Cultures

Pure bacterial isolates were cultivated in 5 mL of Tryptic Soy Broth (TSB) at 27 °C with shaking at 150 rpm for 48 h. Subsequently, 1 mL aliquots of each culture were harvested by centrifugation at 13,000 × g for 3 min. Genomic DNA was extracted using the Wizard® SV Genomic DNA Purification Kit (Promega, Italy). Extracted DNA was stored at −20 °C until further analysis.

2.6.1.2 BOX-PCR

The technique was applied to group microbial isolates based on their genetic profiles. PCR amplifications were performed using the A1R BOX primer (5′-CTACGGCAAGGCGACGCTGACG-3′) (Andreolli et al., 2011; Van Belkum et al., 1996).

PCR Reaction

PCR reactions were performed in a final volume of 25 µL for each sample. A negative control, containing all reaction components except template DNA, was included in each PCR run.

Each PCR reaction mixture consisted of the following components:

- DNA (20–50 ng): 2 µL
- GoTaq® Reaction Buffer 1× (stock 5×, Promega): 5 µL
- Primer A1R BOX (10 pmol/µL: final amount 20 pmol per reaction): 2.0 µL
- dNTPs (0.4 mM; stock 10 mM, Promega): 1 µL
- Taq DNA polymerase (1 U; stock 5 U μL^{-1}, Promega): 0.2 µL
- Sterile distilled water: 14.8 µL

Prepared master mix by counting the number of strains and one as negative control to be sure that there is no contamination at each amplification run.

Thermocycler Program Conditions

- Initial denaturation: 94 °C for 5 min
- 35 Cycles**:**
    - Denaturation: 94 °C for 1 min
    - Annealing: 52 °C for 1 min
    - Extension: 72 °C for 2 min

Agarose Gel Electrophoresis

PCR products were analyzed by electrophoresis on a 1.5% (w/v) agarose gel, run at 100 V for 30 min. A 1 kb DNA ladder and a 100 bp DNA ladder were used as molecular size markers to verify amplicon size.

2.6.1.3 16S rRNA Gene Amplification for Bacterial Isolates

PCR Amplification

Amplification of the 16S rRNA gene was performed using universal bacterial primers fD1 (5′-AGAGTTTGATCCTGGCTCAG-3′) and rP2 (5′-ACGGCTACCTTGTTACGACTT-3′), as previously described (Weisburg et al., 1991).

PCR Reaction

The composition of the PCR reaction mixture (final volume 25 µL) was as follows:

- Genomic DNA (10–50 ng): 2.0 µL
- GoTaq® Reaction Buffer (5×, Promega; final concentration 1×): 5.0 µL
- Primer fD1 (10 pmol/µL; final amount 10 pmol per reaction): 1.0 µL

- Primer rP2 (10 pmol/µL; final amount 10 pmol per reaction): 1.0 µL
- dNTPs (10 mM, Promega; final concentration 0.4 mM): 1.0 µL
- Taq DNA polymerase (5 U/µL, Promega; final amount 1 U per reaction): 0.2 µL
- Nuclease-free water: 14.8 µL

Thermocycler Program Conditions

PCR amplification was carried out in a thermocycler under the following conditions:

- Initial denaturation: 94 °C for 4 min
- 30 cycles of:
    - Denaturation: 94 °C for 45 sec
    - Annealing: 42 °C for 45 sec
    - Extension: 72 °C for 2 min
- Final extension: 72 °C for 5 min

2.6.2.4 ITS Amplification for Fungal Isolates

Fungal isolates were grown on agar plates for 5 days at 27 °C. A small amount of mycelium was directly collected from the colony using a sterile tip and suspended in 20 µL of sterile double distilled H_2O. The suspension was used directly as template DNA for PCR amplification.

For isolates that did not show amplification in the first PCR attempt, a slightly larger amount of mycelium was suspended in 100 µL sterile double distilled H_2O and subjected to thermal lysis at 90 °C for 10 min. After thermal degradation, 20 µL of the lysate was used as template DNA for PCR.

PCR Amplification

Amplification of the fungal ITS rRNA region was performed using universal primers ITS1 (5′-TCCGTAGGTGAACCTGCGG-3′) and ITS4 (5′-TCCTCCGCTTATTGATATGC-3′) as described by White et al. (1990).

PCR Reaction

The composition of the PCR reaction mixture (final volume 50 µL) was as follows:

- Nuclease-free water (ddH_2O): 3.6 µL
- GoTaq® Reaction Buffer (5×, Promega; final concentration 1×): 10.0 µL
- dNTPs (10 mM, Promega; final concentration 0.4 mM): 2.0 µL
- ITS1 primer (10 pmol/µL; final amount 10 pmol per reaction): 2.0 µL

- ITS4 primer (10 pmol/µL; final amount 10 pmol per reaction): 2.0 µL
- BSA (2 µg/µL; final amount 20 µg per reaction): 10.0 µL
- Taq DNA polymerase (5 U/µL, Promega; final amount 1 U per reaction): 0.4 µL
- Mycelium suspension (template DNA): 20.0 µL

Thermocycler Program Conditions

PCR amplification was carried out in a thermocycler under the following conditions:

- Initial denaturation: 95 °C for 6 min
- 35 cycles of:
    - Denaturation: 94 °C for 1 min
    - Annealing: 50 °C for 1 min
    - Extension: 72 °C for 1 min
- Final extension: 72 °C for 6 min

2.6.1.4 Agarose Gel Electrophoresis, DNA Purification

PCR products corresponding to the 16S rRNA gene (bacteria) and the ITS region (fungi) were analyzed on 1% (w/v) agarose gels. A 100 bp DNA ladder was used as a molecular size marker to verify amplicon size. Bands of the expected size were excised under UV illumination and purified using the QIAEX II Gel Extraction Kit (QIAGEN, Milan, Italy), according to the manufacturer's instructions.

2.6.1.5 Preliminary Taxonomic Identification

Purified PCR products were submitted for Sanger sequencing to Eurofins Genomics (Germany). The obtained sequences, representing partial 16S rRNA gene fragments for bacterial isolates and ITS regions for fungal isolates, were manually inspected to remove low-quality regions, trimmed, and assembled using BioEdit Sequence Alignment Editor (version 7.7.1) (Hall, 1999).

Taxonomic identification was performed by comparing the processed sequences against reference databases using the BLASTN algorithm (Altschul et al., 1990), implemented in the NCBI database. Sequence similarity searches were used to assign taxonomic identity based on the closest matching sequences. For bacterial isolates, identification was further refined using the EzBioCloud database, with searches restricted to type strains to improve taxonomic accuracy (Yoon et al., 2017).

Sequence-based identification was based on partial gene regions, which are widely used as molecular markers for taxonomic classification, although they may not always allow discrimination at the species level.

2.6.2 Cryopreservation of Pure Strains

Pure microbial cultures were stored at -80 °C for further studies. To ensure purity and physiological stability, each isolate was streaked three times on Tryptic Soy Agar (TSA). Single colonies were inoculated into liquid medium and incubated for 48 h under appropriate growth conditions.

Following incubation, cell suspensions were mixed with sterile glycerol to obtain a final glycerol concentration of 25% (v/v). Briefly, 800 µL of culture was combined with 800 µL of a sterile 50% (v/v) glycerol solution in cryovials, mixed thoroughly, and immediately stored at −80 °C until further use.

2.7 PFAS-Related Functional Experiments

2.7.1 Evaluation of PFAS Abatement Using Enriched Microbiomes

2.7.1.1 Preparation of Inocula from Enrichment Cultures

For each biological microbiome replica (Soil A, Soil B, Sed A and Sed B) two technical enriched cultures replica were previously performed (for instance, Soil Aa and Soil Ab). Here, for each enrichment-derived microbiome, the two technical replicates were combined to obtain a representative inoculum. Specifically, 2.5 mL from each technical replicate was pooled in a sterile tube, resulting in a total volume of 5 mL per sample. The third replica was obtained, merging the combined technical replica. Therefore, the experiment was performed in a triplicate. From each pooled sample, 1 mL was used to inoculate new batch cultures for PFAS biodegradation experiments. The experimental design included microbiomes derived from original soil (Soil) and sediment (Sed) samples at different storage times (T0 and T3).

2.7.1.2 Batch Culture Setup for PFAS Biodegradation

Batch experiments were conducted using Minimal Defined (DM) medium supplemented with perfluorooctanoic acid (PFOA) and perfluorohexane sulfonic acid (PFHxS) at final concentrations of 25 mg L^{-1} and 10 mg L^{-1}, respectively. For each microbiome condition, glass vials were prepared containing 24 mL of PFAS-amended DM medium, to which 1 mL of the corresponding inoculum was added, resulting in a final working volume of 25 mL per vial.

Control Experiments

To distinguish biotic from abiotic PFAS removal, the following controls were included:

- **Initial chemical controls (T0):** PFAS-amended DM medium analyzed prior to inoculation to determine initial PFAS concentrations.
- **Abiotic controls (Abiot):** PFAS-amended DM medium without microbial inoculum

Incubation Conditions

All batch cultures were incubated under the following conditions:

- **Temperature:** 27 °C

- **Agitation:** 200 rpm
- **Incubation time:** 87 days

2.7.1.3 PFAS Quantification

PFAS concentrations were quantified according to ASTM D7979-20. Samples were collected at the beginning of the experiment (T0) and after 87 days of incubation (T87). PFAS removal was evaluated by comparing PFOA and PFHxS concentrations at T0 and T87 in biotic cultures inoculated with enrichment-derived microbiomes from soil and sediment stored for 0 (T0) and 12 months (T3), as well as in abiotic controls.

2.7.1.4 Microbial Enumeration

Prior to PFAS addition, 100 µL of each pooled inoculum was withdrawn for total bacterial count analysis to determine the initial microbial load of each enriched microbiome. Additional samples were collected after 1, 7, 10, and 13 weeks from the beginning of the experiment. Total bacterial counts were determined by plating appropriate serial dilutions on tryptic soy agar (TSA). Plates were incubated at 27 °C for 5 days, after which colony-forming units (CFU) were counted and expressed as CFU per millilitre of culture.

2.8 PFAS-Exposed Isolates Screening and Selection for Defluorination Assays

Strains isolated and identified from enrichment cultures at all time points (T0, T1, T2, and T3) were screened to identify PFAS-tolerant candidates suitable for subsequent experiments evaluating PFAS biotransformation potential. Briefly, isolates were pre-cultured in 5 mL Tryptic Soy Broth (TSB) at 27 °C and 150 rpm for 72 h to obtain sufficient biomass. Cells were harvested by centrifugation (5,000 rpm, 10 min) and washed twice with sterile physiological solution (0.9% NaCl) to remove residual nutrients prior to exposure assays.

To test growth and tolerance, two strategies were used:

- **General viability control:** first streaking was directly applied from a TSB culture onto tryptic soy agar (TSA) plates to assess growth and provide a reference control.
- **PFAS exposure screening:** the washed cell suspension was spotted and streaked onto (i) DM agar amended with perfluorooctanoic acid (PFOA; 50 mg L^{-1}) and tested as the sole carbon source and (ii) DM agar control plates

To assess the stability and reproducibility of PFOA tolerance, the colonies growing on DM agar with PFOA were streaked repeatedly on the same medium. A second streaking was carried out from colonies grown after the first exposure, and a third streak from colonies grown after the second exposure. This enabled us to confirm the stable growth in the presence of PFOA, rather

than the result of residual nutrients and/or physiological adaptation. Only isolates exhibiting consistent growth on DM agar plates containing PFOA (50 mg L^{-1}) and successive streaking steps were used for PFAS biotransformation and defluorination experiments.

2.9 Experiments with PFAS

Isolates showing stable growth and tolerance in the presence of perfluorooctanoic acid (PFOA) during the enrichment and screening steps were selected for further test. These PFAS-exposed isolates were further tested for their ability to bio transform and de-fluorinate organic compounds in biotransformation and defluorination assays, respectively. All these experiments were performed in the Environmental Biotechnology and Resources Research Group at CBQF - Centre for Biotechnology and Fine Chemistry at Universidade Católica Portuguesa, Escola Superior de Biotecnologia (ESB-UCP), Porto, Portugal, under controlled laboratory conditions.

2.9.1 General experimental Conditions

Unless otherwise stated, all experiments were conducted in sealed glass vials containing 75 mL of minimal medium (MM). Biotic assays were inoculated to an initial OD_{600}-equivalent value of 0.05, adjusted according to culture type. Cultures were incubated at 25 °C with shaking at 130 rpm. Target compounds were added at a final concentration of 10 mg L^{-1}. Sampling schedules varied depending on the experimental design and are detailed below.

2.9.2 Fluoxetine Biotransformation and Defluorination Experiments

Fluoxetine (FLX) biotransformation experiments were performed first to evaluate the ability of selected fungal and bacterial isolates to transform a fluorinated pharmaceutical compound and to assess associated defluorination activity.

Cultures were prepared in 75 mL of minimal medium (MM) and inoculated to an initial OD_{600}-equivalent value of 0.05. Fluoxetine was added at a final concentration of 10 mg L^{-1}. Experiments were conducted for 28 days at 25 °C under shaking at 130 rpm.

Three nutritional conditions were tested:
(i) FLX as the sole added compound,
(ii) FLX with D-glucose added at the start of the experiment (0.5 g L^{-1}), and
(iii) FLX with D-glucose supplied weekly at 0.5 g L^{-1}.

At defined time points, 3 mL samples were withdrawn and centrifuged. The clarified supernatant was used for fluoxetine quantification by HPLC and for fluoride ion (F^-) analysis to monitor defluorination.

2.9.3 PFOA Defluorination Experiments with Single Isolates

Following FLX experiments, defluorination assays were conducted using perfluorooctanoic acid (PFOA). Triplicate experiments with fungal and bacterial isolates, as well as abiotic controls, were included.

Perfluorooctanoic acid (PFOA) was supplied from a stock solution to reach a final concentration of 10 mg L^{-1}. Cultures were incubated under typical conditions, and samples were collected weekly for 84 days (T0 to T12). Culture samples (2 mL) were taken and processed only for fluoride ion (F^-) determination.

2.9.4 PFOA Defluorination Experiments with a Mixed Microbial Consortium

Besides single-isolate tests, a consortium of microorganisms was tested for co-defluorination. Bacterial and fungal isolates were cultivated separately, and the appropriate volumes were directly added to the experimental vials so that the group inoculum amounted to an initial OD_{600}-equivalent of 0.05. The consortium was comprised of both fungi and bacteria. The final concentration of PFOA was 10 mg L^{-1}. The experiment was performed for 61 days with sampling at T0-T3 (Day 0-61). 2 mL samples were withdrawn for fluoride (F^-) analysis.

PFOA was added at a final concentration of 10 mg L^{-1}. The experiment was conducted for 61 days, with sampling at T0–T3 (Day 0–61). At each time point, 2 mL of culture were collected for fluoride ion (F^-) analysis.

2.9.5 Experiments with other PFAS Compounds

Lastly, other PFAS were tested using the same protocol as described above to determine defluorination potential across structurally diverse PFAS. The compounds tested were 8:2 fluorotelomer sulfonic acid (8:2 FTS), perfluorooctane sulfonate (PFOS), GenX (HFPO dimer acid), 3-perfluoroheptyl propanoic acid (7:3 FTCA), and nonafluoro-3,6-dioxaheptanoic acid (NFDHA).

Each isolate was incubated separately with each PFAS compound at a final concentration of 10 mg L^{-1}. Experiments were conducted for 47 days with sampling at T0–T4 (Day 0–47). Samples were processed for fluoride ion (F^-) analysis to assess defluorination activity.

2.10 Analytical Methods

2.10.1 Fluoride Analysis

For fluoride analysis, biomass was removed from culture samples by centrifugation at 14 000 rpm for 10 min at 4 °C. The concentration of fluoride ions in the clarified supernatant was determined using an ion-selective combination electrode (model Orion 96-09, Thermo Electron Corporation, Beverly, MA). The electrode was calibrated using sodium fluoride (NaF) standards ranging from 0.005 to 5 mM prepared in minimal medium (MM).

The ionic strength of both standards and samples was adjusted by the addition of a total ionic strength adjustment buffer (TISAB). The TISAB solution consisted of NaCl (1 M), CH_3COOH (0.25 M), CH_3COONa (0.75 M), and sodium citrate (0.002 M). Fluoride ion measurements were performed for all experimental conditions, including fluoxetine (FLX), PFOA, and other PFAS experiments. Fluoride analysis was carried out following the analytical approach described in the study on enantioselective biodegradation of fluoxetine by *Labrys portucalensis* F11 (Moreira et al., 2014).

2.10.1.1 Calibration Curve for Fluoride Ion Analysis

A calibration curve for fluoride ion quantification was prepared using sodium fluoride (NaF) standards. A 50 mM NaF stock solution was prepared by dissolving 0.105 g of NaF in 50 mL of distilled water. The solution was mixed for approximately 30 min until complete dissolution and stored as the primary stock solution. Working fluoride standards were prepared by serial dilution of the stock solution to obtain concentrations in the range 0.0025–5 mM (50, 5, 1, 0.5, 0.1, 0.01, 0.005, and 0.0025 mM), using minimal medium as the diluent to match the sample matrix.

Table 9. Concentrations of fluoride standards prepared from NaF for calibration.

[F] (mM)	log10	E (mV)
0.0025	-2.60206	172.1
0.005	-2.30103	158.4
0.01	-2	140
0.05	-1.30103	100.3
0.1	-1	85
0.5	-0.30103	45.7
1	0	28.4
5	0.69897	-8.9

Fluoride measurements were performed using a fluoride ion-selective electrode. For each standard, 1 mL of NaF solution was mixed with 1 mL of total ionic strength adjustment buffer (TISAB) prior to measurement. Electrode potential (mV) was measured for each concentration once it was stabilized. A calibration curve was drawn with fluoride concentration (mM) against the electrode potential (mV). The curve was applied for the quantification of fluoride ions released in fluoxetine, PFOA and other PFAS experiments.

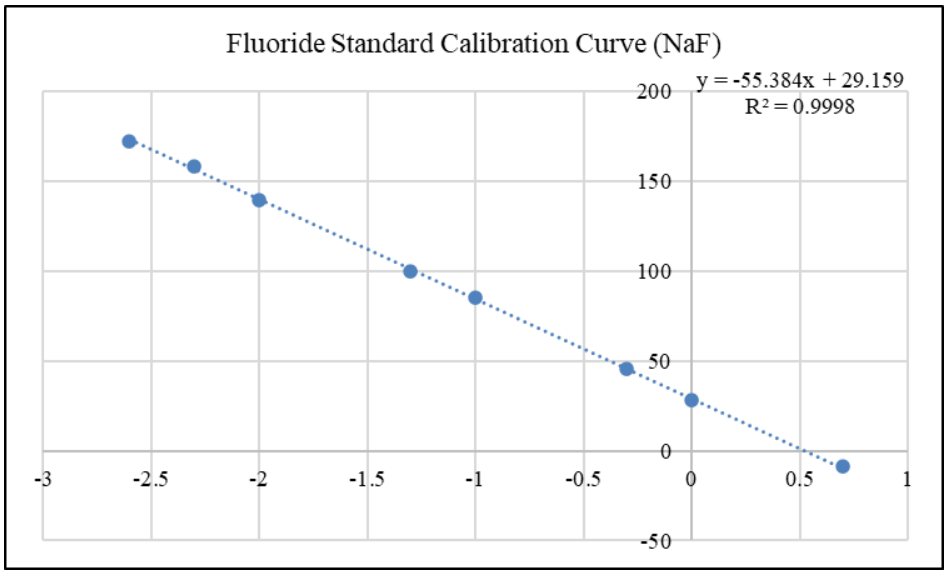

Figure 8. Fluoride standard calibration curve generated using sodium fluoride (NaF) standards.

2.10.2 HPLC Analysis of Fluoxetine

High-performance liquid chromatography (HPLC) was used to quantify fluoxetine (FLX) concentrations in culture samples. Prior to HPLC analysis, the biomass was removed by centrifuging the sample at 14 000 rpm for 10 min; the supernatant was used for analysis. HPLC analyses were conducted with Waters e2695 Separations Module and Waters 2998 photodiode array (PDA) detector. The separation was conducted under gradient elution with acidified water (trifluoroacetic acid, TFA; pH 2.14) used as mobile phase A and acetonitrile used as mobile phase B. The flow rate was 1.0 mL min^{-1}. The gradient program comprised an increase in the percentage of the organic solvent (mobile phase B) that reduced the retention of fluoxetine on the stationary phase and, consequently, earlier elution of the analyte with better peak shape.

Fluoxetine concentrations were determined by means of external calibration curves, which were prepared by analysis of FLX standards of varying concentrations under the same chromatographic conditions.

2.10.2.1 Fluoxetine calibration and quantification by HPLC

The concentration of fluoxetine (FLX) was determined by external calibration. A stock solution of 10,000 mg L^{-1} FLX was prepared and diluted to prepare a series of standards. Standard calibration solutions ranging from 0.1-200 mg L^{-1} (0.1, 0.2, 0.5, 1, 2, 5, 10, 20 and 200 mg L^{-1}) were prepared and processed under identical conditions as the samples.

Table 10. Fluoxetine standard concentrations and corresponding HPLC peak responses are used for calibration.

FLX (mg/L)	Area (µV+sec)
0.5	3792
1	13542
5	148875
10	310460
20	591207

Standards were injected into the HPLC, and peak areas measured. The linear response observed over the concentration range allowed the construction of a calibration curve by plotting FLX concentration (mg L^{-1}) versus peak area. A high correlation coefficient ($R^2 \approx 0.998$) between concentration and the detector response indicated that the method was fit for quantitative analysis. The detected concentrations of fluoxetine in culture samples were determined by extrapolating the calibration curve and corrected for dilution factors, where applicable.

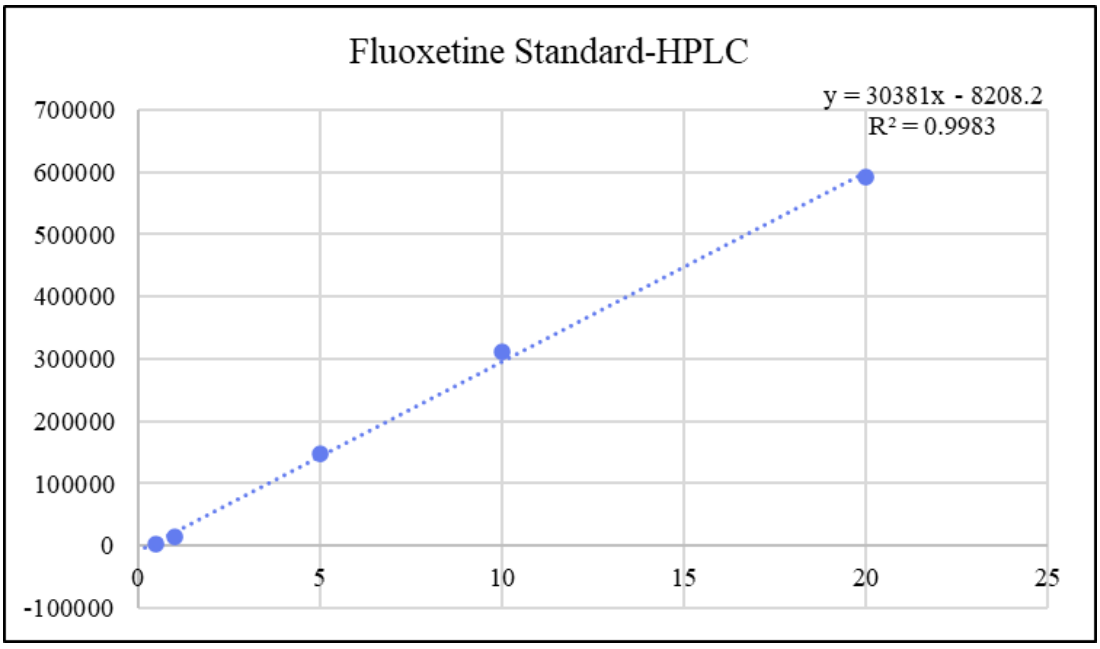

Figure 9. HPLC-based calibration curve showing the relationship between fluoxetine concentration and peak response.

Chapter 3. Results

The effect of cryogenic preservation on microbiomes from two PFAS-impacted matrices, soil, and sediment, was evaluated using both culture-dependent and culture-independent approaches. Enrichment cultures derived from preserved microbiomes were established to assess responses to PFAS exposure and to perform microbial isolation. Additionally, the potential application of preserved microbiomes for bioremediation was investigated.

3.1 Effect of Cryogenic Preservation on Microbial Communities

Culture-based total bacterial counts were employed to assess the effects of cryopreservation on the culturability of microorganisms over time (T0, T1, T2, and T3). In soil samples (Figure 10-A), bacterial counts were constant from T0 to T2, with no significant difference between these time points (all in significance group A). This time range maintained bacterial concentrations in the range of 10^6 - 10^7 CFU g^{-1}. However, a significant decrease was recorded after 12 months (T3, group B) with bacterial counts dropping to 10^5 CFU g^{-1}, suggesting a loss of culturable bacterial abundance during long-term storage.

In sediment (Figure 10-B), bacterial counts showed a significant time-dependent decline during preservation. Bacterial counts were comparable at T1 and T2 and were lowest at T3 in comparison with T0. The T0 value (group AB) was intermediate and statistically comparable to T1 and T2, indicating that initial storage did not have a significant influence on culturable bacterial abundance. While less marked than in soil, the bacterial count in sediment samples also showed a significant decline between T0 and T3, confirming the effect of storage on culturable bacteria.

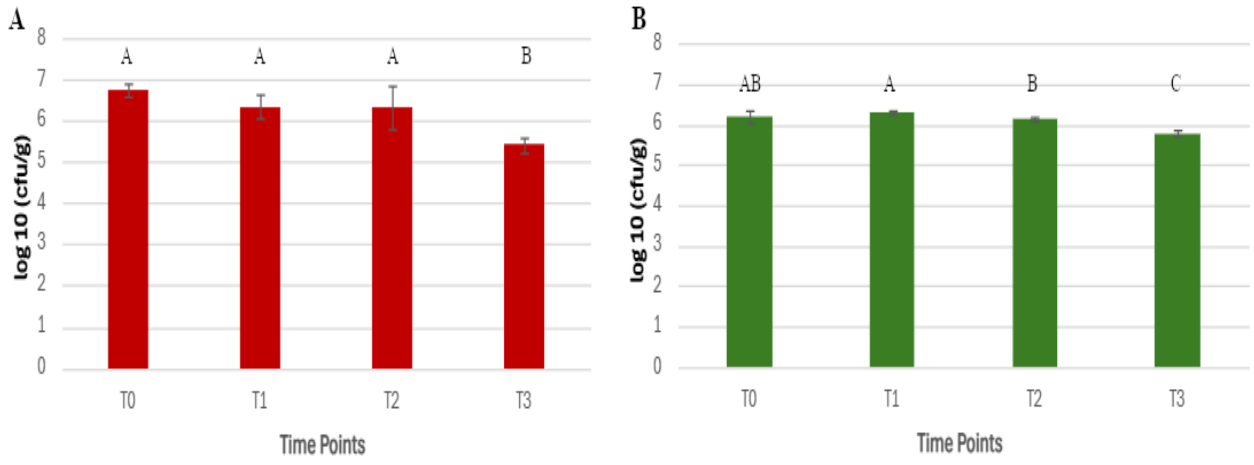

Figure 10. Bacterial total counts performed in Soil (A) and Sediment (B) samples at T0, T1, T2 and T3. Error bars show the standard deviation. Mean values marked by the same letter are not significantly different at $P < 0.05$.

Total fungal counts were evaluated to determine the impact of cryopreservation on culturable fungal communities in soil and sediment (Figure 11). In the soil (Figure 11-A), counts were relatively stable and ranged between 10^4 and 10^5 CFU g^{-1}. T1 and T2 belonged to group AB and

were not significantly different from T0 (A) or T3 (B). However, significant variation in fungal cell counts was detected between T0 and T3, suggesting a slight decrease in culturable fungal populations after 12 months of storage.

In sediments (Figure 11-B), fungal cell counts remained unchanged throughout the preservation period. There were no significant differences between time points (all in group A) and fungal cell concentrations remained in the range of 10^4-10^5 CFU g^{-1}. This finding indicates successful maintenance of culturable fungal communities in sediment.

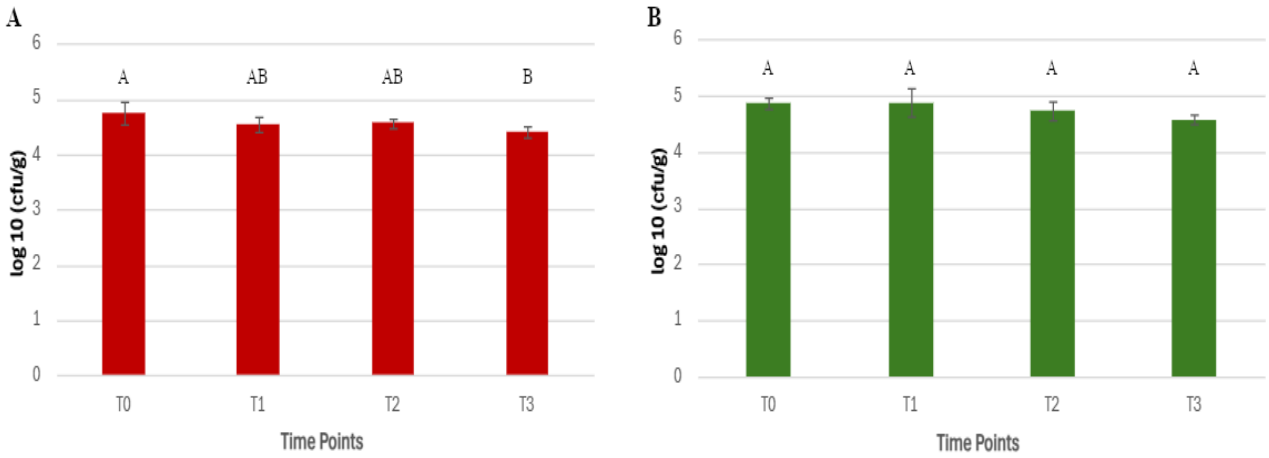

Figure 11. Fungal total counts performed in Soil (A) and Sed (B) samples at T0, T1, T2 and T3. Error bars show the standard deviation. Mean values marked by the same letter are not significantly different at $P < 0.05$.

Overall, soil samples exhibited a significant reduction in both bacterial and fungal counts after 12 months of preservation, with bacterial populations being more markedly affected. In sediment samples, bacterial concentrations showed a significant decrease between T0 and T3, whereas fungal populations remained stable throughout the entire experimentation period.

3.2 Assessment of Microbial Metabolic Activity

Microbial metabolic activity was assessed at four time points (T0, T1, T2, and T3) using Biolog EcoPlates™ to characterize functional change in the communities. The resulting heatmap reflects changes in substrate utilization patterns over time, which reflect changes in microbial metabolic potential (Figure 12).

Overall, the Biolog EcoPlate results showed that there was higher initial metabolic activity in soil compared with the sediment. However, in soil, the ability to utilize diverse carbon sources such as Tween80, beta Methyl-D-Glucoside, N-Acetyl-D-Glucosamine, and Glucose-1-Phosphate dropped dramatically by T3 indicating loss of specific metabolic functions. In comparison, the sediment communities showed a more gradual decrease in substrate use, with progressive declines between time points (e.g. D-Malic Acid at T1, β-Methyl-D-Glucoside, γ-Aminobutyric Acid and L-Asparagine at T2, and D-Galactonic Acid γ-lactone at T3).

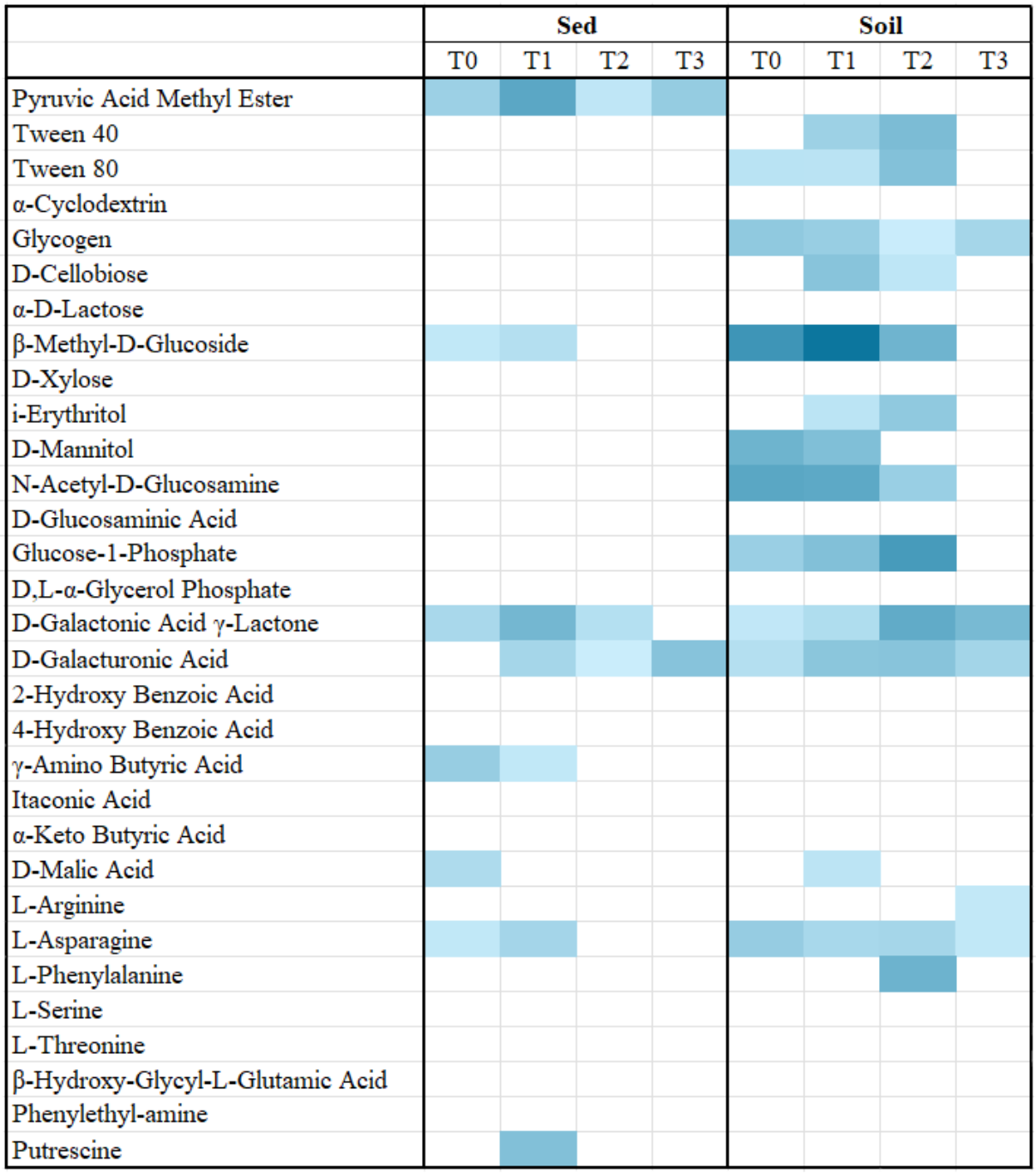

Figure 12. The metabolic activities of the microbiome were evaluated by Biolog EcoPlaltesTM. Blank cells show no activity. Color intensity indicates activity magnitude, with dark representing high activity and light representing less activity. Each data point represents the mean signal intensity of an individual sample after $OD_{590} - OD_{750}$ and background subtractions. A sample is considered positive only when the difference between the sample and its corresponding control exceeds 0.15

The Principal Component Analysis (PCA) (Figure 13-A) revealed a clear discrimination between soil and sediment samples, suggesting the different substrate utilization pattern between the two environmental matrices. The soil samples revealed a significant shift along Component 1 for T3,

indicating a major shift in metabolic profiles during preservation, especially between T2 and T3. In contrast, sediment samples grouped more closely together reflecting greater functional stability and a gradual decline in metabolic activity.

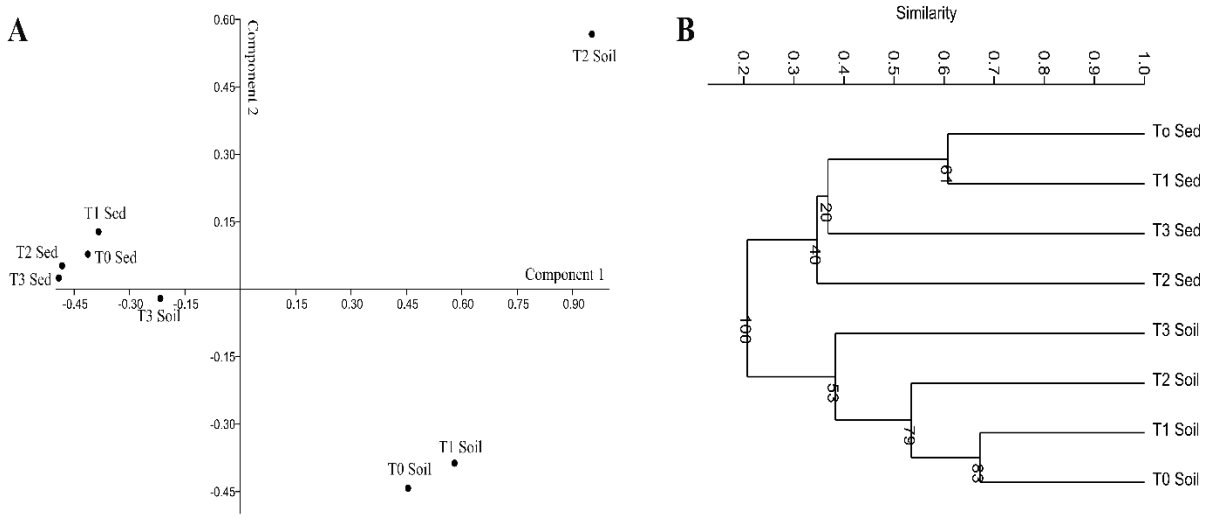

Figure 13. Statistical analysis of Biolog EcoPlates™ results displayed in Fig. 3. (A) Principal Component Analysis and (B) Beta diversity analysis conducted using the UPGMA clustering algorithm with the Bray–Curtis method and 1,000 bootstrap.

The dendrogram (Figure 13-B) also supports these observations identifying two main clusters, separating soil from sediment communities. Moreover, the data support that the most significant metabolic change in soil takes place between T2 and T3. On the other hand, although less pronounced, the main change in sediment occurs from T1 to T2. Collectively, these findings indicate that while both matrices experienced reductions in metabolic potential during long-term preservation.

3.3 Microbial Community Composition

Total genomic DNA was extracted from soil and sediment samples collected at four time points (T0, T1, T2, and T3). Extractions were performed in duplicate for each sample type (SedA, SedB, SoilA, and SoilB), and the results are reported in Table 11. The DNA was eluted in 75 µL of buffer C6 (DNeasy PowerSoil Pro kit®).

Table 11. Qualitative and quantitative analysis of total DNA extracted from Soil and Sediment samples at T0, T1, T2, and T3. The 260/280 and 260/230 ratios (NANODROP) were used to assess DNA purity, whereas DNA concentration (ng/µL and µg/g) was quantified using the QUBIT. Only QUBIT values were used for downstream molecular analysis.

Samples			260/280	260/230	DNA (ng/µL)	DNA (µg/g)
T0-Sed	**SedA**	A1	1.31	0.99	173	14.78 ± 4.86
		A2	1.33	1.1	93.2	
	SedB	B1	1.31	1.68	111	
		B2	1.83	1.13	87.2	

T1-Sed	**SedA**	A1	1.9	0.88	167	22.17 ± 2.57
		A2	1.89	1.84	163	
	SedB	B1	1.9	2	173	
		B2	1.9	1.65	207	
T2-Sed	**SedA**	A1	1.93	0.83	139	17.79 ± 2.44
		A2	1.93	1.07	164	
	SedB	B1	1.92	1.01	154	
		B2	1.92	1.02	119	
T3-Sed	**SedA**	A1	1.91	0.83	220	30.25 ± 2.18
		A2	1.92	1.07	243	
	SedB	B1	1.92	1.01	260	
		B2	1.93	1.02	257	
T0-Soil	**SoilA**	A1	1.32	0.23	35.6	3.23 ± 0.88
		A2	1.93	0.41	20.6	
	SoilB	B1	1.88	0.1	25.6	
		B2	2.08	0.1	21.4	
T1-Soil	**SoilA**	A1	1.85	0.54	33.9	4.61 ± 1.23
		A2	1.9	0.41	47.5	
	SoilB	B1	1.86	0.14	24.9	
		B2	1.9	0.65	41.9	
T2-Soil	**SoilA**	A1	1.85	0.29	16.4	3.61 ± 1.45
		A2	1.96	1.48	21.8	
	SoilB	B1	1.97	0.77	41	
		B2	1.94	0.15	37.4	
T3-Soil	**SoilA**	A1	1.89	0.29	15.4	7.40 ± 3.80
		A2	1.91	1.48	69	
	SoilB	B1	1.91	0.77	67.6	
		B2	1.91	0.15	87.3	

DNA extraction results revealed substantially higher DNA yields in sediment samples (approximately 15–30 µg g^{-1}) compared to soil samples (approximately 3–7.5 µg g^{-1}).
Microbial community composition was characterized through DNA barcoding analysis targeting both bacterial and fungal populations. The relative abundances in sediment and soil samples are presented in Figure 14**.** Alpha diversity was assessed using the Shannon index (Table 12)**,** while beta diversity patterns are illustrated in Figure 15**.**
The Shannon index integrates two key components of diversity:

- **species richness**, representing the number of taxa detected, and
- **species evenness**, describing the relative distribution of abundances within the community.

This index is widely applied in microbial ecology to characterize complex environmental communities and to detect changes in community structure over time (Magurran, 2004).

Table 12. Shannon-index values analyzed at T0, T1, T2, and T3. The bacterial population was assessed at both class and family levels, while the fungal population was evaluated at the class level.

Sample	Bacteria		Fungi
	Class	Family	Class
T0-Sed	2.34 ± 0.05	3.28 ± 0.061	0.89 ± 0.004
T1-Sed	2.31 ± 0.112	3.28 ± 0.013	1.04 ± 0.088
T2-Sed	2.41 ± 0.0318	3.43 ± 0.090	1.1 ± 0.039
T3-Sed	2.13 ± 0.349	2.9 ± 0.54	0.99 ± 0.050
T0-Soil	2.22 ± 0.109	3.47 ± 0.110	1.22 ± 0.137
T1-Soil	2.08 ± 0.127	3.33 ± 0.11	1.28 ± 0.058
T2-Soil	2.21 ± 0.166	3.37 ± 0.13	1.46 ± 0.014
T3-Soil	1.94 ± 0.365	3.32 ± 0.231	1.27 ± 0.095

The Shannon index revealed no substantial differences in microbial (bacterial and fungal) biodiversity, although a slight reduction in bacterial diversity was observed in both soil and sediment at T3.

3.3.1 Microbiome Metagenomic Profiling

Microbial community composition was characterized through DNA barcoding analysis targeting both bacterial and fungal populations. The relative abundances in sediment and soil samples are presented in Figure 14. The fungal community was dominated by the class *Sordariomycetes*, accounting for 34-39% of sequences in sediment and 17-30% in soil samples, respectively. Further, sediment samples had a relatively high proportion of *Dothideomycetes* (~7-13.3%) while soil samples were dominated by *Tremellomycetes* (~4.5-11%) and *Eurotiomycetes* (~3-6%). In both soil and sediment samples, the bacterial community was dominated by *Actinobacteria* (~6.5-25%), *Betaproteobacteria* (~5.5-20%), *Gammaproteobacteria* (~3.5-11.5%) and *Alphaproteobacteria* (~10-20.5%).

Interestingly, *Bacilli* and *Thermoleophilia* had a higher relative abundance in soil (~1-7% and ~14.5-19%) than in sediment (~1-2.3% and ~1.5-8%). In contrast, *Cytophagia* and were more prevalent in sediment (~3-10%) than in soil (~2-3%). At the family level, sediment samples were more abundant in *Comamonadaceae* (~3.5-5.5%) and *Nitrospiraceae* (~2.5-4.5%), while Soil samples were characterized by higher relative abundances of *Bacillaceae* (~2.5–4.5%), *Micrococcaceae* (~2.5–5.5%), and *Oxalobacteraceae* (~2–3.5%).

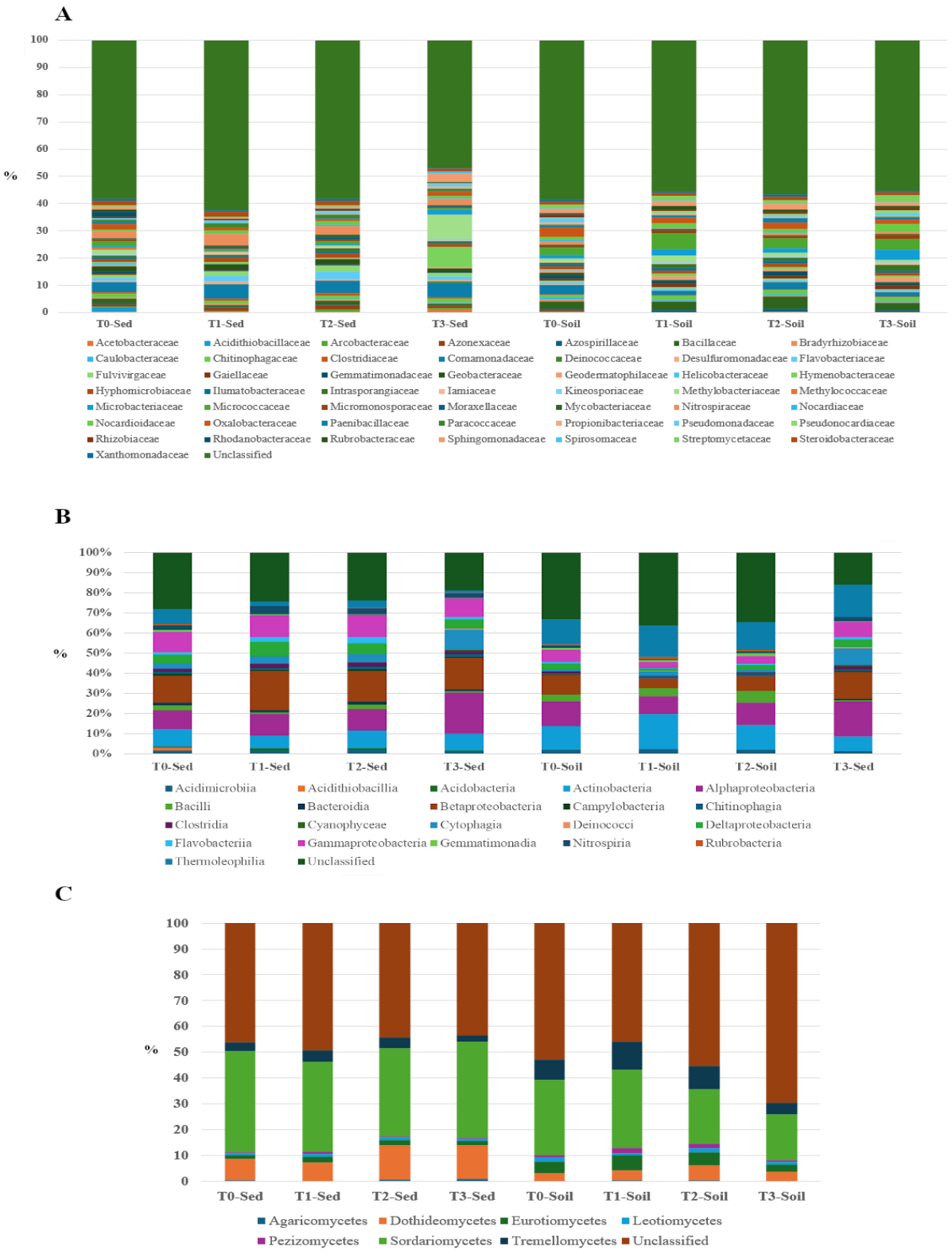

Figure 14. Relative abundances of bacterial communities at the family (A) and class (B) levels, and fungal communities at the class (C) level. Percentages represent the mean values obtained from two biological replicates.

3.3.2 Temporal Dynamics of Microbial Diversity and Community Structure

Microbial diversity was evaluated by distinguishing between alpha diversity, which describes diversity within individual samples, and beta diversity, which describes differences in community composition among samples and across time points (Anderson et al., 2011; Author & Whittaker, 1960; Magurran, 2004).

Beta diversity was investigated using multivariate statistical approaches to compare microbial community composition among samples enabled:

- identification of the main gradients driving sample separation, and
- comparison of microbial community dynamics across sampling times (T0–T3) and between environmental matrices (soil and sediment) (Ramette, 2007).

The relative abundance of bacterial phyla across enrichment samples is presented in Figure 15 for Sediment-derived microbiomes (A1) and Soil-derived microbiomes (A2). The heatmaps illustrate variations in community composition across different preservation time points (T0–T3). The bacterial communities from both matrices were dominated by *Proteobacteria*, *Bacteroidota* and *Actinobacteriota*, which were consistently present in all samples, showing the presence of a mutual core microbiome. Other phyla such as *Campylobacterota*, *Cyanobacteria*, and *Deinococcota* were present in all samples, but with varying relative abundances. By contrast, minor phyla, including *Acidobacteriota*, *Gemmatimonadota*, *Verrucomicrobiota*, and *Nitrospirota* exhibited greater variability, likely reflecting differential tolerances to preservation and enrichment conditions.

Metabarcoding and clustering analyses showed that the overall community structure remained largely preserved across T0–T3 in both soil and sediment microbiomes. No clear temporal clustering of samples was observed, as samples from different time points and replicates were intermixed, with no clear grouping observed.

Figure 15 also shows the relative abundance of fungal classes in enrichment samples derived from Sediment (B1) and Soil (B2) microbiomes. In both matrices, fungal communities were dominated by *Agaricomycetes*, *Leotiomycetes* and *Pezizomycetes*, which were present at high abundance in all samples, suggesting the retention of a core fungal community structure following preservation. *Dothideomycetes* and *Eurotiomycetes* were present in moderate abundance, whereas *Sordariomycetes* and *Tremellomycetes* were generally less abundant and more variable. In both Sed and Soil derived microbiomes (B1), class-level profiles were relatively uniform across T0–T3, with only minor fluctuations in relative abundance. Like bacterial communities, the overall fungal community structure was largely preserved over time, with no clear temporal clustering of samples observed.

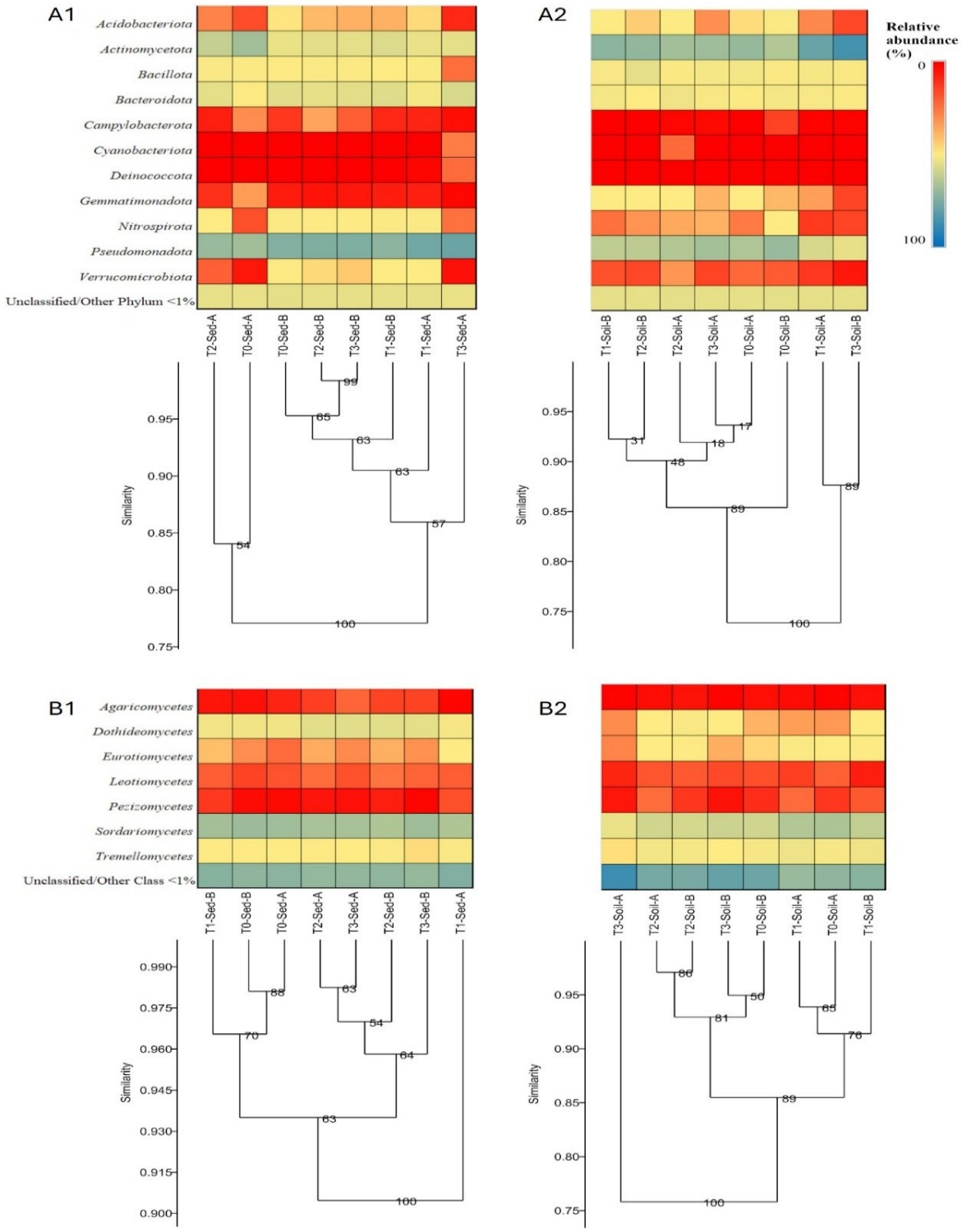

Figure 15. Metabarcoding-based community composition across samples (T0–T3) without replicate averaging. Bacterial phyla in sediment (A1) and soil (A2); (B1–B2) fungal classes in sediment (B1) and soil (B2). Heatmaps show relative abundance (%), and dendrograms represent Bray–Curtis (UPGMA) clustering of individual samples.

3.4 Temporal Variation in DNA Yield from Enrichment Cultures

Enrichment cultures were established using PFOA as the selective compound at a concentration of 300 mg L^{-1} to 600 mg L^{-1} in minimal defined medium. At each time point (T0, T1, T2, and T3), DNA was extracted in duplicate from enrichment cultures derived from Soil A, Soil B, Sed A, and Sed B. For each extraction, 10 mL of enrichment culture was processed, and DNA was eluted in 80 µL of Soultion EB (DNeasy PowerWater Pro kit®). DNA yield results are reported in Table 13.

Table 13. Qualitative and quantitative analysis of DNA extracted from enrichment cultures at different time points (T0–T3). DNA purity was assessed using NanoDrop 260/280 and 260/230 absorbance ratios for each sample. DNA concentration measured by NanoDrop is reported as ng μL^{-1} for each replicate, while DNA yield quantified per culture volume is expressed as µg mL^{-1} and reported as mean ± standard deviation for each time point.

Samples			260/280	260/230	DNA (ng/µL)	DNA (µg/mL)
T0-Sed	**SedA**	A1	1.91	1.8	180.3	**1.5134 ± 0.4689**
		A2	1.89	1.54	163.1	
	SedB	B1	1.15	1.30	273.5	
		B2	1.89	2.00	139.8	
T1-Sed	**SedA**	A1	1.79	0.29	32.2	**0.5886 ± 0.3166**
		A2	1.88	1.30	125.0	
	SedB	B1	1.83	1.02	56.5	
		B2	1.81	0.60	80.6	
T2-Sed	**SedA**	A1	1.89	2.01	66.2	**0.8318 ± 0.2139**
		A2	1.96	2.00	113.4	
	SedB	B1	1.93	2.22	128.8	
		B2	1.90	1.87	107.5	
T3-Sed	**SedA**	A1	2.15	2.00	235.6	**1.8198 ± 0.3806**
		A2	2.11	2.09	291.6	
	SedB	B1	1.86	1.42	190.4	
		B2	1.89	0.84	192.3	
T0-Soil	**SoilA**	A1	1.88	0.93	78.8	**0.5918 ± 0.3657**
		A2	1.90	1.28	136.3	
	SoilB	B1	1.83	0.4	47.7	
		B2	1.90	1.58	33.1	
T1-Soil	**SoilA**	A1	1.91	0.73	47.2	**0.2884 ± 0.1108**
		A2	1.75	0.40	21.7	
	SoilB	B1	1.73	1.15	26.7	
		B2	1.62	0.56	48.6	
T2-Soil	**SoilA**	A1	1.91	2.00	69.4	**0.4784 ± 0.1543**
		A2	1.84	1.91	46.0	
	SoilB	B1	1.86	1.87	41.6	
		B2	1.89	2.12	82.2	
T3-Soil	**SoilA**	A1	2.09	0.71	62.2	
		A2	2.26	0.53	129.7	

	SoilB	B1	1.88	0.84	29.9	**0.5242 ± 0.3588**
		B2	2.00	1.00	40.3	

DNA concentrations showed variability among replicates and across time points for both soil- and sediment-derived enrichment cultures. In comparison to soil enrichment cultures, sediment enrichment cultures generally exhibited higher DNA yields. The DNA concentration in sediment samples varied over time between 0.58 ± 0.32 and 1.82 ± 0.38 µg mL^{-1}, with the highest concentrations found at T3. DNA yields in all soil-derived enrichment cultures were lower, with a range of 0.29 + 0.11 to 0.59 + 0.37 µg mL^{-1}, with moderate variability over time of preservation.

Despite variability among individual replicates, DNA was successfully recovered from all samples and time points, confirming suitability for downstream molecular analyses.

3.5 Comparative DGGE Profiling of Enriched Microbiomes

Following enrichment, changes in microbial community structure were assessed by PCR-DGGE analysis of bacterial 16S rRNA gene fragments for both sediment and soil samples (Figure 16).

Both environmental matrices displayed complex and time-dependent banding profiles in DGGE profiles. Several bands were observed at all the time points in sediment samples, which revealed that there were bacterial populations that could survive under PFOA-selective conditions. Although multiple bands were preserved during preservation time points (T0-T3), changes in band intensity and the emergence of bands were noted, indicating changes in the community after enrichment.

Significant temporal changes were observed in soil samples. The variations between replicate samples (A and B) were low and showed good reproducibility of the DGGE patterns. In general, the PCR-DGGE analysis showed dynamic time-dependent changes in the composition of the microbial communities that occurred in both soil and sediment microbiomes.

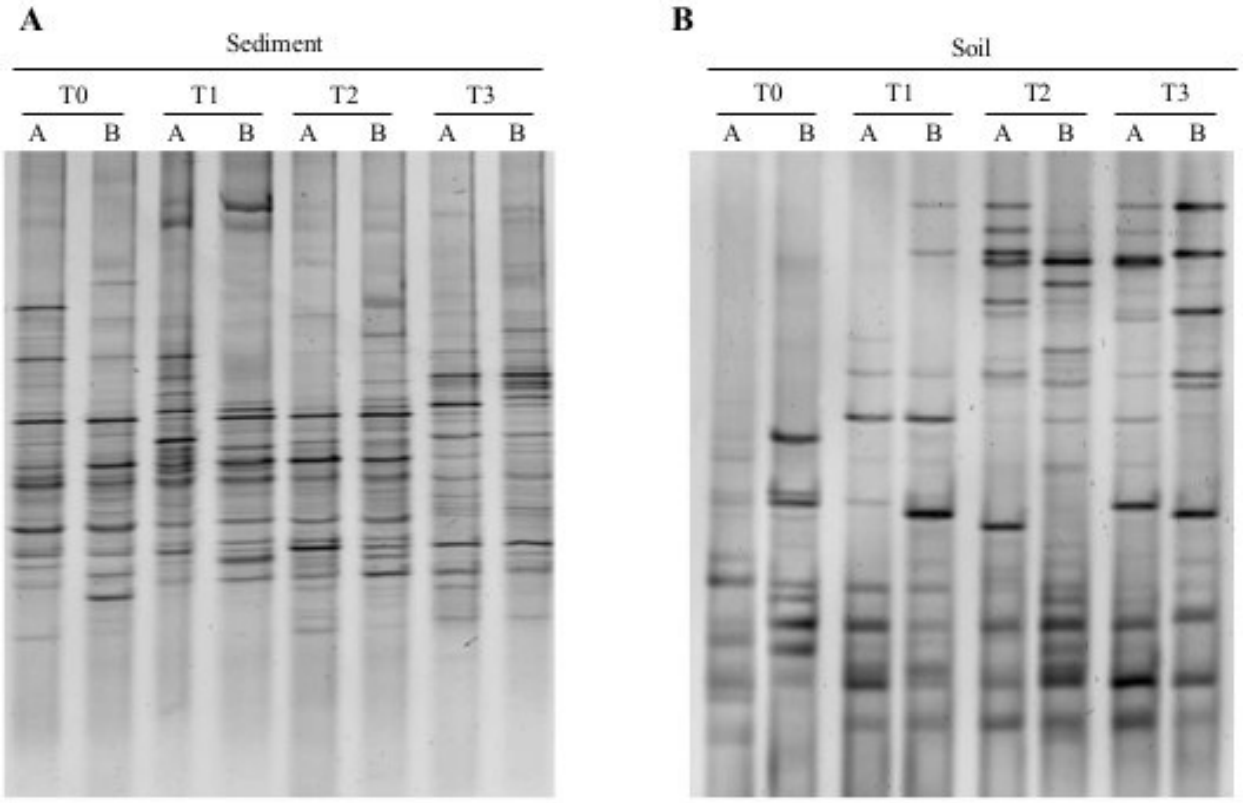

Figure 16. DGGE electrophoresis gels obtained from T0, T1, T2 and T3 of Sediment (A) and Soil (B) samples.

3.5.1 UPGMA Cluster Analysis of DGGE Profiles

The dendrograms constructed based on the UPGMA clustering algorithm depict the similarity relationships between the DGGE profiles of the enriched sediment (A1) and soil (B1) microbiomes at various time points (T0-T3) (Figure 17). Presence of bands were used to cluster and indices of similarity are represented in terms of percentage of similarity.

In the case of samples of sediment (A1), the replicate profiles (A and B) at the same time points were clustered close to each other. T1 and T2 samples were more similar, whereas T0 and T3 were further divided into two distinct clusters, indicating that community structure changed progressively during the enrichment with PFOA. In the case of soil samples (B1), there was a simlar temporal separation. The earliest enrichment stages (T0) were concentrated in a single cluster, whereas T1 and T2 samples were included into distinct branches with lower similarity indices. Eventually, T3 formed a separated unique cluster. The clustering of replicates at each time point verified consistency in duplicate enrichments.

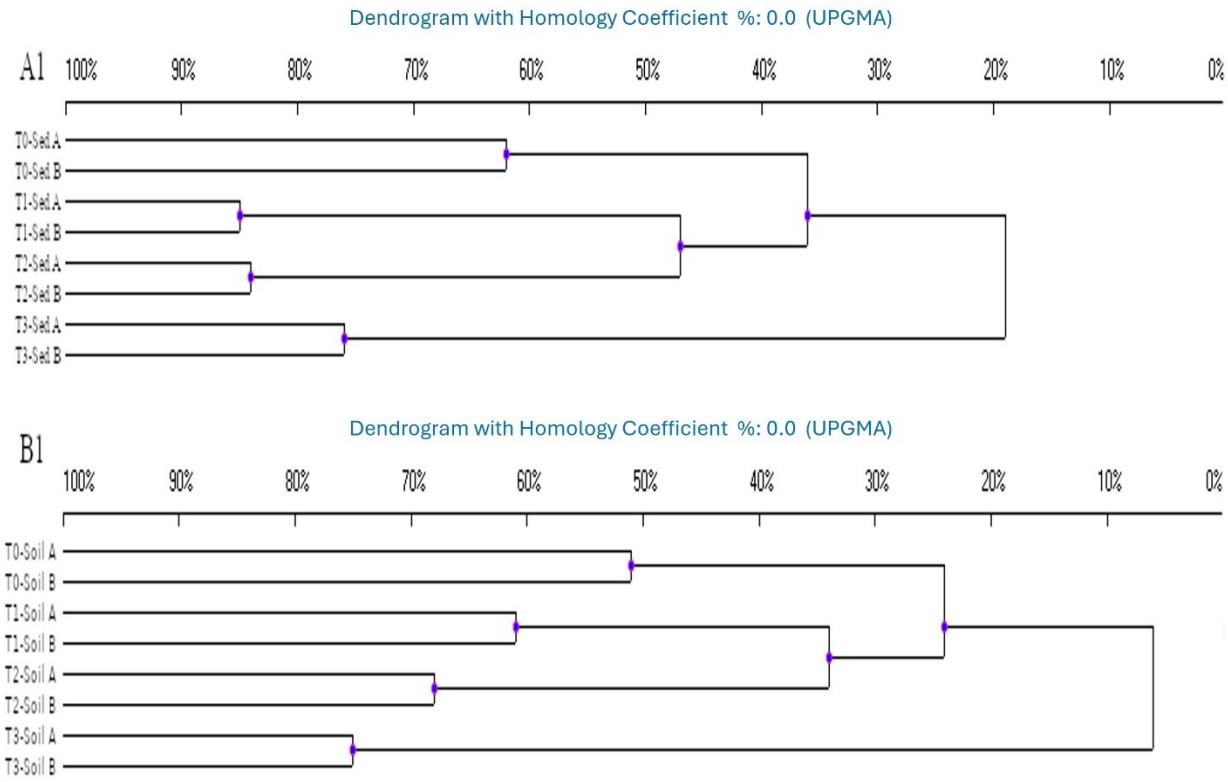

Figure 17. Dendrograms based on PCR-DGGE profiles showing similarity relationships among enriched microbial communities from sediment (A1) and soil (B1) samples collected at different time points (T0–T3). Replicate enrichments (A and B) are shown for each time point. Dendrogram with homology coefficient %: 0.0 (UPGMA)

Overall, approximately 35% and 25% similarity were observed between T0 and T1/T2 clusters in sediment and soil samples, respectively. Moreover, similarity between T0 and T3 decreased to about 20% in sediment and 5% in soil. These clustering patterns reveal time-dependent structuring of microbial communities in both sediment and soil enrichment cultures, with soil microbiomes exhibiting greater divergence across enrichment stages than sediment microbiomes.

3.6 Total Microbial Count from Enrichment Cultures

Both for bacterial and fungal total count for each environmental matrix, analyses were conducted at the end of the enrichment culture in two biological replicates (A and B). Each biological replicate was further analyzed in duplicate as technical replicates. Total viable bacterial counts were monitored in both soil and sediment samples at each enrichment time (T0, T1, T2, and T3) (Figure 18). In soil-derived samples (Figure 18-A), bacterial counts in enrichment culture performed at T0 showed about 10^7 CFU mL^{-1}, reaching values of approximately 10^9 CFU mL^{-1} at T2.

After that a decrease in bacterial count was observed at T3, which was comparable to T0, indicating sustained bacterial growth under enrichment conditions. In sediment-derived samples (Figure 18-B), enrichment cultures at T0 and T1 showed approximately same total count values, around 10^7 CFU mL^{-1}, T2 showed higher counts approximately 10^8 CFU mL^{-1},T3 showed a slight decrease in counts. Overall, enrichment cultures at T2, consistently exhibited higher bacterial counts in both soil and sediment-derived cultures.

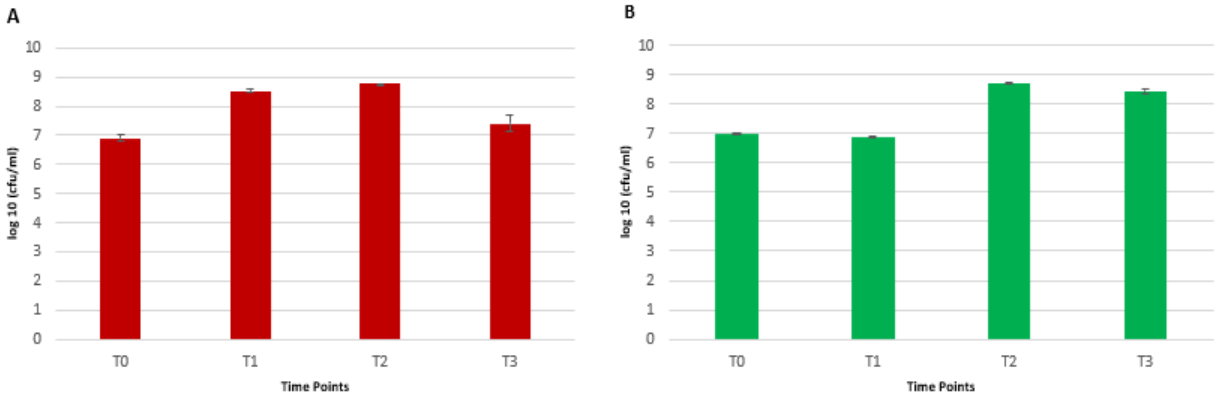

Figure 18. Total viable bacterial counts from enrichment cultures at different time points (T0–T3). A: soil-derived enrichment cultures; B: sediment-derived enrichment cultures. Values represent mean ± standard deviation.

Fungal total counts from enrichment cultures are presented in Figure 19. In soil-derived enrichment cultures (Figure 19-A), fungal counts increased from approximately 10^5 CFU mL^{-1} at T0 to an approximate number of around 10^7 CFU mL^{-1} at T1, T2 and T3.

In sediment-derived samples (Figure 19-B), fungal counts were approximately 10^5 CFU mL^{-1} in enrichment cultures at T0 and increased markedly at T1 to values close to 10^8 CFU mL^{-1}.At T2, counts that remained high near to 10^8 CFU mL^{-1}, followed by a moderate decrease at T3 to approximately 10^7 CFU mL^{-1}.

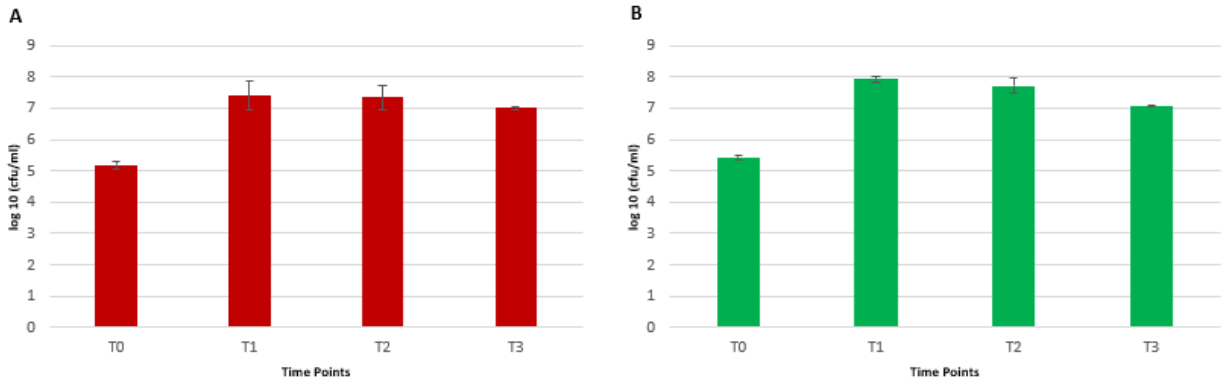

Figure 19. Total viable fungal counts from enrichment cultures at different time points (T0–T3). A: soil-derived enrichment cultures; B: sediment-derived enrichment cultures. Values represent mean ± standard deviation.

3.7 Microbial Isolates from Enrichment Cultures

Microbial isolation (both bacterial and fungal) was carried out using a direct isolation approach. Enrichment cultures obtained at each time point (T0, T1, T2, and T3) were serially diluted and spread onto appropriate solid media to allow colony development. Plates were incubated at 27 °C for 5 days, after which well-isolated and morphologically distinct colonies were selected. These colonies were transferred onto fresh media and sub-cultured through three successive streaking steps to obtain pure cultures. The number of isolates obtained from soil and sediment enrichment cultures at different time points is summarized in Tables 14 and 15.

Table 14. Number of bacterial isolates obtained from TSA plates following enrichment cultures at different time points.

Time point	Soil	Sediment
T0	19	15
T1	18	19
T2	16	16
T3	18	17
Total	71	67
Total	138	

Table 15. Number of fungal isolates obtained from MALT plates following enrichment cultures at different time points.

Time Point	Soil	Sediment
T0	7	6
T1	6	6
T2	7	7
T3	8	6

Total	28	25
Total	53	

3.7.1 Molecular Characterization of Isolated Strains

3.7.1.1 BOX-PCR Fingerprinting of the Isolated Strains

Genotypic diversity of culturable isolates was evaluated using BOX-PCR fingerprinting. Each isolate was subjected to genomic DNA extraction; amplification products were separated using agarose gel electrophoresis, and visual comparison of banding pattern was performed. Isolates with the same BOX- PCR patterns were classified into one operational taxonomic unit (OTU), regardless of the time of sampling.

Soil. BOX-PCR profiles from soil-derived isolates (LA/LB groups) resolved into 51 bacterial OTUs, indicating substantial genotypic heterogeneity within the soil culturable fraction.

Sediment. BOX-PCR profiles from sediment-derived isolates (SA/SB groups) resolved into 55 bacterial OTUs, showing slightly higher genotypic richness compared to soil.

There were only two OTUs that overlapped between soil and sediment, (Table 16). Three isolates (3T2SA, 4T2SB, and 6T2SA) were subsequently identified as fungal by ITS sequencing and were excluded from the bacterial OTU dataset.

Table 16. Bacterial OTU richness by matrix based on BOX-PCR fingerprinting.

Matrix	Number of OTUs
Soil	51
Sediment	55
OTUs shared between matrices	2
Total Bacterial OTUs	**103**

3.7.1.2 Taxonomic Identification by 16S rRNA Gene Sequencing

Following BOX-PCR genotyping, selected bacterial isolates were preliminarily identified by partial 16S rRNA gene sequencing. The obtained sequences were quality-checked, trimmed, and assembled using BioEdit Sequence Alignment Editor (version 7.7.1) (Hall, 1999) prior to analysis. Taxonomic identification was performed using BLASTN searches against the NCBI database and further refined using the EzBioCloud database with restriction to type strains.

Sequence-based identification was based on partial 16S rRNA gene regions, which are widely used as molecular markers for taxonomic classification, although they may not always allow

discrimination at the species level ((Altschul et al., 1990; Yoon et al., 2017). The length of the sequences utilized for taxonomic identification was approximately 700–900 bp, consistent with partial 16S rRNA gene sequencing.

These bacterial isolates are from enrichment cultures exposed to increasing PFOA concentrations (300 mg L^{-1} for 7 days, followed by 600 mg L^{-1} for an additional 7 days). Soil A (LA) and Soil B (LB) represent two biological replicates derived from the Lonigo site (L). T denotes recovery on tryptic soy agar (TSA) plates, while T0–T3 indicate the respective enrichment time points (Table 17).

Table 17. Taxonomic identification of isolates recovered from soil enrichment cultures (LA and LB) following PFOA exposure (300–600 mg L^{-1}). The table reports matrices of origin, isolate codes, closest type strain matches based on 16S rRNA gene sequencing, identity percentages, and phylogenetic affiliations.

Matrices	Strain	Taxon with the higher % similarity	Identity %	Phylogeny
Soil A T0	**1T0LA**	*Achromobacter animicus* LMG 26690^T	99.75	Betaproteobacteria
	2T0LA	*Klebsiella aerogenes* KCTC 2190^T	99.88	Gammaproteobacteria
	3T0LA	*Citrobacter portucalensis* A60^T	100	Gammaproteobacteria
	4T0LA	*Achromobacter aegrifaciens* LMG 26852^T	99.87	Betaproteobacteria
	5T0LA (6T0LA)	*Achromobacter agilis* LMG 3411^T	99.88	Betaproteobacteria
	7T0LA	*Achromobacter animicus* LMG 26690^T	100	Betaproteobacteria
Soil B T0	**1T0LB** (6T0LB, 9T0LB, 12T0LB, 2T2LB 7T2LB)	*Pseudomonas plecoglossicida* NBRC 103162^T	100	Gammaproteobacteria
		Pseudomonas ceruminis BML-PP028^T	100	Gammaproteobacteria
	2T0LB	*Stenotrophomonas nitritireducens* DSM 12575^T	99.72	Gammaproteobacteria
	3T0LB	*Stenotrophomonas maltophilia* MTCC 434^T	99.88	Gammaproteobacteria
	4T0LB	*Stenotrophomonas nitritireducens* DSM 12575^T	95.97	Gammaproteobacteria
	7T0LB (11T0LB)	*Brevundimonas olei* MJ15^T	100	Alphaproteobacteria
	10T0LB	*Shinella zoogloeoides* ATCC 19623^T	100	Alphaproteobacteria
Soil A T1	**1T1LA**	*Pseudomonas hibiscicola* ATCC 19867^T	100	Gammaproteobacteria
	2T1LA(3T1LA, 4T1LA)	*Pseudomonas plecoglossicida* NBRC 103162^T	100	Gammaproteobacteria
	5T1LA	*Brucella cytisi* ESC1^T	100	Alphaproteobacteria
	6T1LA	*Leclercia adecarboxylata* NBRC 102595^T	99.41	Gammaproteobacteria
	7T1LA	*Silvania hatchlandensis* H19S6^T	99.46	Gammaproteobacteria
Soil B T1	**8T1LA**	*Citrobacter portucalensis* A60^T	99.25	Gammaproteobacteria
	1T1LB	*Pseudomonas alloputida* Kh7^T	100	Gammaproteobacteria
	2T1LB	*Achromobacter ruhlandii* ATCC 15749^T	92.97	Betaproteobacteria

	3T1LB	*Pseudomonas plecoglossicida* NBRC 103162^T	100	Gammaproteobacteria
		Pseudomonas ceruminis BML-PP028^T	100	Gammaproteobacteria
	4T1LB	*Stenotrophomonas indicatrix* WS40^T	100	Gammaproteobacteria
	5T1LB	*Brucella daejeonensis* MJ11^T	98.71	Alphaproteobacteria
	6T1LB	*Stenotrophomonas nitritireducens* DSM 12575^T	99.07	Gammaproteobacteria
	7T1LB (6T2LB)	*Pseudomonas urmiensis* SWRI10^T	99.25	Gammaproteobacteria
	8T1LB (9T1LB)	*Pseudomonas persica* RUB6^T	99.34	Gammaproteobacteria
	10T1LB	*Brucella pseudogrignonensis* CCUG 30717^T	99.23	Alphaproteobacteria
Soil A T2	**1T2LA**	*Stenotrophomonas nitritireducens* DSM 12575^T	99.62	Gammaproteobacteria
	2T2LA	*Microbacterium saccharophilum* K-1^T	99.11	Actinomycetia
	3T2LA (1T2LB)	*Flavobacterium humidisoli* MMS21-Er5^T	98.64	Flavobacteriia
	4T2LA	*Brucella cytisi* ESC1^T	100	Alphaproteobacteria
	5T2LA	*Chryseobacterium cucumeris* GSE06^T	99.75	Flavobacteriia
	6T2LA (7T2LA)	*Shinella zoogloeoides* ATCC 19623^T	100	Alphaproteobacteria
	8T2LA	*Leclercia adecarboxylata* NBRC 102595^T	99.38	Gammaproteobacteria
Soil B T2	**3T2LB**	*Brucella cytisi* ESC1^T	100	Alphaproteobacteria
	4T2LB	*Flavobacterium humidisoli* MMS21-Er5^T	97.68	Flavobacteriia
	5T2LB	*Escherichia hermannii* CIP 103176^T	99.5	Gammaproteobacteria
	8T2LB	*Enterobacter kobei* DSM 13645^T	100	Gammaproteobacteria
	9T2LB	*Sphingobacterium thalpophilum* DSM 11723^T	99.64	Sphingobacteriia
Soil A T3	**1T3LA**	*Microbacterium sufflavum* SSW1-47^T	100	Actinomycetia
	2T3LA	*Microbacterium commune* Re1^T	99.75	Actinomycetia
	3T3LA	*Agromyces chromiiresistens* H3Y2-19a^T	99.39	Actinomycetia
	4T3LA (5T3LA)	*Microbacterium saccharophilum* K-1^T	99.2	Actinomycetia
	6T3LA	*Microbacterium commune* Re1^T	99.73	Actinomycetia
	7T3LA	*Curtobacterium flaccumfaciens* LMG 3645^T	100	Actinomycetia
	8T3LA	*Prescottella equi* DSM 20307^T	100	Actinomycetia
Soil B T3	**1T3LB**	*Microbacterium sufflavum* SSW1-47^T	100	Actinomycetia
	2T3LB	*Sphingomonas montis* DRJ-4^T	100	Alphaproteobacteria
	3T3LB	*Microbacterium sufflavum* SSW1-47^T	100	Actinomycetia
	4T3LB	*Alcaligenes ammonioxydans* HO-1^T	98.37	Betaproteobacteria
	5T3LB	*Microbacterium sufflavum* SSW1-47^T	99.86	Actinomycetia
	6T3LB	*Brevundimonas intermedia* ATCC 15262^T	99.75	Alphaproteobacteria
	7T3LB	*Microbacterium paraoxydans* NBRC 103076^T	99.88	Actinomycetia
	8T3LB	*Stenotrophomonas nitritireducens* DSM 12575^T	99.62	Gammaproteobacteria

Isolates were also obtained from sediment enrichment cultures under increasing PFOA concentrations (300–600 mg L^{-1}). Sediment A (SA) and Sediment B (SB) represent two biological replicates derived from the sediment samples (S), with T indicating TSA recovery plates and T0–T3 denoting enrichment time points (Table 18).

Table 18. Taxonomic identification of isolates recovered from sediment enrichment cultures (SA and SB) following PFOA exposure. The table reports enrichment time points (T0–T3), isolate codes, closest type strain matches based on 16S rRNA gene sequencing, accession numbers, identity percentages, and phylogenetic affiliations.

Matrices	Strain	Taxon with the higher % similarity	Identity %	Phylogeny
Sediment A T0	**1T0SA**	*Klebsiella aerogenes KCTC 2190*^{T}	99.73	Gammaproteobacteria
	2T0SA	*Raoultella ornithinolytica* JCM 6096^{T}	99.37	Gammaproteobacteria
	3T0SA	*Stenotrophomonas pictorum* JCM 9942 ^{T}	100	Gammaproteobacteria
	4T0SA (5T0SA)	*Pseudomonas chlororaphis subsp. Aureofaciens* NBRC 3521^{T}	100	Gammaproteobacteria
	6T0SA (7T0SA, 8T0SA)	*Stenotrophomonas maltophilia* MTCC 434 ^{T}	99.73	Gammaproteobacteria
	9T0SA (7T2SB)	*Pseudomonas monsensis* PGSB 8459^{T}	100	Gammaproteobacteria
Sediment B T0	**1T0SB** (2T0SB)	*Citrobacter portucalensis* A60^{T}	100	Gammaproteobacteria
	3T0SB	*Leclercia adecarboxylata* NBRC 102595^{T}	99.88	Gammaproteobacteria
	4T0SB	*Stenotrophomonas cyclobalanopsidis* ^{T}	98.45	Gammaproteobacteria
	5T0SB	*Stenotrophomonas indicatrix* WS40^{T}	99.37	Gammaproteobacteria
	6T0SB	*Brucella cytisi* ESC1^{T}	100	Alphaproteobacteria
Sediment A T1	**2T1SA**	*Pseudomonas nitroreducens DSM 14399*^{T}	98.66	Gammaproteobacteria
		Pseudomonas nitritireducens WZBFD3-5A2^{T}	98.66	Gammaproteobacteria
	3T1SA	*Stenotrophomonas mori* DY006^{T}	99.15	Gammaproteobacteria
	4T1SA	*Stenotrophomonas acidaminiphila* JCM 13310^{T}	99.47	Gammaproteobacteria
	5T1SA	*Pseudomonas nitroreducens* DSM 14399^{T}	99.76	Gammaproteobacteria
	6T1SA	*Pseudomonas nitroreducens* DSM 14399^{T}	99.53	Gammaproteobacteria
	7T1SA (6T1SB)	*Raoultella ornithinolytica* JCM 6096^{T}	100	Gammaproteobacteria
Sediment B T1	**2T1SB**	*Klebsiella huaxiensis* WCHKl090001^{T}	95.72	Gammaproteobacteria
	3T1SB	*Pseudomonas nitroreducens* DSM 14399^{T}	99.14	Gammaproteobacteria
	4T1SB (11T1SB)	*Brucella cytisi* ESC1^{T}	100	Alphaproteobacteria
	5T1SB	*Leclercia adecarboxylata* NBRC 102595^{T}	99.88	Gammaproteobacteria
	7T1SB	*Stenotrophomonas terrae* DSM 18941^{T}	99.65	Gammaproteobacteria
	8T1SB	*Pseudomonas nitroreducens* DSM 14399^{T}	99.75	Gammaproteobacteria
	9T1SB	*Glutamicibacter uratoxydans* NBRC 15515^{T}	98.59	Actinomycetia
	10T1SB	*Raoultella terrigena* ATCC 33257^{T}	99.5	Gammaproteobacteria
Sediment A T2	**1T2SA**	*Klebsiella pneumoniae* subsp. *pneumoniae* DSM 30104^{T}	99.74	Proteobacteria
	2T2SA	*Klebsiella variicola* subsp. *variicola* DSM 15968^{T}	99.87	Proteobacteria
	4T2SA	*Brucella cytisi* ESC1^{T}	100	Alphaproteobacteria
	5T2SA	*Brucella cytisi* ESC1^{T}	100	Alphaproteobacteria
	7T2SA	*Pectobacterium carotovorum* NCPPB 312^{T}	100	Gammaproteobacteria
	8T2SA	*Brucella pseudogrignonensis* CCUG 30717^{T}	98.83	Alphaproteobacteria
	1T2SB (3T2SB)	*Klebsiella pneumoniae* subsp. *rhinoscleromatis* ATCC 13884^{T}	99.75	Proteobacteria

Sediment B T2	**5T2SB**	*Klebsiella pneumoniae* subsp. *rhinoscleromatis* ATCC 13884^T	99.75	Proteobacteria
	6T2SB	*Brucella cytisi* ESC1^T	100	Alphaproteobacteria
	8T2SB	*Microbacterium tenebrionis* YMB-B2^T	99.76	Actinomycetia
	9T2SB	*Brevundimonas intermedia* ATCC 15262^T	99.87	Alphaproteobacteria
Sediment A T3	**1T3SA**	*Brevundimonas diminuta* ATCC 11568^T	99.88	Alphaproteobacteria
	2T3SA	*Raoultella ornithinolytica* JCM 6096^T	100	Gammaproteobacteria
	3T3SA	*Rhodanobacter soli* DCY45^T	98.75	Gammaproteobacteria
	4T3SA	*Stenotrophomonas nitritireducens* DSM 12575^T	99.6	Gammaproteobacteria
	5T3SA	*Sphingobacterium mizutaii* NCTC 12149^T	99.76	Sphingobacteriia
	6T3SA	*Herbaspirillum huttiense* subsp. *huttiense* ATCC 14670^T	99.86	Betaproteobacteria
	7T3SA	*Brucella pseudogrignonensis* CCUG 30717^T	99.88	Alphaproteobacteria
		Brucella thiophenivorans DSM 7216^T	98.88	Alphaproteobacteria
	8T3SA	*Pusillimonas noertemannii* DSM 10065^T	99.88	Betaproteobacteria
Sediment B T3	**1T3SB**	*Klebsiella variicola* subsp. *tropica* SB5531^T	100.00	Gammaproteobacteria
	2T3SB	*Pseudomonas nitroreducens* DSM 14399^T	99.77	Gammaproteobacteria
	3T3SB	*Citrobacter portucalensis* A60^T	100	Gammaproteobacteria
	4T3SB	*Brevundimonas intermedia* ATCC 15262^T	99.36	Alphaproteobacteria
	5T3SB	*Rhodococcoides fascians* LMG 3623^T	99.63	Actinomycetia
	6T3SB	*Brucella cytisi* ESC1^T	100	Alphaproteobacteria
	8T3SB (7T3SB)	*Brevundimonas intermedia* ATCC 15262^T	95.23	Alphaproteobacteria

The distribution of bacterial genera isolated from soil showed temporal variation across enrichment time points (T0–T3). At T0, multiple genera were detected, with a relatively balanced distribution among dominant taxa. At T1, with a clear predominance of *Pseudomonas*. At T2, community composition shifted, showing a more even distribution among several genera, including *Flavobacterium*, *Brucella*, and *Chryseobacterium*. At T3, *Microbacterium* became the dominant genus, while other taxa were present in lower numbers (Figure 20).

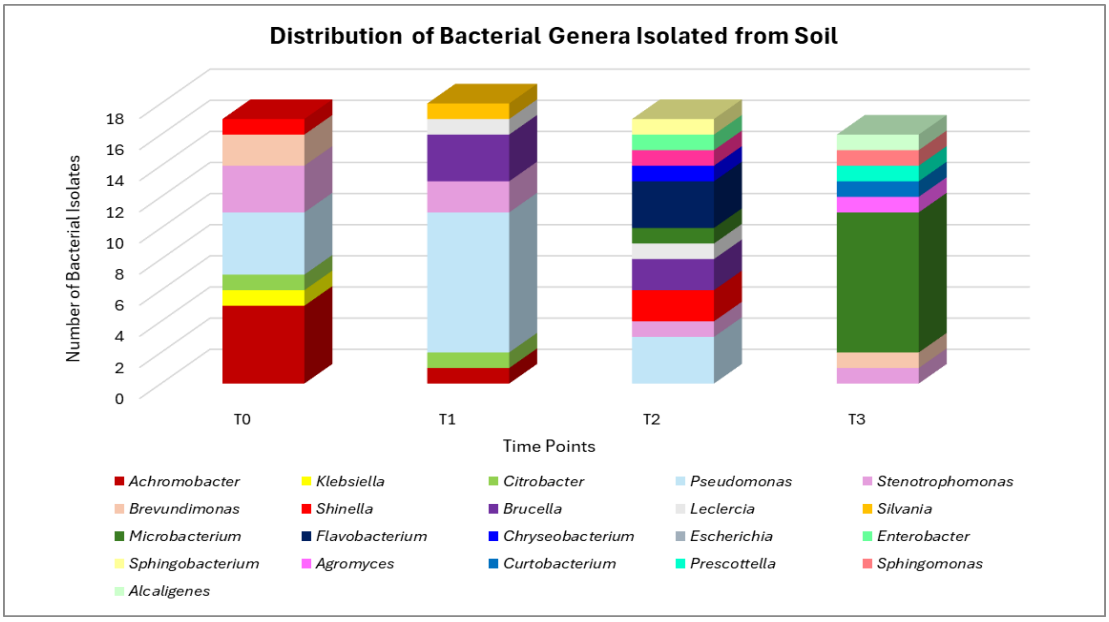

Figure 20. Temporal variation in soil-derived bacterial genera during enrichment (T0–T3).

Overall, the results indicate dynamic changes in the cultivable soil bacterial community during the enrichment process, with shifts in dominant genera over time.

The bacterial genera isolated from sediment differs in terms of distribution across enrichment time points (T0–T3). Several genera were detected at T0, with *Stenotrophomonas* and *Pseudomonas* among the dominant taxa. At T1, there is a wider distribution of genera, including *Pseudomonas*, *Raoultella*, and *Brucella*. At T3, there was more diversity, with multiple genera represented, including *Brevundimonas*, *Rhodanobacter*, and some minor taxa (Figure 21). Overall, the sediment-derived bacterial community exhibited temporal shifts during enrichment, with changes in dominant genera across time points.

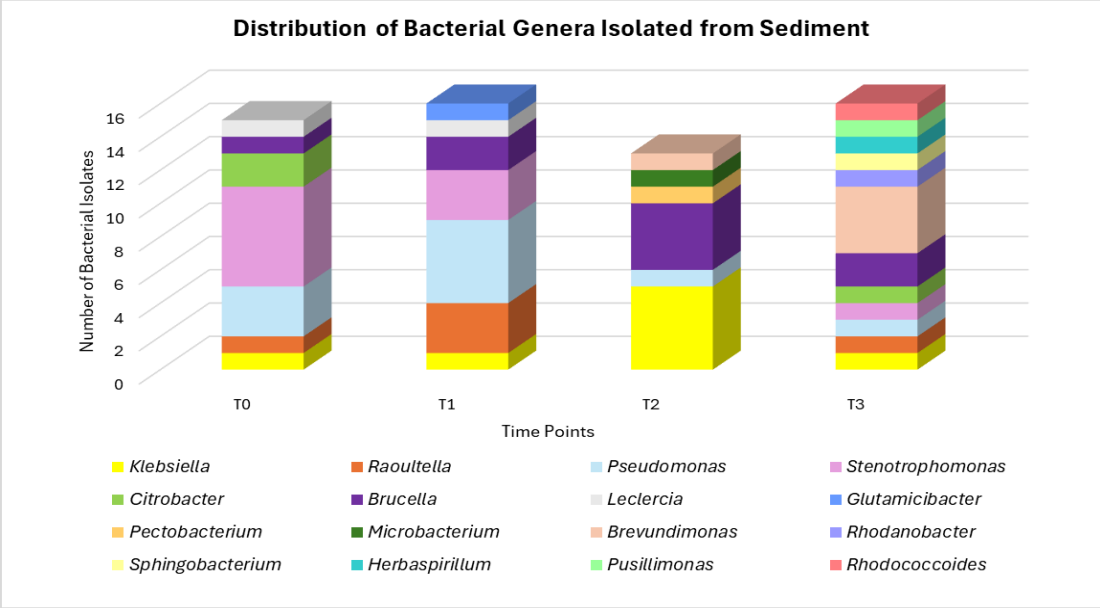

Figure 21. Temporal variation in sediment-derived bacterial genera during enrichment (T0–T3).

The class-level composition of the cultivable bacterial isolates was analyzed across enrichment time points (T0–T3) for both soil and sediment matrices. The distribution of major bacterial classes altered over time, indicating changes in community structure during PFOA enrichment. Differences were observed between matrices as well as between biological replicates, reflecting selective pressures imposed during the enrichment process (Figure 22, 23).

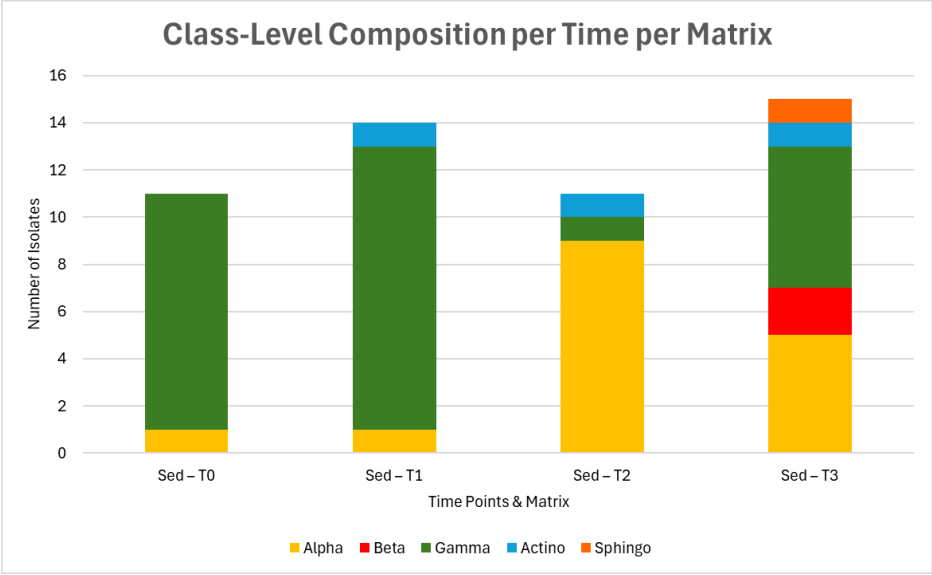

Figure 22. Class-level composition of bacterial isolates from sediment (both Sed A and Sed B) across enrichment time points (T0–T3).

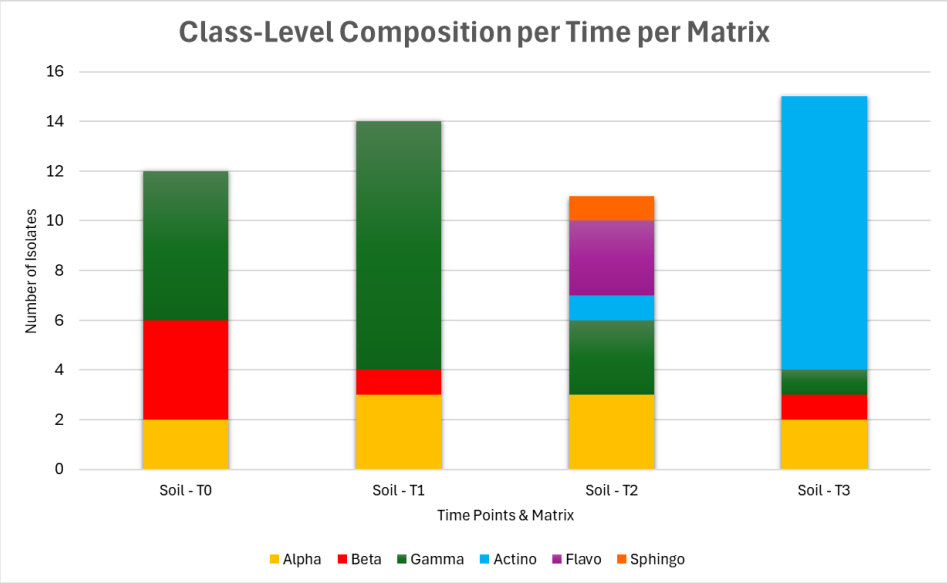

Figure 23. Class-level composition of bacterial isolates from soil (both Soil A and Soil B) across enrichment time points (T0–T3).

3.7.2 Taxonomic Identification by ITS Region Sequencing

A total of 53 fungal isolates were obtained from enrichment cultures on MALT agar plates at different sampling time points (Table 18), including 28 isolates from soil samples and 25 from sediment samples. However, not all isolates were subjected to molecular identification. Only isolates displaying distinct and unique morphological characteristics were selected for molecular identification through amplification and sequencing of the ITS region.

Using this approach, 20 isolates were identified, among these, three strains that were initially isolated as bacterial isolates did not yield amplification with 16S rRNA gene primers but were successfully amplified and sequenced using ITS primers, indicating that they belonged to fungal taxa. Fungal isolates were identified by partial ITS region sequencing. The obtained sequences were quality-checked and trimmed prior to analysis using BioEdit Sequence Alignment Editor (version 7.7.1) (Hall, 1999).

Taxonomic identification was performed using BLASTN searches against the NCBI database to determine the closest matching sequences and assign taxonomic affiliations (Altschul et al., 1990). The length of the ITS sequences utilized for taxonomic identification was approximately 450–500 bp.

The identified fungal taxa were predominantly affiliated with genera such as *Barnettozyma*, *Trichosporon*, *Galactomyces*, *Candida*, *Geotrichum*, *Fusarium*, and *Cyberlindnera*, indicating their persistence across enrichment cultures. The list of isolates selected for ITS sequencing and their identification results are reported in Table 19.

Table 19. Taxonomic identification of selected fungal isolates recovered from PFAS-enriched soil and sediment microbiomes using ITS sequencing. The table reports enrichment time points (T0–T3), isolate codes, closest type strain matches based on ITS sequencing, accession numbers, and identity percentages.

Strain	Taxon with the highest % similarity	Accession Number	Identity %
1M0LA	*Geotrichum pandrosioniae*	OR122285.1	99.3
1M0SA	*Barnettozyma californica*	KY101725.1	93.26
1M0SB	*Candida tropicalis*	AF218992.1	99.24
1M1LA	*Barnettozyma californica*	KY101725.1	96
1M1LB	*Cyberlindnera saturnus*	NR_165971.1	99.31
2M1LB	*Trichosporon asahii*	FJ943429.1	99.41
2M1SA	*Trichosporon asahii*	MN809444.1	99.6
3M1SA	*Barnettozyma californica*	NR_138212.1	96.98
2M1SB	*Galactomyces pseudocandidum*	JN974291.1	91.45
3M1SB	*Trichosporon japonicum*	NR_073263.1	100
1M2LA	*Barnettozyma californica*	NR_138212.1	96.98
3M2LA	*Fusarium falciforme*	NR_164424.1	99.63
3M2LB	*Fusarium hordeum*	MW016578.1	99.41
2M2SA	*Cyberlindnera saturnus*	NR_165971.1	99.76
3M3LA	*Galactomyces pseudocandidum*	JN974291.1	97.95
2M3LB	*Galactomyces pseudocandidum*	JN974291.1	98.23
3M3LB	*Cutaneotrichosporon moniliiforme*	KY103024.1	99.56
3T2SA	*Geotrichum silvicola*	NR_077071.1	97.96
6T2SA	*Candida tropicalis*	KU729064.1	99.76
4T2SB	*Candida palmioleophila*	NR_077076.1	100

3.8 PFOA and PFHxS- Exposed Cultures

Batch cultures were established in Minimal Defined (DM) medium supplemented with PFOA and PFHxS at final concentrations of 25 mg L^{-1} and 10 mg L^{-1}, respectively, and incubated for 87 days to evaluate the degradation potential of enriched new microbiomes.

3.8.1 Microbial Growth

To estimate the changes in microbial abundance, a total bacterial count was performed after PFOA and PFHxS exposure. The first bacterial total count at experiment commence (0 days) was used to validate the fact that a measurable and comparable microbial load could be found in all enrichment-derived microbiomes. There were changes in bacterial load between 0 days and 87 days in soil cultures. Total Bacterial counts expressed as $\log_{10}$ CFU mL^{-1}, and the results showed a more pronounced increase in soil T3 (Figure 24), suggesting that preserved microbiomes-maintained viability.

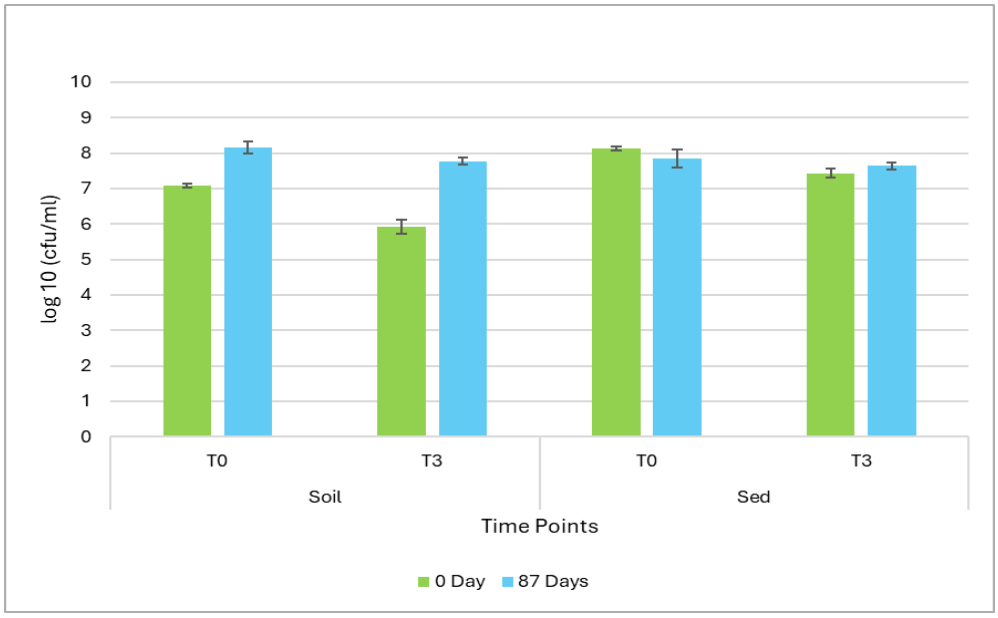

Figure 24.Total viable bacterial counts (log_{10} CFU mL^{-1}) measured at 0 and 87 days in enrichment-derived microbiomes from soil (Soil T0, Soil T3) and sediment (Sed T0, Sed T3). Error bars represent standard deviation of replicate measurements.

In sediment samples, bacterial counts remained relatively stable between 0 days and 87 days, with only minor variations in both T0 and T3 conditions. This refers to a relatively stable microbial population with limited changes in cultivable abundance over time. Overall, these results demonstrate that microbial populations remained viable throughout the abatement experiment, with observable growth in soil-derived microbiomes and stability in sediment-derived communities, reflecting microbial adaptation.

3.8.2 Evaluation of PFOA and PFHxS Removal

Batch experiments were carried out in Minimal Defined (DM) medium amended with PFOA and PFHxS, while appropriate controls were included to distinguish between biological and non-biological effects. The T0 condition (day 0) represents the initial PFAS concentrations measured before microbial inoculation, whereas the abiotic control consisted of PFAS-amended medium without microorganisms and was used to evaluate any non-biological changes during incubation.

After 87 days, the concentrations measured in all treatments (abiotic control, Soil T0, Sed T0, Soil T3, and Sed T3) remained comparable to the initial values for both compounds. Statistical analysis performed separately for each compound showed that all PFOA treatments were grouped within the same significance category (A), while all PFHxS treatments were grouped within a single category (B), indicating no statistically significant differences among treatments within each dataset (Figure 25).

Overall, these results indicate that neither microbial activity nor preservation time had a measurable effect on PFAS concentrations, and no evidence of abatement or biotransformation of PFOA or PFHxS was observed under the tested conditions.

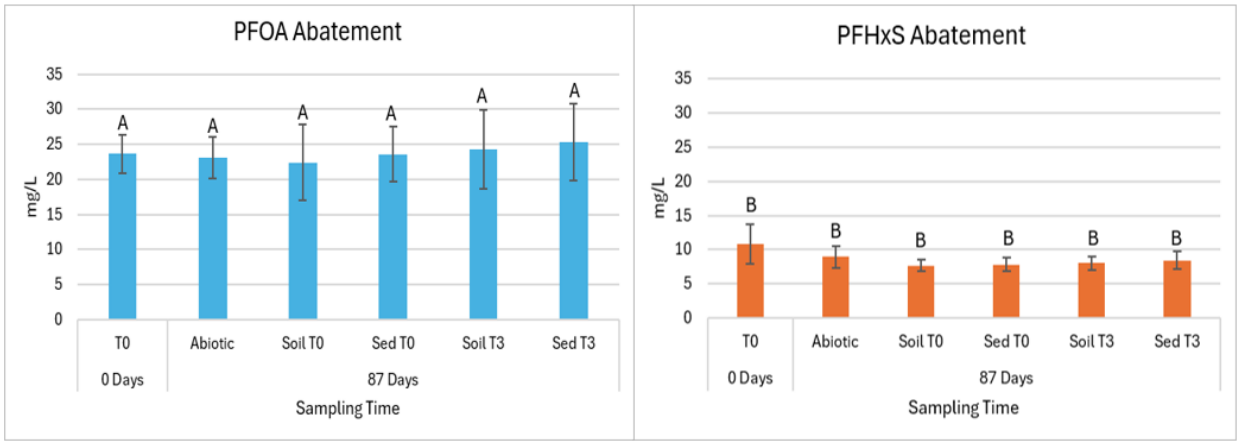

Figure 25. Concentration of PFOA and PFHxS at the beginning of the experiment (T0, day 0) and after 87 days of incubation in abiotic control and enrichment-derived microbiomes from soil (Soil T0, Soil T3) and sediment (Sed T0, Sed T3). Statistical analysis (ANOVA) was performed separately for each compound; different letters indicate significance groups within each compound. Error bars represent standard deviation of replicate measurements.

Although no significant abatement was observed, the slight variation in PFHxS concentrations may indicate non-biological processes such as adsorption, requiring further analysis of the solid (pellet) fraction.

3.9 Screening and Selection of PFOA-Exposed Isolates for Defluorination Assays

DM agar supplemented with PFOA, 50 mg L^{-1}, as the sole carbon source was used to screen isolates obtained from enrichment cultures (T0–T3), and there were limited number of isolates that were able to show growth. Initially, TSA plates were used to streak isolates to verify their viability, following that isolates were streaked on nutrient-limited DM agar and DM agar amended with PFOA. Out of the tested isolates, four bacterial strains were consistently showing growth on PFOA-amended DM agar following successive streaking (second and third streaking):

- *Brevundimonas* sp. 9T2SB
- *Chryseobacterium* sp. 5T2LA
- *Sphingobacterium* sp. 9T2LB
- *Sphingobacterium* sp. 5T3SA

These isolates maintained stable colony morphology and sustained growth under selective conditions, confirming true tolerance to PFOA rather than transient adaptation or growth supported by residual nutrients.

Moreover, two fungal strains were identified.

- *Geotrichum* sp. 3T2SA
- *Candida* sp. 4T2SB

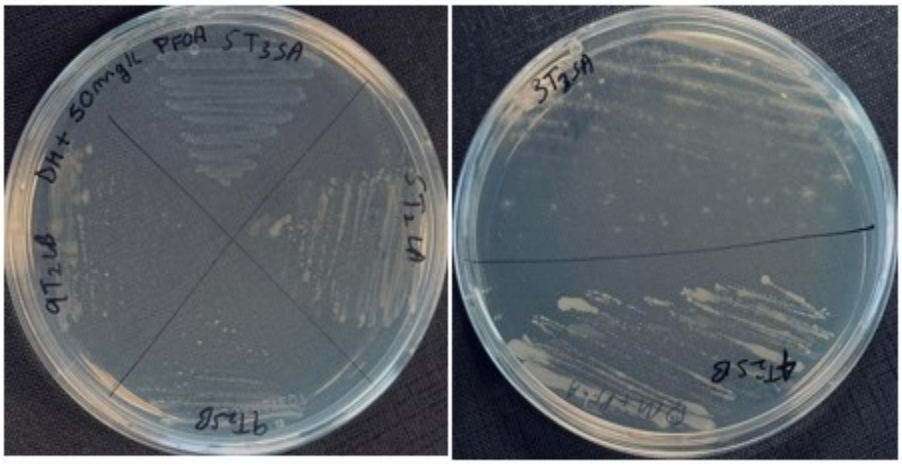

Figure 26. Representative streaking plates showing growth of selected isolates on DM agar supplemented with PFOA (50 mg L^{-1}) under selective conditions. Visible colony formation across streaking sectors confirms sustained growth after successive passages.

The confirmed bacterial isolates, together with the subsequently identified fungal strains, were used in subsequent biotransformation experiments with fluoxetine, PFOA, and other PFAS compounds to assess their transformation and defluorination potential. Fluoxetine (FLX)is a fluorinated compound containing C–F bonds whose environmental occurrence, persistence, and biodegradation have been well documented. Compared to highly recalcitrant PFAS, FLX represents a more labile model substrate, allowing the investigation of microbial defluorination processes under controlled conditions (Moreira, 2012).

3.10 Biotransformation and Defluorination Outcomes

3.10.1 Fluoxetine Biotransformation and Fluoride Release Patterns

The biotransformation assays using fluoxetine revealed that the tested isolates had a different response under the three nutritional conditions. The alterations in the fluoxetine concentration and fluoride release during the incubation (28 days) was monitored using HPLC and ion-selective electrode analysis, respectively, to determine the degradation and the defluorination activity associated with the degradation.

i. Fluoxetine Biotransformation in the Absence of Additional Carbon Source

With fluoxetine as the only carbon and energy source, no significant growth of any of the tested bacterial or fungal isolates was detected within the 28 days of incubation. OD_{600} values were found to be low and constant during the experiment, which implies that no active increase in biomass was observed under such conditions. Fluoride ion analysis also revealed no measurable release of fluoride at any sampling time. No changes in the fluoride concentration were observed in the abiotic control, which validated that there was no chemical defluorination. HPLC analysis was not conducted in this condition due to the absence of microbial growth and release of fluoride.

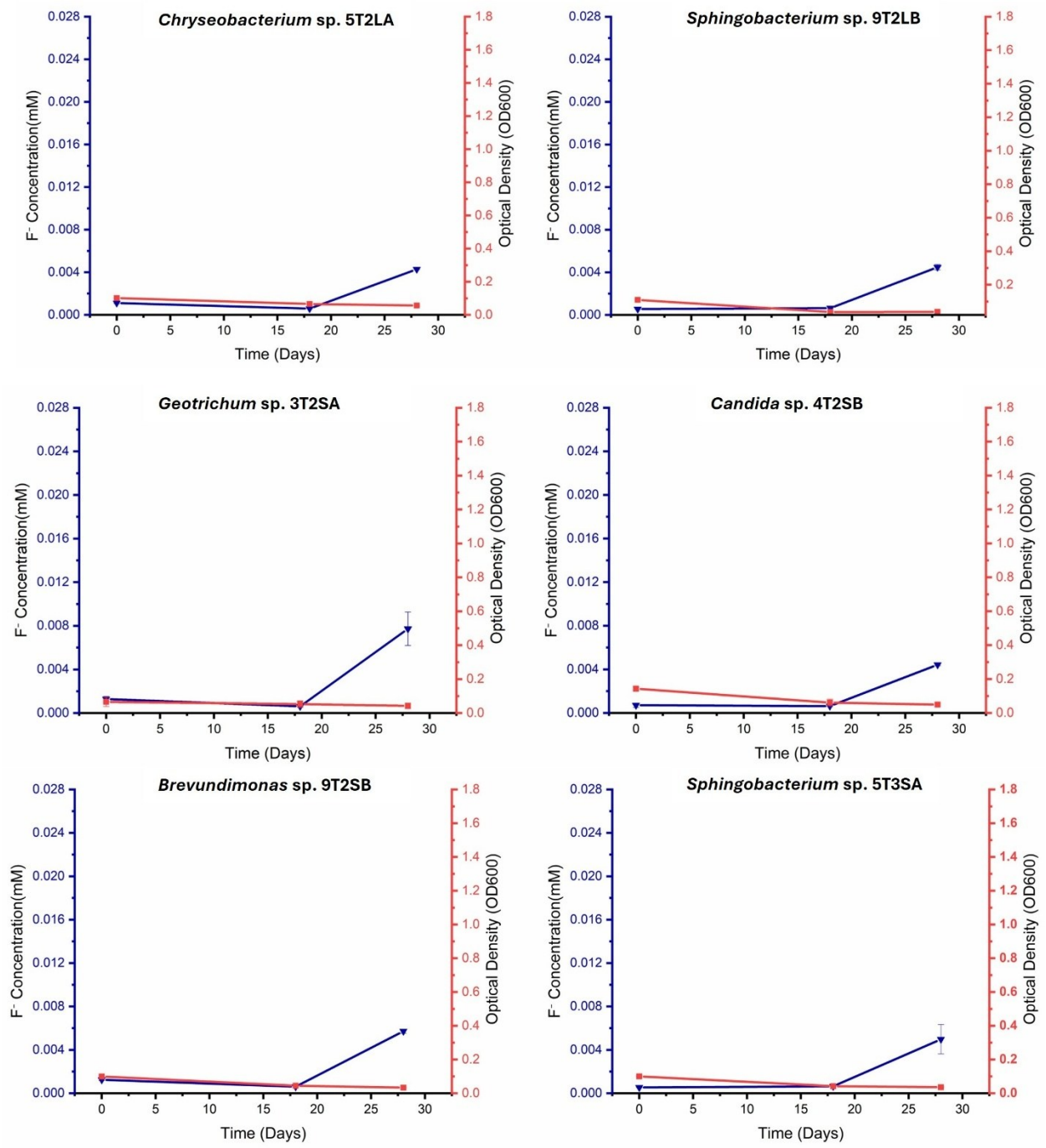

Figure 27. Optical density (OD_{600}) and fluoride ion (F^-) release profiles of six selected isolates incubated with fluoxetine (10 mg L^{-1}) as the sole added compound over 28 days. Experiments were performed in triplicate, including an abiotic control. Values represent mean measurements ± standard deviation.

To conclude, these findings point to the fact that fluoxetine, when provided as the only carbon and energy source, was not able to support microbial activity or defluorination that could be measured under the conditions of the experiment performed.

ii. Enhanced Fluoxetine Biotransformation with Initial Glucose Addition

With the addition of D-glucose (0.5 g L^{-1}) at the start of the experiment along with fluoxetine, all the tested isolates demonstrated a significant growth in OD_{600} in the first week of the experiment, which was a sign of active growth of biomass due to the presence of glucose. Optical density increased the most at Day 7 in all strains with a gradual decrease towards Days 21 and 28. In some of the flasks, fluoride ion concentrations rose in the first week indicating that there was a defluorination activity in the co-metabolic conditions. Nevertheless, the overall level of fluoride was quite low and even declined at later time points.

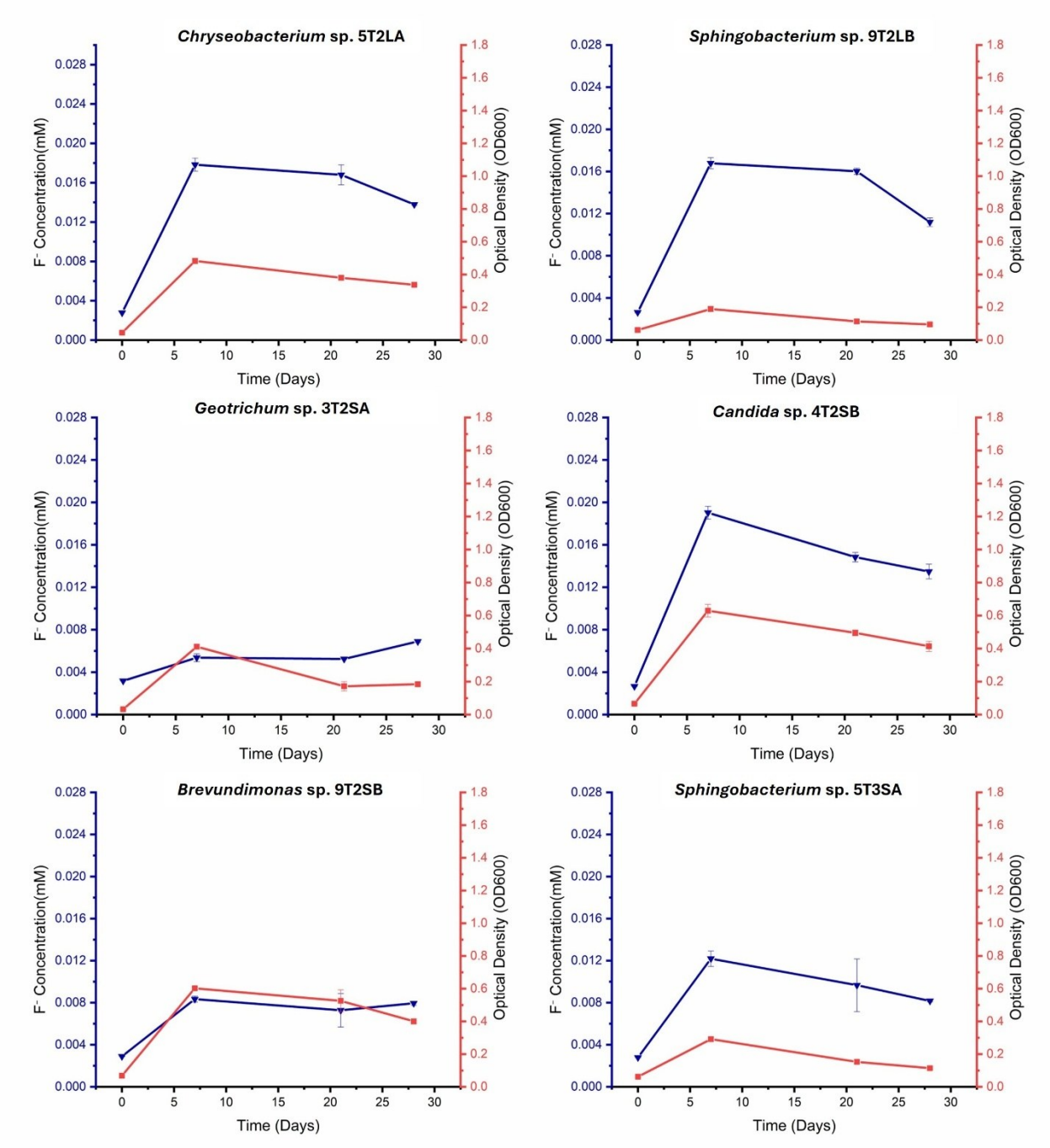

Figure 28. Optical density (OD_{600}) and fluoride ion (F^-) release profiles of six selected isolates incubated with fluoxetine (10 mg L^{-1}) and D-glucose (0.5 g L^{-1}) added at the start of the experiment. Measurements were performed over 28 days. Values represent mean ± standard deviation of triplicate experiments.

It is important to note that the abiotic control also had surprisingly high OD_{600} values, which shows contamination during the experiment. Subculture of the cultures of all the experimental conditions confirmed cross-contamination since similar colony morphologies were found in different treatments.

Three predominant strains were reproducibly obtained in several cultures: 4T2SB, 9T2SB and 5T3SA. These are strains that were then chosen to be experimented on.

iii. Effect of Repeated Glucose Supplementation on Fluoxetine Biotransformation and Fluoride Release

Under the condition where D-glucose (0.5 g L^{-1}) was supplied weekly, all three selected strains (*Candida* sp. 4T2SB, *Brevundimonas* sp. 9T2SB, and *Sphingobacterium* sp. 5T3SA) showed a progressive increase in OD_{600} over the 28-day incubation period, indicating sustained microbial growth supported by continuous carbon supplementation. Fluoride ion concentrations increased steadily with time for all strains, suggesting active defluorination under these co-metabolic conditions. The highest fluoride release was observed toward the final sampling points (Days 21–28), consistent with ongoing transformation activity.

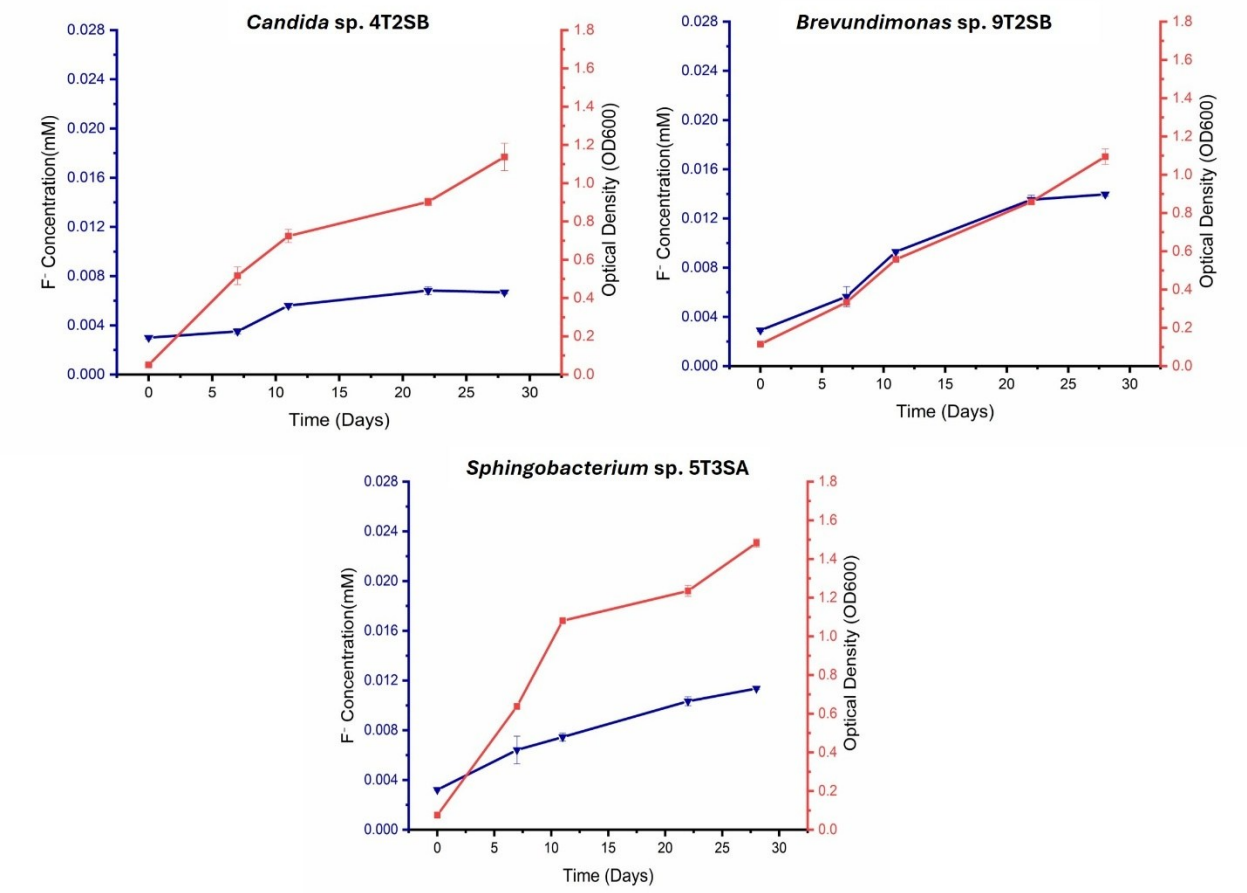

Figure 29. Optical density (OD_{600}) and fluoride ion (F^-) release profiles of Candida sp. *4T2SB, Brevundimonas* sp. *9T2SB, and Sphingobacterium* sp. *5T3SA during incubation with fluoxetine (10 mg L^{-1}) and weekly glucose supplementation (0.5 g L^{-1}). Values represent mean ± standard deviation of triplicate experiments.*

HPLC analysis revealed that there was a corresponding reduction in the fluoxetine level over time. The three strains exhibited a significant FLX removal with the most pronounced reduction observed for *Brevundimonas* sp. 9T2SB and *Sphingobacterium* sp. 5T3SA, while *Candida* sp. 4T2SB also demonstrated clear but comparatively moderate degradation.

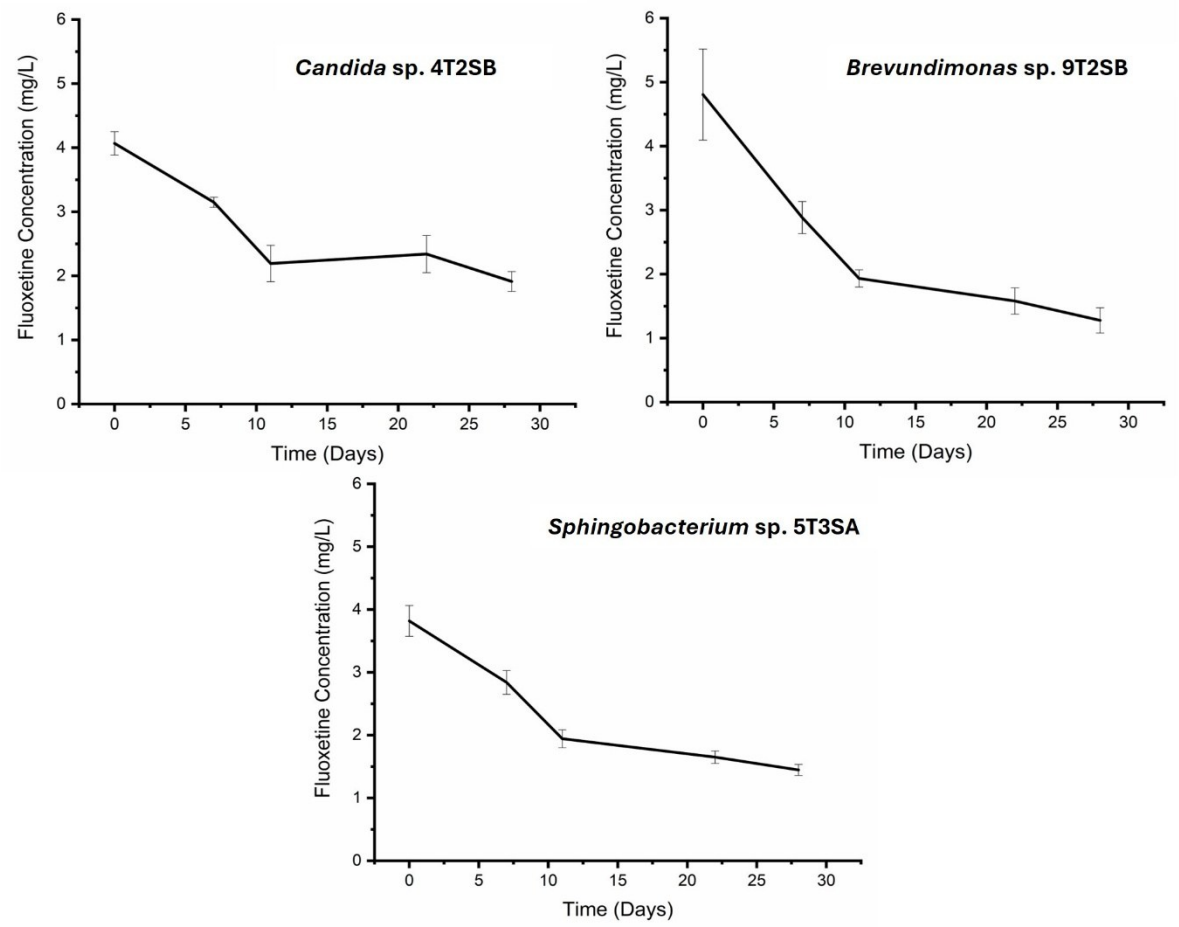

Figure 30. HPLC-monitored fluoxetine concentration profiles during incubation with the three selected strains under weekly glucose supplementation. Data represent mean ± standard deviation of triplicates.

Abiotic control did not reveal any significant differences in the concentration of fluoxetine or fluoride levels, proving that the effects observed were biologically mediated. Overall, weekly glucose supplementation enhanced microbial growth, promoted fluoxetine degradation, and supported measurable defluorination activity.

3.10.2 Defluorination Potential of Isolates and Microbial Consortia

i. Lack of PFOA Defluorination by Single Isolates

Assays of fungal and bacterial isolates incubated with 10 mg L^{-1} of PFOA did not show any measurable release of fluoride ion (F-) during the experimental period. The concentration of

fluoride was similar to the concentration in the abiotic controls at all sampling points, and this revealed that C-F bond cleavage was not measurable under the experimental conditions.

Also, optical density (OD_{600}) did not increase significantly compared to the starting values indicating that PFOA was not able to maintain the growth of microbes as a carbon or energy source. Taken together, these findings indicate that none of the single isolates tested could be shown to de-fluorinate or transform based on growth during the experiment. Collectively, these results indicate that PFOA did not support microbial growth as a sole carbon source, and no defluorination or transformation was detected.

ii. Defluorination Response of the Microbial Consortium

Mixed microbial consortium experiments were established by cultivating bacterial and fungal isolates separately and subsequently combining them to obtain a final inoculum with an initial OD_{600} equivalent of 0.05. Cultures were amended with PFOA (10 mg L^{-1}) and incubated for 61 days (T0–T3). The consortium did not exhibit any significant change in optical density over time, indicating that PFOA did not support microbial growth under the tested conditions. No release of fluoride ions (F^-) was detected throughout the incubation period, as fluoride concentrations remained comparable to those observed in the abiotic controls.

iii. Defluorination Potential Toward Additional PFAS Compounds

In cultures incubated in the presence of structurally diverse PFAS compounds (8:2 FTS, PFOS, GenX, 7:3 FTCA, and NFDHA) at the final concentration of 10 mg L^{-1} during 47 days (T0-T4), no significant increase in optical density (OD_{600}) was found in any of the cultures. This means that all the tested PFAS compounds were not able to support the growth of microbes in the conditions imposed. Simultaneously, in all treatments, no release of fluoride ion (F -) was measured. The fluoride contents were also similar to those of the abiotic controls during the incubation period, and this proves that there was no observable cleavage of the C-F bond.

The consortium did not show any detectable defluorination activity with PFOA or other PFAS compounds assessed. The absence of fluoride release, together with the lack of biomass increase, indicates that these PFAS did not undergo biological conversion through defluorination and could not be utilized as a sole source of carbon and energy under the experimental conditions.

Chapter 4 – Discussion

This study aimed to investigate microbial communities from PFAS-contaminated soil and sediment in terms of preserving their viability, metabolic activity, response to PFOA enrichment, and their potential for fluorinated compound transformations. Two aspects are considered in discussing the results. The first addresses the conservation and maintenance of microbiome viability, metabolic activity, and structure in environmentally contaminated matrices. The second concerns the extent to which preserved microbiomes could be propagated and utilized for bioremediation purposes by enrichment cultures, alongside the isolation of microorganisms as microbial bioresources with potential tolerance or capacities to transform PFAS.

Both dimensions are important because preservation of environmental microbiomes is increasingly recognized as a prerequisite for reproducible and comparable ecological research, biobanking and future biotechnological applications on the other hand, protocols for long-term preservation of complex contaminated matrices are still poorly established (Dully et al., 2021; Pavlovska et al., 2021; Prakash et al., 2020). Moreover, no research on the revitalization and use of the microbiome for PFAS abatement is currently available in the literature.

4.1 Preservation

Native microbiomes need to be preserved over long periods of time to retain their structural integrity, viability, and functional capacity (Hornung et al., 2018; Potts et al., 2022), especially in contaminated environments where distinct taxa and metabolic processes may be destroyed. Moreover, an ideal maintenance of undamaged microbiomes assists in facilitating powerful comparative research and tracing spatiotemporal variations in microbial communities, which can be applied in future culturomics and OMICS investigations (Prakash et al., 2020). It is also vital in the conservation of ecosystems, environmental health, and encourage bioeconomic applications (Raupp et al., 2024; Stephens, 2023).

Although a wide range of preservation techniques has been developed for pure cultures, their direct application to intact environmental microbiomes remains limited. This limitation is particularly evident in complex polluted matrices, such as soils and sediments, where microbial communities are highly diverse and structured through intricate ecological interactions. In such systems, maintaining both community composition and functional potential during storage is challenging, as preservation-induced stress can selectively affect sensitive taxa and disrupt metabolic interactions (Kerckhof et al., 2014; Rubin et al., 2013; Song et al., 2016).

These challenges become even more pronounced in contaminated environments, where microbial communities are often shaped by long-term exposure to pollutants and may include specialized or low-abundance taxa with key ecological roles. In this context, standardized procedures for preserving intact microbiomes are still lacking, particularly for matrices impacted by persistent contaminants (Pavlovska et al., 2021; Prakash et al., 2020). Although some studies have explored

short-term preservation of sediment microbiomes, systematic investigations addressing long-term storage effects on microbial viability, functional capacity, and community stability—particularly in polluted environments—are still scarce (Dully et al., 2021).

PFAS-impacted environments introduce an additional level of complexity. The extreme persistence and bio accumulative nature of PFAS can drive the selection of highly adapted microbial assemblages, in which apparent structural stability does not necessarily correspond to functional resilience or degradative potential (Cousins et al., 2020; Meegoda et al., 2020). Therefore, preserving these microbiomes in a manner that maintains both viability and functional traits represents a critical yet underexplored requirement for advancing PFAS bioremediation research.

Based on current knowledge, this study represents the first in-depth investigation of long-term (12 months) cryopreservation of microbiomes in soil and sediment samples. The evaluation was performed through an integrative approach combining culture-dependent and culture-independent analyses, including microbial enumeration, functional profiling, and DNA-based community characterization across multiple storage time points. There are no previous studies that have systematically assessed the long-term effects of storage conditions on both the structural and functional stability of microbial communities, nor their temporal dynamics in such complex environmental matrices. Consequently, there are no directly comparable datasets in the literature against which the present results can be evaluated.

4.1.1 Rationale for Cryogenic Preservation

Cryogenic storage at −80°C with glycerol 30% (*w/v*) was selected as a novel long-term (twelve months) preservation approach for PFAS-impacted environmental matrices to minimize biological and chemical transformations and to maximize the chance of recovering a representative community after preservation. This approach agrees with other studies in the field of cryobiology, where cryopreservation is recognized as one of the most effective approaches to reduce biological change and retain community properties over time (Hubálek, 2003).

The choice of glycerol was due to its dual capacity in evading the damage of cells caused by ice crystals in the process of freezing and also preventing the destruction of viability and the community structure of the population of microbes (Senaratne & Jayaweera, 2024). Another experimental study by Linde et al. (2018), indicated that glycerol was the best cryoprotectant for *Basidiomycetes* at −80 °C. These findings justify using glycerol as a good cryoprotectant in preserving complex environmental microbiomes when the viability and functionality stability have to be maintained.

Though, the present results also show that preservation should not be interpreted as complete biological stasis. It is possible that even under deep-freezing conditions, can still select on relative survival because of differences in freezing and thawing sensitivity, osmotic response,

cryoprotectant penetration, and possible matrix effects. This is notable as storage is frequently regarded as conceptually neutral in studies on environmental microbiomes, but numerous reports have shown that storage conditions can retain broad patterns of diversity while imparting other changes in taxa or functional groups (Dully et al., 2021; Hubálek, 2003; Lauber et al., 2010).

This is what we observed. The temporal effects of preservation were not completely eliminated, but it was still sufficient for recovery, cultivation, community profiling, and subsequent enrichment. Therefore, the findings support previous studies that have used cryogenic preservation as a practical and valuable approach to microbiomes from PFAS-affected media, while also demonstrating that long-term storage can alter the composition of the preserved microbiome.

4.1.2 Total Cultivable Counts

Total cultivable counts gave information on the vitality of the microbiome during storage. The observed stability for up to eight months (T2) shows that cryogenic preservation was effective in preserving bacterial viability over intermediate time scales. This trend is consistent with Ramírez et al. (2017) who reported that freeze-storage at −20 °C maintained the abundance of culturable soil bacteria for up to eight months, whereas the viability of filamentous fungi and *Bacillus mycoides* declined sharply beyond this period. The vitality decline at twelve months (T3) shows a temporal effect of storage, likely due to cumulative damage on cell membranes.

Nonetheless, this loss should not be mistaken for a loss of viability, as cultivable counts represent only the recoverable phenotype of the microbiome and may not reflect their true abundance. Under prolonged storage conditions, a proportion of the microbiome may persist in a viable-but-non-culturable state, reflecting a shift in physiological status rather than true cell death (Lee et al., 2021). Although sediment samples also exhibited a significant reduction in bacterial abundance at T3, the decrease was less pronounced than in soil, indicating that prolonged storage negatively impacts bacterial viability across distinct environmental matrices.

This difference may be attributed to the intrinsic characteristics of the two matrices: soils are typically more heterogeneous and aerated, exposing microorganisms to greater stress during freezing and thawing, whereas sediments often provide more stable, fine-grained, and organic-rich conditions that can offer physical protection to microbial cells. Consequently, microbial communities in sediments may be less susceptible to preservation-induced damage compared to those in soils. This differential response between soil and sediment further highlights a matrix-dependent effect of preservation which relates to the ecological differences between these environments (Fierer & Jackson, 2006; Lozupone & Knight, 2007; Zinger et al., 2011).

Taken together, these results show that cryogenic preservation impact the viability of microorganisms, it shows a selective effect on the recoverable portion of the microbiome, and this is dependent on the matrix from which the microorganisms were derived. A meta-analysis by Fromin (2025) found that more than 75% of the studies found significant storage effects on culture

independent microbial parameters, but few studies used culture-based techniques to determine actual viability.

This underlines the scarcity of information on long-term survivability of microbes. Here, our experiment is the combined assessment of bacterial and fungal viable counts (CFU g^{-1}) within the microbiomes of soil and sediment in 12 months. Although it was found that culturable populations were maintained over a period of up to eight months, a subsequent decrease suggests a time-dependent loss of viability that cannot be detected by DNA-based methods, and this shows that there is a critical time limit to long-term preservation.

4.1.3 Microbial Metabolic Activity

The Biolog® EcoPlates™ assay (Biolog Inc.), based on community-level physiological profiling (CLPP), is one of the most commonly used methods to evaluate functional changes within microbial communities and to describe patterns of metabolic activity and potential (Feigl et al., 2017).

The results of this study showed that microbiome functional expression was impacted by preservation, with soil-derived communities exhibiting higher initial metabolic activity followed by a more pronounced decline between T2 and T3, which may be related to their high spatial heterogeneity, variable organic inputs, and greater niche diversification. The later decrease implies a loss in functional responsiveness, likely due to the selective reduction of metabolically active populations (Garland & Mills, 1991; Preston-Mafham et al., 2002). By comparison, sediment microbiomes showed a steady decline during preservation period from T0 to T3. These matrix-specific patterns in relative functional responses are common, with substrate use patterns frequently influenced by source environment and community structure (Garland, 1997).

The lower functional diversity observed in sediment systems compared to soils can be attributed to their more selective and constrained environmental conditions. Sediments are often characterized by reduced oxygen availability, limited nutrient diffusion, and relatively stable physicochemical conditions, which favor specialized microbial populations with narrower metabolic capabilities. In contrast, soils are typically more heterogeneous and resource-diverse environments, supporting a broader range of microbial taxa and metabolic functions. This interpretation is consistent with previous studies reporting reduced functional diversity in aquatic and sediment-associated microbial communities compared to soil systems (Brandt et al., 2014).

This analysis of Biolog EcoPlate revealed functional patterns which are consistent with other studies, including Lukhele & Msagati (2024), reported that in heavy metal-contaminated soils, microbial communities have been reported to preserve metabolic activity toward key substrate groups, including amino acids and organic acids, despite reduced overall functional diversity. In the present study, a more detailed analysis of substrate utilization revealed that, in soil, the ability

to metabolize diverse carbon sources such as Tween 80, β-Methyl-D-Glucoside, N-Acetyl-D-Glucosamine, and Glucose-1-Phosphate declined markedly by T3, indicating a loss of specific metabolic functions. In contrast, sediment communities exhibited a more gradual reduction in substrate use, with progressive declines observed across time points (e.g., D-Malic Acid at T1; β-Methyl-D-Glucoside, γ-Aminobutyric Acid, and L-Asparagine at T2; and D-Galactonic Acid γ-lactone at T3).

These findings align with studies on petroleum-contaminated soils have shown sustained utilization of carbohydrates (e.g., simple sugars), amino acids, and carboxylic acids, reflecting the persistence of core metabolic functions despite contamination stress (Garland & Mills, 1991; Preston-Mafham et al., 2002). In such systems, microbial communities often shift toward populations capable of metabolizing both native soil organic matter and contaminant-derived compounds, maintaining functional redundancy. Accordingly, although contamination can reduce the extent of substrate utilization, the capacity to metabolize essential carbon sources is often retained, supporting ecosystem-level functional stability. Even though there was a reduction in substrate use after a period of long-term storage, the capacity to metabolize major carbon sources including polysaccharides and amino acids was retained.

In the context of PFAS-impacted systems, while direct evidence on functional responses remains limited, studies suggest that microbial communities exposed to persistent contaminants often exhibit structural stability but constrained or specialized metabolic activity (Cousins et al., 2020; Meegoda et al., 2020). The partial retention of metabolic capacity observed in this study may therefore reflect the adaptive potential of microbiomes originating from polluted environments, where long-term exposure to contaminants selects for metabolically flexible and stress-tolerant populations. Overall, these findings indicate the strength of the polluted microbiomes and justify the application of CLPP as a sensitive method to identify functional modifications in the conditions of contamination and storage.

4.1.4 Microbial Community Composition

Metabarcoding allowed us to assess the stability of microbial community structure during long-term cryogenic storage. The continued presence of dominant bacterial phyla (*Proteobacteria*, *Bacteroidota* and *Actinobacteriota*) and fungal classes (*Sordariomycetes*, *Agaricomycetes* and *Leotiomycetes*) are consistent with previous studies (Baldrian, 2017; Fierer, 2017). This taxonomic structure aligns with previous studies on subarctic soils (Kim et al., 2014), and plain lake sediments (W. Huang et al., 2017). Sediment samples were particularly enriched in *Comamonadaceae* and *Nitrospiraceae*, whereas soil samples contained higher abundances of *Bacillaceae*, *Micrococcaceae*, and *Oxalobacteraceae*, families commonly associated with microbial adaptation to chemical stressors, including organic contaminants, heavy metals, and persistent pollutants, as well as oxidative and nutrient stress conditions (Baldrian, 2017; Cousins et al., 2020; Fierer, 2017; Lukhele & Msagati, 2024).

The Shannon index revealed no substantial differences in microbial biodiversity across time points from T0 to T2, although a slight reduction in bacterial diversity was detected at T3 in both soil and sediment. Evidence from Kushwaha et al. (2024) also indicated that microbial richness remained largely stable for the first nine weeks of field-temperature storage, but that Shannon diversity declined after three to six weeks, particularly among fungal taxa, underscoring differential temporal sensitivity. Their stability over time suggests that a central community composition may be preserved during storage in terms of culture-independent analysis, despite relative changes in vitality.

Metabarcoding and clustering analyses indicated that the overall community structure was preserved across all time points. No significant temporal clustering of samples was observed, as replicates from different preservation time points did not group distinctly, suggesting that storage duration did not substantially influence the core microbiome composition consistent with reports that cryogenic preservation helps maintain community richness and evenness (Lauber et al., 2010). Variations detected in beta diversity were therefore primarily attributable to shifts in relative abundance rather than fundamental structural changes.

In contrast, differences between environmental matrices were more pronounced. Sediment-derived communities exhibited greater homogeneity, characterized by tighter clustering and lower dispersion, indicating higher structural stability (Zinger et al., 2011). Conversely, soil-derived communities were more heterogeneous, showing higher dispersion. This pattern was consistent for both bacterial and fungal communities, highlighting the dominant role of the environmental matrix in shaping microbiome stability during preservation. Direct comparative evaluations of soil and sediment microbiomes under standardized cryogenic conditions remain limited; our findings therefore extend the current understanding of long-term microbial preservation beyond the durations previously documented.

4.2 Propagation

4.2.1 Community Structure in Enriched Microbiomes

PFOA enrichment was performed to exert a distinct selection pressure, resulting in restructuring of new microbial communities in soil and sediment microbiomes. These changes in community structures are comparable with previous studies. Such shifts in community composition under selective conditions are consistent with previous studies. For example, Muyzer et al. (1993) and Muyzer & Smalla (1998) demonstrated, using DGGE-based approaches, that microbial communities in environmental matrices such as marine systems and soils undergo clear structural shifts in response to environmental gradients and selective pressures. Similarly, Wittebolle et al. (2009) showed that in activated sludge systems exposed to chemical perturbations, the outcome of community restructuring depends on the initial community composition, highlighting the role of selection in shaping microbial assemblages.

The retention of several bands over time suggests an abundant portion of the initial microbiome was not affected by PFOA, and the shifts in band intensity and diversity reflect a change in dominant populations from T0 to T3. Sediment microbiomes showed a relatively high similarity between initial (T0) and intermediate time points (T1 and T2), and progressive divergence at later time points, suggesting progressive but relatively stable community restructuring. Similarly, the soil microbiomes showed a similar pattern but stronger divergence between T0 and T3. Microbial total count in enrichment cultures at different time points suggests that a large proportion of the preserved microbiome was alive and able to proliferate under PFOA selective pressure.

The abundance of microbes, especially in enrichment cultures at T1 and T2, is typical of the initial proliferation of tolerant or adaptable microorganisms in enrichment cultures, while the levelling slight decrease at T3 indicates an establishment of a more defined community structure under sustained selective conditions (Atlas & Bartha, 1998; Madigan et al., 2018). Similar trend was observed in fungal total counts, but sediment-derived enrichments comparatively showed more abundance to soil which is likely due to the more suitable ecological properties of sediment matrices (e.g. higher moisture and organic matter content) (Fierer et al., 2007). It is critical that microbial proliferation under these conditions be regarded as an indicator of tolerance and continued activity rather than PFAS degradation, as growth does not prove compound transformation

4.3 Characterization of Isolates from Enrichment Cultures

The isolation of 103 bacterial operational taxonomic units (OTUs) from soil and sed enrichment cultures suggests that exposure to PFOA resulted in the emergence of a diverse but structured cultivable community. The consistent isolation of strains belonging to genera such as *Pseudomonas*, *Stenotrophomonas,* and *Brevundimonas* agrees with other studies reporting these bacterial genera as stress-resistant and commonly recovered from polluted environments (Guo et al., 2023; Presentato et al., 2020; Senevirathna et al., 2022c). In soil enrichments, the transition from early recovery of genera such as *Pseudomonas*, to the emergence of genera including *Microbacterium*, *Flavobacterium*, *Brucella*, and *Chryseobacterium* at later stages suggests a process of temporal succession during enrichment, where early fast-growing taxa are progressively replaced by more persistent and stress-tolerant populations.

By contrast, sediment-derived enrichments displayed a more gradual and stable restructuring. Instead of rapid dominance shifts, the enrichment process appeared to promote the progressive establishment of persistent and environmentally adapted microorganisms. This difference likely reflects the intrinsic characteristics of sediment systems, which are generally more stable and selective environments compared to soils. The enrichment of genera such as *Rhodanobacter* and *Brevundimonas* at later stages supports this interpretation. *Rhodanobacter* has been widely reported in highly contaminated environments, particularly in metal- and nitrate-impacted subsurface systems, where it is selected under strong chemical stress (Carlson et al., 2019).

Similarly, *Brevundimonas* has been identified in polluted matrices, including wastewater and soils exposed to organic contaminants, indicating its capacity to persist under chemically stressed conditions (Q. Zhang et al., 2019).

With respect to PFAS-related adaptation, the literature provides the strongest evidence for *Pseudomonas*, which has been repeatedly isolated from PFAS-contaminated environments and, in some cases, shown the ability to interact with PFAS compounds through bioaccumulation or transformation processes (Presentato et al., 2020). In contrast, for other genera identified in this study, including *Microbacterium*, *Flavobacterium*, *Chryseobacterium*, *Brevundimonas*, and *Rhodanobacter*, current evidence primarily supports their tolerance to contaminated conditions rather than confirmed PFAS degradation. Their enrichment in this study is therefore more appropriately interpreted as an indication of stress resistance and persistence under PFOA exposure, rather than direct involvement in PFAS biotransformation.

The recovery of fungal genera such as *Candida*, *Trichosporon*, *Galactomyces*, *Geotrichum*, *Cyberlindnera*, and *Fusarium* further indicates that enrichment conditions supported a fungal component within the microbiome. These genera are commonly reported in contaminated environments and are known for their tolerance to chemical stress and metabolic versatility (Harms et al., 2011). However, as with bacterial isolates, direct evidence linking these fungi to PFAS degradation remains limited. Their presence therefore reflects resilience under selective conditions, with potential—but as yet unconfirmed—roles in PFAS-related processes.

Overall, these findings demonstrate that PFOA enrichment selectively favors cultivable microbial communities composed of stress-tolerant and environmentally versatile taxa, with clear differences between soil and sediment matrices. Soil enrichments showed a more dynamic changes, whereas sediment enrichments exhibited greater stability and persistence of adapted taxa over time. Together, these results highlight that enrichment under PFAS-related stress conditions promotes microbial populations capable of surviving prolonged exposure, even though their direct role in PFAS transformation remains to be fully clarified.

4.4 Utilization

4.4.1 PFAS Abatement by Enriched Microbiomes

A key finding of this study is the clear disparity between microbial persistence and PFAS abatement. Although enrichment cultures remained viable during exposure, no significant removal of PFOA or PFHxS was observed. This result is consistent with the well-documented recalcitrance of long-chain PFAS under aerobic conditions, largely due to the strength of the C–F bond, which limits microbial degradation pathways (Parsons et al., 2008). Therefore, the observed microbial growth in the presence of PFAS is more appropriately interpreted as a response of tolerance and persistence rather than evidence of compound utilization. The minor fluctuations observed in

PFHxS concentrations are more plausibly explained by physicochemical processes rather than biodegradation. In particular, sorption of PFAS to biomass and particulate matter is a well-established mechanism influencing apparent concentration changes.

Higgins & Luthy (2006) demonstrated that perfluorinated compounds, including PFOA, can strongly associate with organic matter and solid phases in environmental matrices. This behavior has been further supported by subsequent studies showing that PFAS partitioning to sediments, sludge, and microbial biomass can contribute to apparent removal without actual degradation (Ahrens, 2011; T. M. H. Nguyen et al., 2022). Taken together, these findings indicate that while enriched microbiomes retained metabolic activity under PFAS exposure, this did not translate into measurable PFAS transformation. Instead, the results highlight the dominant role of physicochemical interactions and the inherent resistance of long-chain PFAS to microbial degradation under the tested conditions.

4.5 Screening and Defluorination Experiments

The screening of the enrichment-derived isolates on PFOA-containing DM agar plates revealed that only a few of the enrichment isolates could grow; these included *Brevundimonas*, *Chryseobacterium*, *Sphingobacterium*, *Geotrichum*, and *Candida*. Genera like *Candida*, are typically linked with polluted habitats (Q. Zhang et al., 2019). Although direct microbial degradation of PFOA remains rare, several studies have reported the ability of specific microorganisms to persist under PFAS exposure. For example, Wackett, (2022) discussed bacterial taxa such as *Pseudomonas* spp. and related environmental isolates that can tolerate or interact with PFAS compounds, including perfluorooctanoic acid (PFOA) and other perfluoroalkyl acids, primarily through mechanisms such as bioaccumulation or limited transformation rather than complete mineralization.

Similarly, Parsons et al. (2008) evaluated the biodegradability of fluorinated surfactants, including PFOA and related perfluorinated carboxylates, and concluded that microbial growth observed under such conditions reflects tolerance or co-metabolic processes rather than direct utilization or degradation of PFAS as a carbon source. Taken together, these findings support the interpretation that growth of the isolates observed in this study under PFOA exposure is indicative of tolerance and persistence rather than evidence of PFAS mineralization or defluorination. For all the fluorinated compounds tested, including the several PFAS and the fluoxetine (FLX) pharmaceutical, no growth or fluoride release was observed when these compounds were supplied as sole carbon sources, suggesting that direct growth was not supported under the conditions tested.

While FLX is not a PFAS, it bears C–F bonds, and it is a fluorinated pharmaceutical whose environmental occurrence, persistence, and biodegradation have been well documented. Due to its comparatively lower recalcitrance relative to PFAS, FLX serves as a suitable model compound for

investigating microbial defluorination processes (Moreira, 2012). The increase in biomass, decrease in FLX concentration, and release of fluoride observed in glucose-supplemented systems provide strong evidence for co-metabolic transformation. In this case, FLX was not utilized as a primary carbon source but was transformed incidentally through enzymatic activity sustained by glucose. This behavior is characteristic of co-metabolism, where microorganisms degrade non-growth substrates only in the presence of an additional energy source that supports metabolic activity.

A similar mechanism has been described for chlorinated solvents such as trichloroethylene (TCE) and chloroform, where microbial transformation occurs only when a co-substrate (e.g., formate or methane) is available to sustain growth and enzyme production (Berkley et al., 1991). In such systems, enzymes produced during primary metabolism act non-specifically on structurally unrelated compounds, leading to partial transformation rather than complete mineralization. The relevance of this comparison lies not in the similarity of the compounds, but in the shared metabolic mechanism. In contrast, the co-metabolic transformation of PFAS remains highly limited. Compounds such as perfluorooctanoic acid (PFOA) are extremely recalcitrant due to the strength of the carbon–fluorine bond, which restricts enzymatic attack and prevents their use as growth substrates (Cousins et al., 2020; Parsons et al., 2008).

Although some studies suggest that microorganisms may interact with PFAS under co-metabolic conditions, these interactions are generally limited to partial transformation or bioaccumulation rather than complete defluorination (Wackett, 2022). Taken together, these findings indicate that the defluorination observed for FLX is driven by co-metabolic processes supported by an external carbon source. However, the absence of similar activity for PFAS under the same conditions highlights the fundamental difference between fluorinated pharmaceuticals and perfluoroalkyl substances, emphasizing the extreme resistance of PFAS to microbial transformation even in metabolically active systems.

This is consistent with expectations for the co-metabolic transformation of xenobiotics such as chlorinated solvents (e.g., trichloroethylene), polycyclic aromatic hydrocarbons (PAHs), and certain pharmaceutical compounds, which are not used as primary carbon sources but are transformed incidentally during microbial metabolism (Murphy, 2016). Crucially, these findings suggest that the isolates may possess only a conditional capacity to cleave C–F bonds. In agreement with previous literature, perfluoroalkyl acids are not readily biodegradable because of the high dissociation energy of the C–F bond and the intrinsic stability of their fluorinated carbon chain (Parsons et al., 2008).

Future work should therefore explore conditions that may enhance transformation potential, including comparisons between growing and resting-cell systems, evaluation of co-metabolic regimes with different auxiliary substrates, and the application of more sensitive analytical techniques to better distinguish between sorption and true biotransformation.

Chapter 5. Conclusions

The work presented here describes the first study on the analysis of stored microbiomes derived from different PFAS-impacted environmental matrices. It provides a detailed assessment of the structural and functional integrity of environmental microbiomes from PFAS-impacted soil and sediment after long-term cryogenic storage, as well as their adaptation to PFAS selective pressure. This research bridges community structure and functional potential through the integration of metabarcoding, culturomics and biotransformation testing, connecting community ecology to environmental biotechnology.

The results achieved evidence that cryogenic preservation affect mainly the vitality and metabolic activities of the microbiome. In particularly, soil cryogenic preservation-maintained microbiome viability and comparable metabolic activity for up to eight months of storage, whereas sediment samples showed more consistent changes in microbial vitality and metabolism. Cryogenic preservation at −80 °C with 30% *v/w* glycerol yielded different but complementary results between culture-dependent and culture-independent analyses, demonstrating that both approaches are necessary to obtain a comprehensive understanding of the microbiome. Metabarcoding and clustering analysis showed no significant temporal clustering of samples.

On the other hand, a loss of culturable microorganisms and metabolic activity at a later time of storage (12 months) was observed. These findings illustrate a critical aspect of microbiome preservation: while the DNA molecule can be maintained, vitality and metabolic activity may diminish over time. Thes findings underline the need for molecular and culture-based approaches in assessing preserved environmental samples. When exposed to high PFOA concentrations through enrichment cultures, the preserved microbiomes remain viable and responsive to chemical stress. Successive changes in community structure were detected, suggesting a selection process in response to PFAS.

The isolation of a variety of bacterial and fungi indicates that preserved microbiomes still have a high functional and ecological versatility, despite prolonged storage. Despite the recovery of PFAS-tolerant microbial communities and isolates, no evidence of PFAS biodegradation or defluorination was detected under the tested conditions. This confirms the well-known recalcitrance of perfluorinated compounds and the difficulty of achieving their transformation through microbial processes. However, co-metabolic experiments using fluoxetine demonstrated that selected isolates were capable of defluorination of simpler fluorinated compounds. This indicates that while the necessary enzymatic potential for C–F bond cleavage exists, the structural complexity and stability of PFAS likely require specific environmental or metabolic conditions to enable transformation.

Chapter 6. Final Perspective and Future Directions

Overall, this study demonstrates that cryogenic preservation with the addition of glycerol (30% *w/v*) may be a reliable approach for maintaining environmental microbiomes as potential resources for future biotechnological applications. Although direct PFAS degradation was not achieved, the identification of stress-tolerant microbial taxa and their ability to transform model fluorinated compounds provides a valuable basis for further investigation.

Future work should focus on metabolic studies to identify conditions that stimulate microbial activity toward fluorinated compounds. In particular, the role of co-metabolism should be systematically explored, as no additional carbon or energy sources were supplied alongside PFAS in this study. The addition of suitable co-substrates, such as simple carbohydrates or organic acids, may help induce otherwise unexpressed enzymatic pathways. Further research should examine different physiological states of microorganisms, including comparisons between actively growing cultures and resting-cell systems, and optimize culture conditions (e.g., incubation time, nutrient availability, pH, and temperature) to detect slow or low-efficiency transformation processes.

At the community level, the development of defined microbial consortia may clarify interspecific interactions and reveal cooperative mechanisms, while biofilm-based systems may enhance microbial stability and metabolic activity. Advanced analytical approaches, such as LC-MS/MS and target/non-target screening, will be essential to detect transformation products and distinguish true biotransformation from sorption. Monitoring fluoride release alongside intermediate metabolites will be critical to confirm defluorination pathways.

Subsequently, omics-based approaches can be applied to identify genes and pathways involved in fluorinated compound transformation, particularly those associated with C–F bond activation. Finally, translating these findings into environmental applications, including soil microcosms and bioreactors, will be essential for developing effective PFAS bioremediation strategies. Together, these directions will help bridge the gap between microbial persistence without detectable transformation and practical PFAS remediation.

Bibliography

Abou-Khalil, C., Sarkar, D., Braykaa, P., & Boufadel, M. C. (2022). Mobilization of Per- and Polyfluoroalkyl Substances (PFAS) in Soils: A Review. In *Current Pollution Reports* (Vol. 8, Number 4, pp. 422–444). Springer Science and Business Media Deutschland GmbH. https://doi.org/10.1007/s40726-022-00241-8

Aggelopoulos, C. A. (2026). Innovations in PFAS remediation: a review on the growing role of cold plasma technology. In *Separation and Purification Technology* (Vol. 380). Elsevier B.V. https://doi.org/10.1016/j.seppur.2025.135535

Ahrens, L. (2011). Polyfluoroalkyl compounds in the aquatic environment: A review of their occurrence and fate. *Journal of Environmental Monitoring*, *13*(1), 20–31. https://doi.org/10.1039/c0em00373e

Ahrens, L., & Bundschuh, M. (2014). Fate and effects of poly- and perfluoroalkyl substances in the aquatic environment: A review. *Environmental Toxicology and Chemistry*, *33*(9), 1921–1929. https://doi.org/10.1002/etc.2663

Ahrens, L., Gerwinski, W., Theobald, N., & Ebinghaus, R. (2010). Sources of polyfluoroalkyl compounds in the North Sea, Baltic Sea and Norwegian Sea: Evidence from their spatial distribution in surface water. *Marine Pollution Bulletin*, *60*(2), 255–260. https://doi.org/10.1016/j.marpolbul.2009.09.013

Ahrens, L., Taniyasu, S., Yeung, L. W. Y., Yamashita, N., Lam, P. K. S., & Ebinghaus, R. (2010). Distribution of polyfluoroalkyl compounds in water, suspended particulate matter and sediment from Tokyo Bay, Japan. *Chemosphere*, *79*(3), 266–272. https://doi.org/10.1016/j.chemosphere.2010.01.045

Alexander, J., Atli Auðunsson, G., Benford, D., Cockburn, A., Cravedi, J.-P., Dogliotti, E., Di Domenico, A., Luisa Fernández-Cruz, M., Fink-Gremmels, J., Fürst, P., Galli, C., Grandjean, P., Gzyl, J., Heinemeyer, G., Johansson, N., Mutti, A., Schlatter, J., van Leeuwen, R., van Peteghem, C., & Verger, P. (2008). Perfluorooctane sulfonate (PFOS), perfluorooctanoic acid (PFOA) and their salts Scientific Opinion of the Panel on Contaminants in the Food chain 1 PANEL MEMBERS. In *The EFSA Journal* (Vol. 653).

Allinson, M., Yamashita, N., Taniyasu, S., Yamazaki, E., & Allinson, G. (2019). Occurrence of perfluoroalkyl substances in selected Victorian rivers and estuaries: An historical snapshot. *Heliyon*, *5*(9). https://doi.org/10.1016/j.heliyon.2019.e02472

Altschul, F. S., Warren, G., Webb, M., & Eugene, W. M. (1990). *Altschul*.

Atlas, R. M., & Bartha, R. (1998). *Microbial ecology: Fundamentals and applications* (4th ed.). Benjamin/Cummings Science Publishing.

Aminot, Y., Sayfritz, S. J., Thomas, K. V, Godinho, L., Botteon, E., Boti, V., Albanis, T., Köck-Schulmeyer, M., Diaz-Cruz, S., Barceló, D., Marques, A., & Readman, J. W. (2019). *Environmental Risks Associated with Contaminants of Legacy and Emerging Concern at European 1 Aquaculture Areas 2 3*.

Anderson, M. J., Crist, T. O., Chase, J. M., Vellend, M., Inouye, B. D., Freestone, A. L., Sanders, N. J., Cornell, H. V., Comita, L. S., Davies, K. F., Harrison, S. P., Kraft, N. J. B., Stegen, J. C., & Swenson, N. G. (2011). Navigating the multiple meanings of β diversity: A roadmap for the practicing ecologist. *Ecology Letters*, *14*(1), 19–28. https://doi.org/10.1111/j.1461-0248.2010.01552.x

Agency for Toxic Substances and Disease Registry (ATSDR). (2021). *Toxicological profile for perfluoroalkyls*. U.S. Department of Health and Human Services.

Andreolli, M., Lampis, S., Brignoli, P., & Vallini, G. (2021). Mesocosm-based simulations to optimize a bioremediation strategy for the effective restoration of wildfire-impacted soils contaminated with high-molecular-weight hydrocarbons. *Journal of Applied Microbiology*, *131*(3), 1249–1260. https://doi.org/10.1111/jam.15018

Andreolli, M., Lampis, S., Zenaro, E., Salkinoja-Salonen, M., & Vallini, G. (2011). Burkholderia fungorum DBT1: A promising bacterial strain for bioremediation of PAHs-contaminated soils. In *FEMS Microbiology Letters* (Vol. 319, Number 1, pp. 11–18). https://doi.org/10.1111/j.1574-6968.2011.02259.x

Author, C., & Whittaker, R. H. (1960). Vegetation of the Siskiyou Mountains. In *Source: Ecological Monographs* (Vol. 30, Number 3).

Bah Abbas. (2022). *ASSESSING THE VIABILITY OF MICROALGAE AS A BIOREMEDIATION METHOD FOR PER-AND POLYFLUOROALKYL SUBSTANCES (PFAS)-2022 by Abbass Bah*.

Baldrian, P. (2017). Forest microbiome: Diversity, complexity and dynamics. *FEMS Microbiology Reviews*, *41*(2), 109–130. https://doi.org/10.1093/femsre/fuw040

Berg, G., Rybakova, D., Fischer, D., Cernava, T., Vergès, M. C. C., Charles, T., Chen, X., Cocolin, L., Eversole, K., Corral, G. H., Kazou, M., Kinkel, L., Lange, L., Lima, N., Loy, A., Macklin, J. A., Maguin, E., Mauchline, T., McClure, R., … Schloter, M. (2020). Microbiome definition re-visited: old concepts and new challenges. In *Microbiome* (Vol. 8, Number 1). BioMed Central Ltd. https://doi.org/10.1186/s40168-020-00875-0

Berhanu, A., Mutanda, I., Taolin, J., Qaria, M. A., Yang, B., & Zhu, D. (2023). A review of microbial degradation of per- and polyfluoroalkyl substances (PFAS): Biotransformation

routes and enzymes. In *Science of the Total Environment* (Vol. 859). Elsevier B.V. https://doi.org/10.1016/j.scitotenv.2022.160010

Bhattacharya, A., Fathima, J., Varghese, S., Chatterjee, P., & Gadhamshetty, V. (2025). Advances in bioremediation strategies for PFAS-contaminated water and soil. In *Soil and Environmental Health* (Vol. 3, Number 1). Elsevier B.V. https://doi.org/10.1016/j.seh.2024.100126

Banks, R. E., Smart, B. E., & Tatlow, J. C. (Eds.). (2013). *Organofluorine chemistry: Principles and commercial applications*. Springer.

Bolyen, E. , G. C. J., Botkin, J. R., & McGuire, A. L. (2019). Clarify the HIPAA right of access to individuals' research data. In *Nature Biotechnology* (Vol. 37, Number 8, pp. 850–852). Nature Publishing Group. https://doi.org/10.1038/s41587-019-0190-3

Brusseau, M. L., Anderson, R. H., & Guo, B. (2020). PFAS concentrations in soils: Background levels versus contaminated sites. *Science of the Total Environment*, *740*. https://doi.org/10.1016/j.scitotenv.2020.140017

Buck, R. C., Franklin, J., Berger, U., Conder, J. M., Cousins, I. T., Voogt, P. De, Jensen, A. A., Kannan, K., Mabury, S. A., & van Leeuwen, S. P. J. (2011). Perfluoroalkyl and polyfluoroalkyl substances in the environment: Terminology, classification, and origins. *Integrated Environmental Assessment and Management*, *7*(4), 513–541. https://doi.org/10.1002/ieam.258

Butt, C. M., Muir, D. C. G., & Mabury, S. A. (2014). Biotransformation pathways of fluorotelomer-based polyfluoroalkyl substances: A review. *Environmental Toxicology and Chemistry*, *33*(2), 243–267. https://doi.org/10.1002/etc.2407

Cao, X., Wang, C., Lu, Y., Zhang, M., Khan, K., Song, S., Wang, P., & Wang, C. (2019). Occurrence, sources and health risk of polyfluoroalkyl substances (PFASs) in soil, water and sediment from a drinking water source area. *Ecotoxicology and Environmental Safety*, *174*, 208–217. https://doi.org/10.1016/j.ecoenv.2019.02.058

Carlson, H. K., Price, M. N., Callaghan, M., Aaring, A., Chakraborty, R., Liu, H., Kuehl, J. V., Arkin, A. P., & Deutschbauer, A. M. (2019). The selective pressures on the microbial community in a metal-contaminated aquifer. *ISME Journal*, *13*(4), 937–949. https://doi.org/10.1038/s41396-018-0328-1

Che, S., Jin, B., Liu, Z., Yu, Y., Liu, J., & Men, Y. (2021). Structure-specific aerobic defluorination of short-chain fluorinated carboxylic acids by activated sludge communities. *Environmental Science and Technology Letters*, *8*(8), 668–674. https://doi.org/10.1021/acs.estlett.1c00511

Chetverikov, S. P., Sharipov, D. A., Korshunova, T. Y., & Loginov, O. N. (2017). Degradation of perfluorooctanyl sulfonate by strain Pseudomonas plecoglossicida 2.4-D. *Applied*

Biochemistry and Microbiology, *53*(5), 533–538. https://doi.org/10.1134/S0003683817050027

Cocolin, L., Bevivino, A., Alduina, R., Andreolli, M., Bianco, A., Capozzi, V., Costa, C., Costanzo, M., Curtoni, A., Di Gregorio, L., Elsayed, A., Felis, G., Ferrara, M., Ferrocino, I., Fiore, A., Franzetti, A., Gaglio, R., Gallo, G., Garello, M., … Giovanna Varese, C. (2024). *STANDARD OPERATING PROCEDURES (SOPs) FOR SAMPLING OF MICROBIOME IN DIFFERENT ECOSYSTEMS*.

Colosi, L. M., Pinto, R. A., Huang, Q., & Weber, W. J. (2009). PEROXIDASE-MEDIATED DEGRADATION OF PERFLUOROOCTANOIC ACID. *Environmental Toxicology and Chemistry*, *28*(2), 264–271. https://doi.org/10.1897/08-282.S1

Cordner, A., Brown, P., Cousins, I. T., Scheringer, M., Martinon, L., Dagorn, G., Aubert, R., Hosea, L., Salvidge, R., Felke, C., Tausche, N., Drepper, D., Liva, G., Tudela, A., Delgado, A., Salvatore, D., Pilz, S., & Horel, S. (2024). PFAS Contamination in Europe: Generating Knowledge and Mapping Known and Likely Contamination with "Expert-Reviewed" Journalism. *Environmental Science and Technology*, *58*(15), 6616–6627. https://doi.org/10.1021/acs.est.3c09746

Cousins, I. T., Dewitt, J. C., Glüge, J., Goldenman, G., Herzke, D., Lohmann, R., Ng, C. A., Scheringer, M., & Wang, Z. (2020). The high persistence of PFAS is sufficient for their management as a chemical class. In *Environmental Science: Processes and Impacts* (Vol. 22, Number 12, pp. 2307–2312). Royal Society of Chemistry. https://doi.org/10.1039/d0em00355g

Cranwill, A. (2022). *Potential of a Laccase from Trametes versicolor to Degrade Per-and Polyfluoroalkyl Substances in Water*.

Curtzwiler, G. W., Silva, P., Hall, A., Ivey, A., & Vorst, K. (2021). Significance of Perfluoroalkyl Substances (PFAS) in Food Packaging. *Integrated Environmental Assessment and Management*, *17*(1), 7–12. https://doi.org/10.1002/ieam.4346

Cao, L., Xu, W., Wan, Z., Li, G., & Zhang, F. (2022). Occurrence of PFASs and its effect on soil bacteria at a fire-training area using PFOS-restricted aqueous film-forming foams. *iScience, 25*(4). https://doi.org/10.1016/j.isci.2022.104084

Chemical & Engineering News. (2022). European court rejects Chemours's arguments on GenX classification. *Chemical & Engineering News*. https://cen.acs.org/environment/persistent-pollutants/European-court-rejects-Chemourss-arguments/100/i8

ChemTrust. (2023). *Forever chemicals: Antwerp factory pollution raises serious concerns*. https://chemtrust.org/news/forever-chemicals-antwerp-factory/

Chambers, R. D. (2004). *Fluorine in organic chemistry*. CRC Press.

Davis, K. L., Aucoin, M. D., Larsen, B. S., Kaiser, M. A., & Hartten, A. S. (2007). Transport of ammonium perfluorooctanoate in environmental media near a fluoropolymer manufacturing facility. *Chemosphere*, *67*(10), 2011–2019. https://doi.org/10.1016/j.chemosphere.2006.11.049

De Silva, A. O., Armitage, J. M., Bruton, T. A., Dassuncao, C., Heiger-Bernays, W., Hu, X. C., Kärrman, A., Kelly, B., Ng, C., Robuck, A., Sun, M., Webster, T. F., & Sunderland, E. M. (2021). PFAS Exposure Pathways for Humans and Wildlife: A Synthesis of Current Knowledge and Key Gaps in Understanding. In *Environmental Toxicology and Chemistry* (Vol. 40, Number 3, pp. 631–657). Wiley Blackwell. https://doi.org/10.1002/etc.4935

DeLuca, N. M., Angrish, M., Wilkins, A., Thayer, K., & Cohen Hubal, E. A. (2021). Human exposure pathways to poly- and perfluoroalkyl substances (PFAS) from indoor media: A systematic review protocol. *Environment International*, *146*. https://doi.org/10.1016/j.envint.2020.106308

Dewapriya, P., Chadwick, L., Gorji, S. G., Schulze, B., Valsecchi, S., Samanipour, S., Thomas, K. V., & Kaserzon, S. L. (2023). Per- and polyfluoroalkyl substances (PFAS) in consumer products: Current knowledge and research gaps. *Journal of Hazardous Materials Letters*, *4*. https://doi.org/10.1016/j.hazl.2023.100086

Dias, D., Bons, J., Kumar, A., Kabir, M. H., & Liang, H. (2024). Forever Chemicals, Per-and Polyfluoroalkyl Substances (PFAS), in Lubrication. In *Lubricants* (Vol. 12, Number 4). Multidisciplinary Digital Publishing Institute (MDPI). https://doi.org/10.3390/lubricants12040114

Dixon, P. (2003). VEGAN, a package of R functions for community ecology. In *Journal of Vegetation Science* (Vol. 14, Number 6, pp. 927–930). Opulus Press AB. https://doi.org/10.1111/j.1654-1103.2003.tb02228.x

Domingo, J. L., & Nadal, M. (2017). Per- and polyfluoroalkyl substances (PFASs) in food and human dietary intake: A review of the recent scientific literature. In *Journal of Agricultural and Food Chemistry* (Vol. 65, Number 3, pp. 533–543). American Chemical Society. https://doi.org/10.1021/acs.jafc.6b04683

Dreyer, A., Matthias, V., Weinberg, I., & Ebinghaus, R. (2010). Wet deposition of poly- and perfluorinated compounds in Northern Germany. *Environmental Pollution*, *158*(5), 1221–1227. https://doi.org/10.1016/j.envpol.2010.01.030

Dully, V., Rech, G., Wilding, T. A., Lanzén, A., MacKichan, K., Berrill, I., & Stoeck, T. (2021). Comparing sediment preservation methods for genomic biomonitoring of coastal marine ecosystems. *Marine Pollution Bulletin*, *173*. https://doi.org/10.1016/j.marpolbul.2021.113129

Ellis, D. A., Martin, J. W., De Silva, A. O., Mabury, S. A., Hurley, M. D., Sulbaek Andersen, M. P., & Wallington, T. J. (2004). Degradation of fluorotelomer alcohols: A likely atmospheric source of perfluorinated carboxylic acids. *Environmental Science and Technology*, *38*(12), 3316–3321. https://doi.org/10.1021/es049860w

EMEP/EEA. (2019). *EMEP/EEA air pollutant emission inventory guidebook 2019*. https://www.eea.europa.eu/publications/emep-eea-guidebook-2019

EFSA Panel on Contaminants in the Food Chain (CONTAM Panel), Schrenk, D., Bignami, M., Bodin, L., Chipman, J. K., del Mazo, J., et al. (2020). Risk to human health related to the presence of perfluoroalkyl substances in food. *EFSA Journal, 18*(9), e06223.

Evich, M. G., Davis, M. J. B., McCord, J. P., Acrey, B., Awkerman, J. A., Knappe, D. R. U., Lindstrom, A. B., Speth, T. F., Tebes-Stevens, C., Strynar, M. J., Wang, Z., Weber, E. J., Henderson, W. M., & Washington, J. W. (2022). Per- and polyfluoroalkyl substances in the environment. *Science*, *375*(6580). https://doi.org/10.1126/science.abg9065

Fang, C., Megharaj, M., & Naidu, R. (2017). Electrochemical Advanced Oxidation Processes (EAOP) to degrade per- and polyfluoroalkyl substances (PFASs). *Journal of Advanced Oxidation Technologies*, *20*(2). https://doi.org/10.1515/jaots-2017-0014

Fang, S., Chen, X., Zhao, S., Zhang, Y., Jiang, W., Yang, L., & Zhu, L. (2014). Trophic magnification and isomer fractionation of perfluoroalkyl substances in the food web of Taihu Lake, China. *Environmental Science and Technology*, *48*(4), 2173–2182. https://doi.org/10.1021/es405018b

Feigl, V., Ujaczki, É., Vaszita, E., & Molnár, M. (2017). Influence of red mud on soil microbial communities: Application and comprehensive evaluation of the Biolog EcoPlate approach as a tool in soil microbiological studies. *Science of the Total Environment*, *595*, 903–911. https://doi.org/10.1016/j.scitotenv.2017.03.266

Fernandez, N. A., Rodriguez-Freire, L., Keswani, M., & Sierra-Alvarez, R. (2016). Effect of chemical structure on the sonochemical degradation of perfluoroalkyl and polyfluoroalkyl substances (PFASs). *Environmental Science: Water Research and Technology*, *2*(6), 975–983. https://doi.org/10.1039/c6ew00150e

Ferrocino, I., Ferrara, M., Garello, M., Turchetti, B., Andreolli, M., Arena, M. P., Alduina, R., Aloi, F., Bevivino, A., Bruno, E., Capozzi, V., Coronas, R., De Vero, L., Di Renzo, T., Franzetti, A., Gaglio, R., Gallo, G., Gullo, M., Guarcello, R., … Cocolin, L. (2025). Standardizing microbiome research: interlaboratory validation of SOPs for sample preparation and DNA extraction from food and environmental ecosystems. *Environmental Microbiome*, *21*(1). https://doi.org/10.1186/s40793-025-00833-z

Fierer, N. (2017). Embracing the unknown: Disentangling the complexities of the soil microbiome. In *Nature Reviews Microbiology* (Vol. 15, Number 10, pp. 579–590). Nature Publishing Group. https://doi.org/10.1038/nrmicro.2017.87

Fierer, N., Bradford, M. A., & Jackson, R. B. (2007). Toward an ecological classification of soil bacteria. *Ecology*, *88*(6), 1354–1364. https://doi.org/10.1890/05-1839

Fierer, N., & Jackson, R. B. (2006). *The diversity and biogeography of soil bacterial communities*. www.pnas.orgcgidoi10.1073pnas.0507535103

Frassinetti, S., Setti, L., Corti, A., Farrinelli, P., Montevecchi, P., & Vallini, G. (1998). *Biodegradation of dibenzothiophene by a nodulating isolate of Rhizobium meliloti*.

Fromin, N. (2025). Impacts of soil storage on microbial parameters. In *SOIL* (Vol. 11, Number 1, pp. 247–265). Copernicus Publications. https://doi.org/10.5194/soil-11-247-2025

Fuchigami, T., & Inagi, S. (2020). Recent Advances in Electrochemical Systems for Selective Fluorination of Organic Compounds. *Accounts of Chemical Research*, *53*(2), 322–334. https://doi.org/10.1021/acs.accounts.9b00520

Gaines, L. G. T. (2023). Historical and current usage of per- and polyfluoroalkyl substances (PFAS): A literature review. In *American Journal of Industrial Medicine* (Vol. 66, Number 5, pp. 353–378). John Wiley and Sons Inc. https://doi.org/10.1002/ajim.23362

Gandolfi, I., Canedoli, C., Rosatelli, A., Covino, S., Cappelletti, D., Sebastiani, B., Tatangelo, V., Corengia, D., Pittino, F., Padoa-Schioppa, E., Báez-Matus, X., Hernández, L., Seeger, M., Saati-Santamaría, Z., García-Fraile, P., López-Mondéjar, R., Ambrosini, R., Papacchini, M., & Franzetti, A. (2024). Microbiomes of urban trees: unveiling contributions to atmospheric pollution mitigation. *Frontiers in Microbiology*, *15*. https://doi.org/10.3389/fmicb.2024.1470376

Gao, K., Zhuang, T., Liu, X., Fu, J., Zhang, J., Fu, J., Wang, L., Zhang, A., Liang, Y., Song, M., & Jiang, G. (2019). Prenatal Exposure to Per- and Polyfluoroalkyl Substances (PFASs) and Association between the Placental Transfer Efficiencies and Dissociation Constant of Serum Proteins-PFAS Complexes. *Environmental Science and Technology*, *53*(11), 6529–6538. https://doi.org/10.1021/acs.est.9b00715

Garland, J. L. (1997). Analysis and interpretation of community-level physiological profiles in microbial ecology. *FEMS Microbiology Ecology*, *24*(4), 289–300. https://doi.org/10.1111/j.1574-6941.1997.tb00446.x

Garland, J. L., & Mills, A. L. (1991). Classification and Characterization of Heterotrophic Microbial Communities on the Basis of Patterns of Community-Level Sole-Carbon-Source Utilization. In *APPLIED AND ENVIRONMENTAL MICROBIOLOGY* (Vol. 57, Number 8). https://journals.asm.org/journal/aem

Giglioli, S., Colombo, L., & Azzellino, A. (2023). Cluster and multivariate analysis to study the diffuse contamination of emerging per- and polyfluoroalkyl substances (PFAS) in the Veneto Region plain (North-eastern Italy). *Chemosphere*, *319*. https://doi.org/10.1016/j.chemosphere.2023.137916

Glüge, J., Scheringer, M., Cousins, I. T., Dewitt, J. C., Goldenman, G., Herzke, D., Lohmann, R., Ng, C. A., Trier, X., & Wang, Z. (2020). An overview of the uses of per- And polyfluoroalkyl substances (PFAS). *Environmental Science: Processes and Impacts*, *22*(12), 2345–2373. https://doi.org/10.1039/d0em00291g

Guelfo, J. L., & Higgins, C. P. (2013). Subsurface transport potential of perfluoroalkyl acids at aqueous film-forming foam (AFFF)-impacted sites. *Environmental Science and Technology*, *47*(9), 4164–4171. https://doi.org/10.1021/es3048043

Guelfo, J. L., Korzeniowski, S., Mills, M. A., Anderson, J., Anderson, R. H., Arblaster, J. A., Conder, J. M., Cousins, I. T., Dasu, K., Henry, B. J., Lee, L. S., Liu, J., McKenzie, E. R., & Willey, J. (2021). Environmental Sources, Chemistry, Fate, and Transport of Per- and Polyfluoroalkyl Substances: State of the Science, Key Knowledge Gaps, and Recommendations Presented at the August 2019 SETAC Focus Topic Meeting. In *Environmental Toxicology and Chemistry* (Vol. 40, Number 12, pp. 3234–3260). John Wiley and Sons Inc. https://doi.org/10.1002/etc.5182

Guo, C., Ahrens, L., Bertilsson, S., Coolen, M. J. L., & Tang, J. (2023). Riverine microbial communities impacted by per- and polyfluoroalkyl substances (PFAS) emissions from a fluoropolymer-manufacturing plant. *Journal of Hazardous Materials*, *457*. https://doi.org/10.1016/j.jhazmat.2023.131803

Hall, A. T. (1999). *BioEdit_a_user_friendly_biological_seque*.

Han, M., Qin, C., & Gao, Y. (2025). Sources and transport of per- and polyfluoroalkyl substance (PFAS) in agricultural soil–plant systems. *New Contaminants*, *1*(1), 0–0. https://doi.org/10.48130/newcontam-0025-0007

Harding-Marjanovic, K. C., Houtz, E. F., Yi, S., Field, J. A., Sedlak, D. L., & Alvarez-Cohen, L. (2015). Aerobic Biotransformation of Fluorotelomer Thioether Amido Sulfonate (Lodyne) in AFFF-Amended Microcosms. *Environmental Science and Technology*, *49*(13), 7666–7674. https://doi.org/10.1021/acs.est.5b01219

Harms, H., Schlosser, D., & Wick, L. Y. (2011). Untapped potential: Exploiting fungi in bioremediation of hazardous chemicals. In *Nature Reviews Microbiology* (Vol. 9, Number 3, pp. 177–192). https://doi.org/10.1038/nrmicro2519

Harris, B. A., Zhou, J., Clarke, B. O., & Leung, I. K. H. (2025). Enzymatic Degradation of PFAS: Current Status and Ongoing Challenges. In *ChemSusChem* (Vol. 18, Number 2). John Wiley and Sons Inc. https://doi.org/10.1002/cssc.202401122

Hartz, W. F., Björnsdotter, M. K., Yeung, L. W. Y., Hodson, A., Thomas, E. R., Humby, J. D., Day, C., Jogsten, I. E., Kärrman, A., & Kallenborn, R. (2023). Levels and distribution profiles of Per- and Polyfluoroalkyl Substances (PFAS) in a high Arctic Svalbard ice core. *Science of the Total Environment*, *871*. https://doi.org/10.1016/j.scitotenv.2023.161830

Hedgespeth, M. L., Taylor, D. L., Balint, S., Schwartz, M., & Cantwell, M. G. (2023). Ecological characteristics impact PFAS concentrations in a U.S. North Atlantic food web. *Science of the Total Environment*, *880*. https://doi.org/10.1016/j.scitotenv.2023.163302

Higgins, C. P., & Luthy, R. G. (2006). Sorption of perfluorinated surfactants on sediments. *Environmental Science and Technology*, *40*(23), 7251–7256. https://doi.org/10.1021/es061000n

Hornung, B., Martins dos Santos, V. A. P., Smidt, H., & Schaap, P. J. (2018). Studying microbial functionality within the gut ecosystem by systems biology. In *Genes and Nutrition* (Vol. 13, Number 1). BioMed Central Ltd. https://doi.org/10.1186/s12263-018-0594-6

Houde, M., De Silva, A. O., Muir, D. C. G., & Letcher, R. J. (2011a). Monitoring of perfluorinated compounds in aquatic biota: An updated review. In *Environmental Science and Technology* (Vol. 45, Number 19, pp. 7962–7973). https://doi.org/10.1021/es104326w

Houde, M., De Silva, A. O., Muir, D. C. G., & Letcher, R. J. (2011b). Monitoring of perfluorinated compounds in aquatic biota: An updated review. In *Environmental Science and Technology* (Vol. 45, Number 19, pp. 7962–7973). https://doi.org/10.1021/es104326w

Hu, X. C., Andrews, D. Q., Lindstrom, A. B., Bruton, T. A., Schaider, L. A., Grandjean, P., Lohmann, R., Carignan, C. C., Blum, A., Balan, S. A., Higgins, C. P., & Sunderland, E. M. (2016). Detection of Poly- and Perfluoroalkyl Substances (PFASs) in U.S. Drinking Water Linked to Industrial Sites, Military Fire Training Areas, and Wastewater Treatment Plants. *Environmental Science and Technology Letters*, *3*(10), 344–350. https://doi.org/10.1021/acs.estlett.6b00260

Huang, S., & Jaffe, P. R. (2019). Defluorination of Perfluorooctanoic Acid (PFOA) and Perfluorooctane Sulfonate (PFOS) by Acidimicrobium sp. Strain A6. *Environmental Science and Technology*, *53*(19), 11410–11419. https://doi.org/10.1021/acs.est.9b04047

Huang, S., Smorada, C., Schaefer, C. E., & Jaffé, P. R. (2024). Stimulating Acidimicrobium sp. Strain A6 in iron-rich, acidic sediments from AFFF-impacted sites for PFAS defluorination. *Science of the Total Environment*, *955*. https://doi.org/10.1016/j.scitotenv.2024.176801

Huang, W., Chen, X., Jiang, X., & Zheng, B. (2017). Characterization of sediment bacterial communities in plain lakes with different trophic statuses. *MicrobiologyOpen*, *6*(5). https://doi.org/10.1002/mbo3.503

Hubálek, Z. (2003). Protectants used in the cryopreservation of microorganisms. In *Cryobiology* (Vol. 46, Number 3, pp. 205–229). Academic Press Inc. https://doi.org/10.1016/S0011-2240(03)00046-4

Hunter Anderson, R., Adamson, D. T., & Stroo, H. F. (2019). Partitioning of poly- and perfluoroalkyl substances from soil to groundwater within aqueous film-forming foam source zones. *Journal of Contaminant Hydrology*, *220*, 59–65. https://doi.org/10.1016/j.jconhyd.2018.11.011

Hu, X. C., Andrews, D. Q., Lindstrom, A. B., Bruton, T. A., Schaider, L. A., Grandjean, P., et al. (2016). Detection of poly- and perfluoroalkyl substances (PFASs) in US drinking water linked to industrial sites, military fire training areas, and wastewater treatment plants. *Environmental Science & Technology Letters, 3*(10), 344–350.

Interstate Technology & Regulatory Council (ITRC). (2022). *PFAS technical and regulatory guidance document and fact sheets (PFAS-1)*. https://pfas-1.itrcweb.org/

Interstate Technology & Regulatory Council (ITRC). (2023). *PFAS technical and regulatory guidance document and terminology update*. https://pfas-1.itrcweb.org/wp-content/uploads/2023/12/Full-PFAS-Guidance-12.11.2023.pdf

Interstate Technology & Regulatory Council (ITRC). (2026). *PFAS — Per- and polyfluoroalkyl substances*. https://pfas-1.itrcweb.org/

International Agency for Research on Cancer (IARC). (2023). *IARC monographs on the evaluation of carcinogenic risks to humans: Perfluorooctanoic acid (PFOA) and perfluorooctane sulfonate (PFOS)*.

Itumoh, E. J., Data, S., Chen, J. L. Y., Kah, M., Padhye, L. P., & Leitao, E. M. (2024). Addressing the persistence of per- and poly-fluoroalkyl substances (PFAS): current challenges and potential solutions. In *RSC Sustainability* (Vol. 2, Number 11, pp. 3183–3201). Royal Society of Chemistry. https://doi.org/10.1039/d4su00152d

Jaffé, P. R., Huang, S., Park, J., Ruiz-Urigüen, M., Shuai, W., & Sima, M. (2024). Defluorination of PFAS by Acidimicrobium sp. strain A6 and potential applications for remediation. In *Methods in Enzymology* (Vol. 696, pp. 287–320). Academic Press Inc. https://doi.org/10.1016/bs.mie.2024.01.013

Kelly, B. C., Ikonomou, M. G., Blair, J. D., Surridge, B., Hoover, D., Grace, R., & Gobas, F. A. P. C. (2009). Perfluoroalkyl contaminants in an arctic marine food web: Trophic magnification and wildlife exposure. *Environmental Science and Technology*, *43*(11), 4037–4043. https://doi.org/10.1021/es9003894

Kerckhof, F. M., Courtens, E. N. P., Geirnaert, A., Hoefman, S., Ho, A., Vilchez-Vargas, R., Pieper, D. H., Jauregui, R., Vlaeminck, S. E., Van De Wiele, T., Vandamme, P., Heylen, K., & Boon,

N. (2014). Optimized cryopreservation of mixed microbial communities for conserved functionality and diversity. *PLoS ONE*, *9*(6). https://doi.org/10.1371/journal.pone.0099517

Kim, H. M., Jung, J. Y., Yergeau, E., Hwang, C. Y., Hinzman, L., Nam, S., Hong, S. G., Kim, O. S., Chun, J., & Lee, Y. K. (2014). Bacterial community structure and soil properties of a subarctic tundra soil in Council, Alaska. *FEMS Microbiology Ecology*, *89*(2), 465–475. https://doi.org/10.1111/1574-6941.12362

Kim, M. H., Wang, N., & Chu, K. H. (2014). 6:2 Fluorotelomer alcohol (6:2 FTOH) biodegradation by multiple microbial species under different physiological conditions. *Applied Microbiology and Biotechnology*, *98*(4), 1831–1840. https://doi.org/10.1007/s00253-013-5131-3

Kim, M. H., Wang, N., Mcdonald, T., & Chu, K.-H. (2012). *Biodefluorination and Biotransformation of Fluorotelomer Alcohols by Two Alkane-Degrading Pseudomonas Strains*. https://doi.org/10.1002/bit.24561/abstract

Klindworth, A., Pruesse, E., Schweer, T., Peplies, J., Quast, C., Horn, M., & Glöckner, F. O. (2013). Evaluation of general 16S ribosomal RNA gene PCR primers for classical and next-generation sequencing-based diversity studies. *Nucleic Acids Research*, *41*(1). https://doi.org/10.1093/nar/gks808

Kotalik, C. J., Hubbard, L. E., Perrotta, B. G., Walters, D. M., Kolpin, D. W., Gray, J. L., Zachritz, A. M., Kraus, J. M., Givens, C. E., Lamberti, G. A., & Kidd, K. A. (2025). Bioaccumulation and Transfer of Per- and Polyfluoroalkyl Substances (PFAS) in a Stream and Riparian Food Web Contaminated by Food Processing Wastewater. *Environmental Science & Technology*, *59*(36), 19444–19456. https://doi.org/10.1021/acs.est.5c04867

Krafft, M. P., & Riess, J. G. (2015). Selected physicochemical aspects of poly- and perfluoroalkylated substances relevant to performance, environment and sustainability-Part one. *Chemosphere*, *129*, 4–19. https://doi.org/10.1016/j.chemosphere.2014.08.039

Kurwadkar, S., Dane, J., Kanel, S. R., Nadagouda, M. N., Cawdrey, R. W., Ambade, B., Struckhoff, G. C., & Wilkin, R. (2022). Per- and polyfluoroalkyl substances in water and wastewater: A critical review of their global occurrence and distribution. In *Science of the Total Environment* (Vol. 809). Elsevier B.V. https://doi.org/10.1016/j.scitotenv.2021.151003

Kushwaha, P., Soto Velázquez, A. L., McMahan, C., & Neilson, J. W. (2024). Field to Greenhouse: How Stable Is the Soil Microbiome after Removal from the Field? *Microorganisms*, *12*(1). https://doi.org/10.3390/microorganisms12010110

Kwon, B. G., Lim, H. J., Na, S. H., Choi, B. I., Shin, D. S., & Chung, S. Y. (2014). Biodegradation of perfluorooctanesulfonate (PFOS) as an emerging contaminant. *Chemosphere*, *109*, 221–225. https://doi.org/10.1016/j.chemosphere.2014.01.072

Kirsch, P. (2006). *Modern fluoroorganic chemistry: Synthesis, reactivity, applications* (2nd ed.). Wiley-VCH.

Kissa, E. (Ed.). (2001). *Fluorinated surfactants and repellents* (Vol. 97). CRC Press.

Liu, J., Edwards, E., Van Hamme, J., Manefield, M., Higgins, C. P., Blotevogel, J., et al. (2023). Correspondence on "Defluorination of perfluorooctanoic acid (PFOA) and perfluorooctane sulfonate (PFOS) by *Acidimicrobium* sp. strain A6." *Environmental Science & Technology, 57*(48), 20440–20442.

Lauber, C. L., Zhou, N., Gordon, J. I., Knight, R., & Fierer, N. (2010). Effect of storage conditions on the assessment of bacterial community structure in soil and human-associated samples. *FEMS Microbiology Letters*, *307*(1), 80–86. https://doi.org/10.1111/j.1574-6968.2010.01965.x

Lee, J., Kim, H. S., Jo, H. Y., & Kwon, M. J. (2021). Revisiting soil bacterial counting methods: Optimal soil storage and pretreatment methods and comparison of culturedependent and -independent methods. *PLoS ONE*, *16*(2 February). https://doi.org/10.1371/journal.pone.0246142

Linde, G. A., Luciani, A., Lopes, A. D., Valle, J. S. do, & Colauto, N. B. (2018). Long-term cryopreservation of basidiomycetes. In *Brazilian Journal of Microbiology* (Vol. 49, Number 2, pp. 220–231). Elsevier Editora Ltda. https://doi.org/10.1016/j.bjm.2017.08.004

Lindstrom, A. B., Strynar, M. J., Delinsky, A. D., Nakayama, S. F., McMillan, L., Libelo, E. L., Neill, M., & Thomas, L. (2011). Application of WWTP biosolids and resulting perfluorinated compound contamination of surface and well water in Decatur, Alabama, USA. *Environmental Science and Technology*, *45*(19), 8015–8021. https://doi.org/10.1021/es1039425

Liu, J., & Mejia Avendaño, S. (2013). Microbial degradation of polyfluoroalkyl chemicals in the environment: A review. In *Environment International* (Vol. 61, pp. 98–114). Elsevier Ltd. https://doi.org/10.1016/j.envint.2013.08.022

Lozupone, C. A., & Knight, R. (2007). *Global patterns in bacterial diversity*. www.pnas.org/cgi/content/full/

Lukhele, T., & Msagati, T. A. M. (2024). Assessment of functional diversity of heterotrophic microbial communities in polluted environments through community level physiological profiles. *Biologia*, *79*(3), 1027–1039. https://doi.org/10.1007/s11756-024-01608-6

Luo, Q., Lu, J., Zhang, H., Wang, Z., Feng, M., Chiang, S. Y. D., Woodward, D., & Huang, Q. (2015). Laccase-Catalyzed Degradation of Perfluorooctanoic Acid. *Environmental Science and Technology Letters*, *2*(7), 198–203. https://doi.org/10.1021/acs.estlett.5b00119

Ma, T., Ye, C., Wang, T., Li, X., & Luo, Y. (2022). Toxicity of Per- and Polyfluoroalkyl Substances to Aquatic Invertebrates, Planktons, and Microorganisms. In *International Journal of Environmental Research and Public Health* (Vol. 19, Number 24). MDPI. https://doi.org/10.3390/ijerph192416729

Madigan, M. T., Bender, K. S., Buckley, D. H., Sattley, W. M., & Stahl, D. A. (2018). *Brock biology of microorganisms* (15th ed.). Pearson Education Limited.

Mishra, S. K., Dey Chowdhury, S., Bhunia, P., Sarkar, A., Surampalli, R. Y., & Zhang, T. C. (2025). A cyclic problem of disposal of products and materials containing per- and polyfluoroalkyl substances. In *PFAS in the environment: Occurrence, characterization, treatment, and management* (pp. 161–186).

Macdonald, R. W., Barrie, L. A., Bidleman, T. F., Diamond, M. L., Gregor, D. J., Semkin, R. G., Strachan, W. M. J., Li, Y. F., Wania, F., Alaee, M., Alexeeva, L. B., Backus, S. M., Bailey, R., Bewers, J. M., Gobeil, C., Halsall, C. J., Harner, T., Hoff, J. T., Jantunen, L. M. M., … Yunker, M. B. (2000). Contaminants in the Canadian Arctic: 5 years of progress in understanding sources, occurrence and pathways. In *The Science of the Total Environment* (Vol. 254).

Manzano-Salgado, C. B., Casas, M., Lopez-Espinosa, M. J., Ballester, F., Basterrechea, M., Grimalt, J. O., Jiménez, A. M., Kraus, T., Schettgen, T., Sunyer, J., & Vrijheid, M. (2015). Transfer of perfluoroalkyl substances from mother to fetus in a Spanish birth cohort. *Environmental Research*, *142*, 471–478. https://doi.org/10.1016/j.envres.2015.07.020

Moreira, I. S. S. (2012). *Exploiting the Capacity of Labrys Portucalensis Strain F11 for Biotransformation of Fluoroaromatic Compounds* (Doctoral dissertation, Universidade Catolica Portuguesa (Portugal)).

Marchesi, J. R., & Ravel, J. (2015). The vocabulary of microbiome research: a proposal. *Microbiome*, *3*(1). https://doi.org/10.1186/s40168-015-0094-5

McGuire, M. E., Schaefer, C., Richards, T., Backe, W. J., Field, J. A., Houtz, E., Sedlak, D. L., Guelfo, J. L., Wunsch, A., & Higgins, C. P. (2014). Evidence of remediation-induced alteration of subsurface poly- and perfluoroalkyl substance distribution at a former firefighter training area. *Environmental Science and Technology*, *48*(12), 6644–6652. https://doi.org/10.1021/es5006187

Meegoda, J. N., Kewalramani, J. A., Li, B., & Marsh, R. W. (2020). A review of the applications, environmental release, and remediation technologies of per-and polyfluoroalkyl substances. In *International Journal of Environmental Research and Public Health* (Vol. 17, Number 21, pp. 1–26). MDPI AG. https://doi.org/10.3390/ijerph17218117

Méndez, V., Holland, S., Bhardwaj, S., McDonald, J., Khan, S., O'Carroll, D., Pickford, R., Richards, S., O'Farrell, C., Coleman, N., Lee, M., & Manefield, M. J. (2022). Aerobic biotransformation of 6:2 fluorotelomer sulfonate by Dietzia aurantiaca J3 under sulfur-

limiting conditions. *Science of the Total Environment*, *829*. https://doi.org/10.1016/j.scitotenv.2022.154587

Merino, N., Wang, M., Ambrocio, R., Mak, K., O'Connor, E., Gao, A., Hawley, E. L., Deeb, R. A., Tseng, L. Y., & Mahendra, S. (2018). Fungal biotransformation of 6:2 fluorotelomer alcohol. *Remediation*, *28*(2), 59–70. https://doi.org/10.1002/rem.21550

Milinovic, J., Lacorte, S., Vidal, M., & Rigol, A. (2015). Sorption behaviour of perfluoroalkyl substances in soils. *Science of the Total Environment*, *511*, 63–71. https://doi.org/10.1016/j.scitotenv.2014.12.017

Mojiri, A., Nazari Vishkaei, M., Ansari, H. K., Vakili, M., Farraji, H., & Kasmuri, N. (2023). Toxicity Effects of Perfluorooctanoic Acid (PFOA) and Perfluorooctane Sulfonate (PFOS) on Two Green Microalgae Species. *International Journal of Molecular Sciences*, *24*(3). https://doi.org/10.3390/ijms24032446

Möller, A., Ahrens, L., Surm, R., Westerveld, J., Van Der Wielen, F., Ebinghaus, R., & De Voogt, P. (2010). Distribution and sources of polyfluoroalkyl substances (PFAS) in the River Rhine watershed. *Environmental Pollution*, *158*(10), 3243–3250. https://doi.org/10.1016/j.envpol.2010.07.019

Moody, C. A., & Field, J. A. (2000). Perfluorinated surfactants and the environmental implications of their use in fire-fighting foams. In *Environmental Science and Technology* (Vol. 34, Number 18, pp. 3864–3870). https://doi.org/10.1021/es991359u

Moreira, I. S., Ribeiro, A. R., Afonso, C. M., Tiritan, M. E., & Castro, P. M. L. (2014). Enantioselective biodegradation of fluoxetine by the bacterial strain Labrys portucalensis F11. *Chemosphere*, *111*, 103–111. https://doi.org/10.1016/j.chemosphere.2014.03.022

Mudumbi, J. B. N., Ntwampe, S. K. O., Muganza, M., & Okonkwo, J. O. (2014). Susceptibility of Riparian Wetland Plants to Perfluorooctanoic Acid (PFOA) Accumulation. *International Journal of Phytoremediation*, *16*(9), 926–936. https://doi.org/10.1080/15226514.2013.810574

Mussabek, D., Persson, K. M., Berndtsson, R., Ahrens, L., Nakagawa, K., & Imura, T. (2020). Impact of the sediment organic vs. Mineral content on distribution of the per-and polyfluoroalkyl substances (pfas) in lake sediment. *International Journal of Environmental Research and Public Health*, *17*(16), 1–13. https://doi.org/10.3390/ijerph17165642

Muyzer, G., De Waal,' And, E. C., & Uitierlinden2, A. G. (1993). Profiling of Complex Microbial Populations by Denaturing Gradient Gel Electrophoresis Analysis of Polymerase Chain Reaction-Amplified Genes Coding for 16S rRNA. In *APPLIED AND ENVIRONMENTAL MICROBIOLOGY*. https://journals.asm.org/journal/aem

Muyzer, G., & Smalla, K. (1998). Application of denaturing gradient gel electrophoresis (DGGE) and temperature gradient gel electrophoresis (TGGE) in microbial ecology. In *Antonie van Leeuwenhoek* (Vol. 73).

Nayak, S., Sahoo, G., Das, I. I., Mohanty, A. K., Kumar, R., Sahoo, L., & Sundaray, J. K. (2023). Poly- and Perfluoroalkyl Substances (PFAS): Do They Matter to Aquatic Ecosystems? In *Toxics* (Vol. 11, Number 6). Multidisciplinary Digital Publishing Institute (MDPI). https://doi.org/10.3390/toxics11060543

Naidu, R., Mallavarapu, M., Liu, Y., & Umeh, A. (Eds.). (2025). *Per- and polyfluorinated alkyl substances: Occurrence, toxicity and remediation of PFAS*. De Gruyter.

National Academies of Sciences, Engineering, and Medicine. (2024). *Exploring linkages between soil health and human health*. National Academies Press.

Nguyen, M. A., Wiberg, K., Ribeli, E., Josefsson, S., Futter, M., Gustavsson, J., & Ahrens, L. (2017). Spatial distribution and source tracing of per- and polyfluoroalkyl substances (PFASs) in surface water in Northern Europe. *Environmental Pollution*, *220*, 1438–1446. https://doi.org/10.1016/j.envpol.2016.10.089

Nguyen, T. M. H., Bräunig, J., Kookana, R. S., Kaserzon, S. L., Knight, E. R., Vo, H. N. P., Kabiri, S., Navarro, D. A., Grimison, C., Riddell, N., Higgins, C. P., McLaughlin, M. J., & Mueller, J. F. (2022). Assessment of Mobilization Potential of Per- and Polyfluoroalkyl Substances for Soil Remediation. *Environmental Science and Technology*, *56*(14), 10030–10041. https://doi.org/10.1021/acs.est.2c00401

Nkin, G. K. (2025). Remediation of Per-and Polyfluoroalkyl Substances (PFAS)-Contaminated Environments: Emerging Nanomaterials, Electrochemical, and Biological Strategies Graphical abstract. *International Journal of Chemistry and Chemical Processes E-ISSN*, *11*(6), 2025. https://doi.org/10.56201/ijccp.vol.11.no6.2025.pg68.97

Olawade, D. B., Oladipo, P., Ajisafe, O., Egbon, E., Fapohunda, O., & Kade, A. (2025). Genetically engineered microorganisms: A promising frontier for PFAS bioremediation. In *Process Safety and Environmental Protection* (Vol. 202). Institution of Chemical Engineers. https://doi.org/10.1016/j.psep.2025.107699

Pan, C. G., Ying, G. G., Zhao, J. L., Liu, Y. S., Liu, S. S., Du, J., & Kookana, R. S. (2015). Spatial Distribution of Perfluoroalkyl Substances in Surface Sediments of Five Major Rivers in China. *Archives of Environmental Contamination and Toxicology*, *68*(3), 566–576. https://doi.org/10.1007/s00244-014-0113-8

Parsons, J. R., Sáez, M., Dolfing, J., & de Voogt, P. (2008). Biodegradation of perfluorinated compounds. *Reviews of Environmental Contamination and Toxicology*, *196*, 53–71. https://doi.org/10.1007/978-0-387-78444-1_2

Pavlovska, M., Prekrasna, I., Parnikoza, I., & Dykyi, E. (2021). Soil sample preservation strategy affects the microbial community structure. *Microbes and Environments*, *36*(1), 1–7. https://doi.org/10.1264/jsme2.ME20134

Potts, L. D., Douglas, A., Perez Calderon, L. J., Anderson, J. A., Witte, U., Prosser, J. I., & Gubry-Rangin, C. (2022). Chronic Environmental Perturbation Influences Microbial Community Assembly Patterns. *Environmental Science and Technology*, *56*(4), 2300–2311. https://doi.org/10.1021/acs.est.1c05106

Prakash, O., Nimonkar, Y., & Desai, D. (2020). A Recent Overview of Microbes and Microbiome Preservation. In *Indian Journal of Microbiology* (Vol. 60, Number 3). Springer. https://doi.org/10.1007/s12088-020-00880-9

Prakash, O., Nimonkar, Y., & Shouche, Y. S. (2013). Practice and prospects of microbial preservation. In *FEMS Microbiology Letters* (Vol. 339, Number 1, pp. 1–9). https://doi.org/10.1111/1574-6968.12034

PFAS Data Hub. (2024). *Forever pollution map*. https://foreverpollution.eu/map/

Presentato, A., Lampis, S., Vantini, A., Manea, F., Daprà, F., Zuccoli, S., & Vallini, G. (2020). On the ability of perfluorohexane sulfonate (PFHxS) bioaccumulation by two Pseudomonas sp. strains isolated from PFAS-contaminated environmental matrices. *Microorganisms*, *8*(1). https://doi.org/10.3390/microorganisms8010092

Preston-Mafham, J., Boddy, L., & Randerson, P. F. (2002). Analysis of microbial community functional diversity using sole-carbon-source utilisation profiles â€“ a critique. *FEMS Microbiology Ecology*, *42*(1), 1–14. https://doi.org/10.1111/j.1574-6941.2002.tb00990.x

Prevedouros, K., Cousins, I. T., Buck, R. C., & Korzeniowski, S. H. (2006). Sources, fate and transport of perfluorocarboxylates. In *Environmental Science and Technology* (Vol. 40, Number 1, pp. 32–44). https://doi.org/10.1021/es0512475

Rahman, M. F., Peldszus, S., & Anderson, W. B. (2014). Behaviour and fate of perfluoroalkyl and polyfluoroalkyl substances (PFASs) in drinking water treatment: A review. In *Water Research* (Vol. 50, pp. 318–340). Elsevier Ltd. https://doi.org/10.1016/j.watres.2013.10.045

Ramette, A. (2007). Multivariate analyses in microbial ecology. In *FEMS Microbiology Ecology* (Vol. 62, Number 2, pp. 142–160). https://doi.org/10.1111/j.1574-6941.2007.00375.x

Ramírez, M., Muñoz, A., López-Piñeiro, A., Albarrán, Á., Peña, D., Rato Nunes, J. M., Gama, J., & Loures, L. (2017). Evaluation of the microbial viability of soil samples from maize crops in freeze-storage under different management conditions in a semi-arid climate. *Sustainability (Switzerland)*, *9*(5). https://doi.org/10.3390/su9050690

Randazzo, A., Pavan, F., Gea, M., & Maffiotti, A. (2025). Perfluoroalkyl substances (PFASs) in groundwater and surface water in the Turin metropolitan area (Italy): An attempt to unravel

potential point sources and compliance with environmental/drinking water quality standards. *Science of the Total Environment*, *958*. https://doi.org/10.1016/j.scitotenv.2024.177973

Raupp, P., Carrillo, Y., & Nielsen, U. N. (2024). Soil Health to Enhance Ecological Restoration and Conservation. In *Journal of Sustainable Agriculture and Environment* (Vol. 3, Number 4). John Wiley and Sons Inc. https://doi.org/10.1002/sae2.70022

Renella, G., Carletti, P., & Masi, A. (2025). Sustainable Management of Poly- and Perfluoroalkyl Substances (PFASs)-Contaminated Areas: Tackling a Wicked Environmental Problem. *Sustainability (Switzerland)*, *17*(2). https://doi.org/10.3390/su17020510

Rubin, B. E. R., Gibbons, S. M., Kennedy, S., Hampton-Marcell, J., Owens, S., & Gilbert, J. A. (2013). Investigating the Impact of Storage Conditions on Microbial Community Composition in Soil Samples. *PLoS ONE*, *8*(7). https://doi.org/10.1371/journal.pone.0070460

Ruiz-Urigüen, M., Shuai, W., Huang, S., & Jaffé, P. R. (2022). Biodegradation of PFOA in microbial electrolysis cells by Acidimicrobiaceae sp. strain A6. *Chemosphere*, *292*. https://doi.org/10.1016/j.chemosphere.2021.133506

Ruyle, B. J., Thackray, C. P., Butt, C. M., Leblanc, D. R., Tokranov, A. K., Vecitis, C. D., & Sunderland, E. M. (2023). Centurial Persistence of Forever Chemicals at Military Fire Training Sites. *Environmental Science and Technology*, *57*(21), 8096–8106. https://doi.org/10.1021/acs.est.3c00675

Schellenberger, S., Liagkouridis, I., Awad, R., Khan, S., Plassmann, M., Peters, G., Benskin, J. P., & Cousins, I. T. (2022). An Outdoor Aging Study to Investigate the Release of Per- and Polyfluoroalkyl Substances (PFAS) from Functional Textiles. *Environmental Science and Technology*, *56*(6), 3471–3479. https://doi.org/10.1021/acs.est.1c06812

Schiavo, M., Colombani, N., Mastrocicco, M., & Petitta, M. (2025). Stochastic assessment of groundwater PFAS concentrations in North-Eastern Italy. *Stochastic Environmental Research and Risk Assessment*, *39*(8), 3391–3404. https://doi.org/10.1007/s00477-025-03023-y

Senaratne, W. M. T. N., & Jayaweera, J. A. A. S. (2024). Comparison of microbial preservation methods: a narrative review. In *GERMS* (Vol. 14, Number 4, pp. 375–386). European Academy of HIV/AIDS and Infectious Diseases. https://doi.org/10.18683/germs.2024.1447

Senevirathna, S. T. M. L. D., Krishna, K. C. B., Mahinroosta, R., & Sathasivan, A. (2022a). Comparative characterization of microbial communities that inhabit PFAS-rich contaminated sites: A case-control study. *Journal of Hazardous Materials*, *423*. https://doi.org/10.1016/j.jhazmat.2021.126941

Senevirathna, S. T. M. L. D., Krishna, K. C. B., Mahinroosta, R., & Sathasivan, A. (2022b). Comparative characterization of microbial communities that inhabit PFAS-rich contaminated

sites: A case-control study. *Journal of Hazardous Materials*, *423*. https://doi.org/10.1016/j.jhazmat.2021.126941

Senevirathna, S. T. M. L. D., Krishna, K. C. B., Mahinroosta, R., & Sathasivan, A. (2022c). Comparative characterization of microbial communities that inhabit PFAS-rich contaminated sites: A case-control study. *Journal of Hazardous Materials*, *423*. https://doi.org/10.1016/j.jhazmat.2021.126941

Shahid, M., & Shafi, Z. (2026). Microbial and molecular approaches for PFAS transformation in soils: prospects and limitations. In *RSC Advances* (Vol. 16, Number 5, pp. 4184–4203). Royal Society of Chemistry. https://doi.org/10.1039/d5ra07508d

Shahsavari, E., Rouch, D., Khudur, L. S., Thomas, D., Aburto-Medina, A., & Ball, A. S. (2021). Challenges and Current Status of the Biological Treatment of PFAS-Contaminated Soils. In *Frontiers in Bioengineering and Biotechnology* (Vol. 8). Frontiers Media S.A. https://doi.org/10.3389/fbioe.2020.602040

Sharp, S., Sardiña, P., Metzeling, L., McKenzie, R., Leahy, P., Menkhorst, P., & Hinwood, A. (2021). Per- and Polyfluoroalkyl Substances in Ducks and the Relationship with Concentrations in Water, Sediment, and Soil. *Environmental Toxicology and Chemistry*, *40*(3), 846–858. https://doi.org/10.1002/etc.4818

Shaw, D. M. J., Munoz, G., Bottos, E. M., Duy, S. V., Sauvé, S., Liu, J., & Van Hamme, J. D. (2019). Degradation and defluorination of 6:2 fluorotelomer sulfonamidoalkyl betaine and 6:2 fluorotelomer sulfonate by Gordonia sp. strain NB4-1Y under sulfur-limiting conditions. *Science of the Total Environment*, *647*, 690–698. https://doi.org/10.1016/j.scitotenv.2018.08.012

Song, S. J., Amir, A., Metcalf, J. L., Amato, K. R., Xu, Z. Z., Humphrey, G., & Knight, R. (2016). Preservation Methods Differ in Fecal Microbiome Stability, Affecting Suitability for Field Studies. *MSystems*, *1*(3). https://doi.org/10.1128/msystems.00021-16

Stephens, A. E. A. (2023). Introducing the Science & Society Series on Local and Indigenous ecological knowledge. In *Trends in Ecology and Evolution* (Vol. 38, Number 1, pp. 1–2). Elsevier Ltd. https://doi.org/10.1016/j.tree.2022.12.003

Sun, H., Gerecke, A. C., Giger, W., & Alder, A. C. (2011). Long-chain perfluorinated chemicals in digested sewage sludges in Switzerland. *Environmental Pollution*, *159*(2), 654–662. https://doi.org/10.1016/j.envpol.2010.09.020

Sunderland, E. M., Hu, X. C., Dassuncao, C., Tokranov, A. K., Wagner, C. C., & Allen, J. G. (2019). A review of the pathways of human exposure to poly- and perfluoroalkyl substances (PFASs) and present understanding of health effects. In *Journal of Exposure Science and Environmental Epidemiology* (Vol. 29, Number 2, pp. 131–147). Nature Publishing Group. https://doi.org/10.1038/s41370-018-0094-1

Technology ▼ Solutions. (2006). https://pubs.acs.org/sharingguidelines

Thakur, A., Khusnutdinova, A. N., Navarro-Márquez, M., Kumar, V., Ma, H., Golyshin, P. N., Lyu, T., Yakunin, A. F., Kumar, G., Nithya, K., Soto, G. G., Iqbal, H. M. N., Gutierrez, T., Coulon, F., & Parra-Saldívar, R. (2025). Comprehensive strategies for the remediation of per- and polyfluoroalkyl substances (PFAS): Mechanisms, technologies, and future perspectives. In *Ecotoxicology and Environmental Safety* (Vol. 306). Academic Press. https://doi.org/10.1016/j.ecoenv.2025.119374

Tseng, N., Wang, N., Szostek, B., & Mahendra, S. (2014). Biotransformation of 6:2 Fluorotelomer alcohol (6:2 FTOH) by a wood-rotting fungus. *Environmental Science and Technology*, *48*(7), 4012–4020. https://doi.org/10.1021/es4057483

Tshangana, C. S., Nhlengethwa, S. T., Glass, S., Denison, S., Kuvarega, A. T., Nkambule, T. T. I., Mamba, B. B., Alvarez, P. J. J., & Muleja, A. A. (2025). Technology status to treat PFAS-contaminated water and limiting factors for their effective full-scale application. In *npj Clean Water* (Vol. 8, Number 1). Nature Research. https://doi.org/10.1038/s41545-025-00457-3

U.S. Environmental Protection Agency (EPA). (2022). *Remediation technologies for per- and polyfluoroalkyl substances (PFAS)*. https://clu-in.org/contaminantfocus/default.focus/sec/Per-_and_Polyfluoroalkyl_Substances_(PFAS)/cat/Remediation_Technologies/

U.S. Environmental Protection Agency (EPA). (2025). *Per- and polyfluoroalkyl substances (PFAS)*. https://www.epa.gov/pfas

U.S. Environmental Protection Agency (EPA). (2025). *PFAS: Listed in OECD global database*. https://comptox.epa.gov/dashboard/chemical-lists/PFASOECD

Valsecchi, S., Babut, M., Mazzoni, M., Pascariello, S., Ferrario, C., De Felice, B., Bettinetti, R., Veyrand, B., Marchand, P., & Polesello, S. (2021). Per- and Polyfluoroalkyl Substances (PFAS) in Fish from European Lakes: Current Contamination Status, Sources, and Perspectives for Monitoring. *Environmental Toxicology and Chemistry*, *40*(3), 658–676. https://doi.org/10.1002/etc.4815

Van Belkum, A., Sluijter, M., De Groot, R., Verbrugh, H., & Hermans, P. W. M. (1996). Novel BOX Repeat PCR Assay for High-Resolution Typing of Streptococcus pneumoniae Strains. In *JOURNAL OF CLINICAL MICROBIOLOGY* (Vol. 34, Number 5). https://journals.asm.org/journal/jcm

Vartoukian, S. R., Palmer, R. M., & Wade, W. G. (2010). Strategies for culture of "unculturable" bacteria. In *FEMS Microbiology Letters* (Vol. 309, Number 1, pp. 1–7). Blackwell Publishing Ltd. https://doi.org/10.1111/j.1574-6968.2010.02000.x

Wackett, L. P. (2022). Nothing lasts forever: understanding microbial biodegradation of polyfluorinated compounds and perfluorinated alkyl substances. In *Microbial Biotechnology* (Vol. 15, Number 3, pp. 773–792). John Wiley and Sons Ltd. https://doi.org/10.1111/1751-7915.13928

Wang, Q., Ruan, Y., Jin, L., Tao, L. S. R., Lai, H., Li, G., Yeung, L. W. Y., Leung, K. M. Y., & Lam, P. K. S. (2023). Legacy and Emerging Per- and Polyfluoroalkyl Substances in a Subtropical Marine Food Web: Suspect Screening, Isomer Profile, and Identification of Analytical Interference. *Environmental Science and Technology*, *57*(22), 8355–8364. https://doi.org/10.1021/acs.est.3c00374

Wang, X., Chen, M., Gong, P., & Wang, C. (2019). Perfluorinated alkyl substances in snow as an atmospheric tracer for tracking the interactions between westerly winds and the Indian Monsoon over western China. *Environment International*, *124*, 294–301. https://doi.org/10.1016/j.envint.2018.12.057

Wang, X., Halsall, C., Codling, G., Xie, Z., Xu, B., Zhao, Z., Xue, Y., Ebinghaus, R., & Jones, K. C. (2014). Accumulation of perfluoroalkyl compounds in Tibetan mountain snow: Temporal patterns from 1980 to 2010. *Environmental Science and Technology*, *48*(1), 173–181. https://doi.org/10.1021/es4044775

Wang, Z., Buser, A. M., Cousins, I. T., Demattio, S., Drost, W., Johansson, O., Ohno, K., Patlewicz, G., Richard, A. M., Walker, G. W., White, G. S., & Leinala, E. (2021). A New OECD Definition for Per- And Polyfluoroalkyl Substances. In *Environmental Science and Technology* (Vol. 55, Number 23, pp. 15575–15578). American Chemical Society. https://doi.org/10.1021/acs.est.1c06896

Wang, Z., Cousins, I. T., Scheringer, M., Buck, R. C., & Hungerbühler, K. (2014). Global emission inventories for C4-C14 perfluoroalkyl carboxylic acid (PFCA) homologues from 1951 to 2030, part II: The remaining pieces of the puzzle. *Environment International*, *69*, 166–176. https://doi.org/10.1016/j.envint.2014.04.006

Wang, Z., Dewitt, J. C., Higgins, C. P., & Cousins, I. T. (2017). A Never-Ending Story of Per- and Polyfluoroalkyl Substances (PFASs)? *Environmental Science and Technology*, *51*(5), 2508–2518. https://doi.org/10.1021/acs.est.6b04806

White, T. J., Bruns, T., Lee, S., & Taylor, J. (1990). AMPLIFICATION AND DIRECT SEQUENCING OF FUNGAL RIBOSOMAL RNA GENES FOR PHYLOGENETICS. In *PCR Protocols* (pp. 315–322). Elsevier. https://doi.org/10.1016/b978-0-12-372180-8.50042-1

Wijayahena, M. K., Moreira, I. S., Castro, P. M. L., Dowd, S., Marciesky, M. I., Ng, C., & Aga, D. S. (2025). PFAS biodegradation by Labrys portucalensis F11: Evidence of chain shortening

and identification of metabolites of PFOS, 6:2 FTS, and 5:3 FTCA. *Science of the Total Environment*, *959*. https://doi.org/10.1016/j.scitotenv.2024.178348

Williams, A. J., Gaines, L. G. T., Grulke, C. M., Lowe, C. N., Sinclair, G. F. B., Samano, V., Thillainadarajah, I., Meyer, B., Patlewicz, G., & Richard, A. M. (2022). Assembly and Curation of Lists of Per- and Polyfluoroalkyl Substances (PFAS) to Support Environmental Science Research. *Frontiers in Environmental Science*, *10*. https://doi.org/10.3389/fenvs.2022.850019

Wittebolle, L., Marzorati, M., Clement, L., Balloi, A., Daffonchio, D., Heylen, K., De Vos, P., Verstraete, W., & Boon, N. (2009). Initial community evenness favours functionality under selective stress. *Nature*, *458*(7238), 623–626. https://doi.org/10.1038/nature07840

Wu, E., Wang, K., Liu, Z., Wang, J., Yan, H., Zhu, X., Zhu, X., & Chen, B. (2023). Metabolic and Microbial Profiling of Soil Microbial Community under Per- and Polyfluoroalkyl Substance (PFAS) Stress. *Environmental Science and Technology*, *57*(51), 21855–21865. https://doi.org/10.1021/acs.est.3c07020

Xu, R., Tao, W., Lin, H., Huang, D., Su, P., Gao, P., Sun, X., Yang, Z., & Sun, W. (2022). Effects of Perfluorooctanoic Acid (PFOA) and Perfluorooctane Sulfonic Acid (PFOS) on Soil Microbial Community. *Microbial Ecology*, *83*(4), 929–941. https://doi.org/10.1007/s00248-021-01808-6

Yamashita, N., Taniyasu, S., Petrick, G., Wei, S., Gamo, T., Lam, P. K. S., & Kannan, K. (2008). Perfluorinated acids as novel chemical tracers of global circulation of ocean waters. *Chemosphere*, *70*(7), 1247–1255. https://doi.org/10.1016/j.chemosphere.2007.07.079

Yang, Y., Wang, J., Tang, S., Qiu, J., Luo, Y., Yang, C., Lai, X., Wang, Q., & Cao, H. (2025). Per- and Polyfluoroalkyl Substances (PFAS) in Consumer Products: An Overview of the Occurrence, Migration, and Exposure Assessment. In *Molecules* (Vol. 30, Number 5). Multidisciplinary Digital Publishing Institute (MDPI). https://doi.org/10.3390/molecules30050994

Yao, J., Pan, Y., Sheng, N., Su, Z., Guo, Y., Wang, J., & Dai, J. (2020). Novel Perfluoroalkyl Ether Carboxylic Acids (PFECAs) and Sulfonic Acids (PFESAs): Occurrence and Association with Serum Biochemical Parameters in Residents Living near a Fluorochemical Plant in China. *Environmental Science and Technology*, *54*(21), 13389–13398. https://doi.org/10.1021/acs.est.0c02888

Yarwood, G., Kemball-Cook, S., Keinath, M., Waterland, R. L., Korzeniowski, S. H., Buck, R. C., Russell, M. H., & Washburn, S. T. (2007). High-resolution atmospheric modeling of fluorotelomer alcohols and perfluorocarboxylic acids in the North American troposphere. *Environmental Science and Technology*, *41*(16), 5756–5762. https://doi.org/10.1021/es0708971

Ye, M., Zhang, Z., Sun, M., & Shi, Y. (2022). Dynamics, gene transfer, and ecological function of intracellular and extracellular DNA in environmental microbiome. In *iMeta* (Vol. 1, Number 3). John Wiley and Sons Inc. https://doi.org/10.1002/imt2.34

Yoon, S. H., Ha, S. M., Kwon, S., Lim, J., Kim, Y., Seo, H., & Chun, J. (2017). Introducing EzBioCloud: A taxonomically united database of 16S rRNA gene sequences and whole-genome assemblies. *International Journal of Systematic and Evolutionary Microbiology*, *67*(5), 1613–1617. https://doi.org/10.1099/ijsem.0.001755

Yu, Y., Che, S., Ren, C., Jin, B., Tian, Z., Liu, J., & Men, Y. (2022). Microbial Defluorination of Unsaturated Per- and Polyfluorinated Carboxylic Acids under Anaerobic and Aerobic Conditions: A Structure Specificity Study. *Environmental Science and Technology*, *56*(8), 4894–4904. https://doi.org/10.1021/acs.est.1c05509

Yu, Y., Zhang, K., Li, Z., Ren, C., Chen, J., Lin, Y. H., Liu, J., & Men, Y. (2020). Microbial Cleavage of C-F Bonds in Two C6Per- And Polyfluorinated Compounds via Reductive Defluorination. *Environmental Science and Technology*, *54*(22), 14393–14402. https://doi.org/10.1021/acs.est.0c04483

Zhang, J., Naveed, H., Chen, K., & Chen, L. (2025). Toxicity of Per- and Polyfluoroalkyl Substances and Their Substitutes to Terrestrial and Aquatic Invertebrates—A Review. In *Toxics* (Vol. 13, Number 1). Multidisciplinary Digital Publishing Institute (MDPI). https://doi.org/10.3390/toxics13010047

Zhang, K., Huang, J., Yu, G., Zhang, Q., Deng, S., & Wang, B. (2013). Destruction of perfluorooctane sulfonate (PFOS) and perfluorooctanoic acid (PFOA) by ball milling. *Environmental Science and Technology*, *47*(12), 6471–6477. https://doi.org/10.1021/es400346n

Zhang, Q., Zhu, D., Ding, J., Zhou, S., Sun, L., & Qian, H. (2019). Species-specific response of the soil collembolan gut microbiome and resistome to soil oxytetracycline pollution. *Science of the Total Environment*, *668*, 1183–1190. https://doi.org/10.1016/j.scitotenv.2019.03.091

Zhang, S., Szostek, B., McCausland, P. K., Wolstenholme, B. W., Lu, X., Wang, N., & Buck, R. C. (2013). 6:2 and 8:2 fluorotelomer alcohol anaerobic biotransformation in digester sludge from a WWTP under methanogenic conditions. *Environmental Science and Technology*, *47*(9), 4227–4235. https://doi.org/10.1021/es4000824

Zheng, G., Schreder, E., Dempsey, J. C., Uding, N., Chu, V., Andres, G., Sathyanarayana, S., & Salamova, A. (2021). Per- And Polyfluoroalkyl Substances (PFAS) in Breast Milk- And Trends for Current-Use PFAS. *Environmental Science and Technology*, *55*(11), 7510–7520. https://doi.org/10.1021/acs.est.0c06978

Zhou, Q., Pan, G., & Zhang, J. (2013). Effective sorption of perfluorooctane sulfonate (PFOS) on hexadecyltrimethylammonium bromide immobilized mesoporous SiO2 hollow sphere. *Chemosphere*, *90*(9), 2461–2466. https://doi.org/10.1016/j.chemosphere.2012.11.009

Zinger, L., Amaral-Zettler, L. A., Fuhrman, J. A., Horner-Devine, M. C., Huse, S. M., Welch, D. B. M., Martiny, J. B. H., Sogin, M., Boetius, A., & Ramette, A. (2011). Global patterns of bacterial beta-diversity in seafloor and seawater ecosystems. *PLoS ONE*, *6*(9). https://doi.org/10.1371/journal.pone.0024570